

**13th INTERNATIONAL CONFERENCE
ON
PARTICLE-INDUCED X-RAY EMISSION**

PIXE 2013

FOR TECHNOLOGY AND GLOBAL DEVELOPMENT

Gramado, Brazil March 3-8, 2013

Book of Abstracts

Organized by

LLI - Laboratório de Implantação Iônica

IF - Instituto de Física

UFRGS - Universidade Federal do Rio Grande do Sul

SBF – Sociedade Brasileira de Física

In cooperation with

IAEA – International Atomic Energy Agency

Editors

Raul C. Fadanelli Filho, M. Lúcia Yoneama, Johnny F. Dias and Livio Amaral

Cover Design

M. Lúcia Yoneama

Cover picture

Lago Negro – Gramado, RS

Website design

Agenor Hentz

Printed by

UFRGS

Porto Alegre, January 2013.

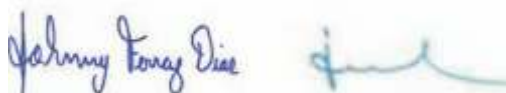
Welcome

The Local Organizing Committee is pleased to welcome all participants to the 13th *International Conference on Particle-Induced X-Ray Emission (PIXE 2013)* held in the city of Gramado (Rio Grande do Sul (RS), Brazil) between March 3 – 8, 2013. The first PIXE conference took place in the city of Lund (Sweden) in 1976. This conference laid the grounds for a long tradition of triennial PIXE conferences (Lund (1980), Heidelberg (1983), Tallahassee (1986), Amsterdam (1989), Tokyo (1992), Padua (1995), Lund (1998), Guelph (2001), Portoroz (2004), Puebla (2007) and Guildford (2010). This year Brazil has the honor and responsibility for organizing the conference. We are proud of undertaking this task because, for the first time, the PIXE conference has crossed the Equator line and is organized in a South-American country.

PIXE conferences have been the perfect forum to discuss recent developments and future perspectives in particle-induced X-ray spectrometry. The conference brings together physicists, engineers, chemists, material scientists, ion beam specialists, biologists and other scientists from different fields. Due to the importance of the PIXE analytical technique in many different fields of research and applied studies, the PIXE 2013 conference will feature a global theme. The theme for the 13th edition of the PIXE conference will be *PIXE for Technology and Global Development*.

The PIXE conference will follow the tradition of the Ion Implantation Laboratory group to organize conferences in Gramado with its beautiful landscape and cozy atmosphere. The Hotel Serra Azul is conveniently located within Gramado's main attraction sites and is surrounded by cafes, restaurants and shops.

We hope that you will find the conference scientifically fruitful, enjoyable and interesting.



Johnny F. Dias Livio Amaral
PIXE 2013 Conference Chairs



Maria Lúcia Yoneama
PIXE 2013 Conference Manager

PIXE 2013 COMMITTEES

International Advisory Committee

M. A. Reis - Portugal (Chair)
T. Calligaro - France
D.D. Cohen - Australia
A. Denker - Germany
J.F. Dias - Brazil
F. Lucarelli - Italy
W. Maenhaut - Belgium
J. Miranda - Mexico
W. Przybylowicz - South Africa
Z. Smit – Slovenia

International Honorary Committee

J.L. Campbell - Canada
G.W. Grime - England
K. Ishii - Japan
P. A. Mando - Italy
C. Ryan - Australia
Z. Szokefalvi-Nagy – Hungary

Local Organizing Committee (IF-UFRGS)

Johnny F. Dias (Conference chair)
Livio Amaral (Conference Chair)
M. Lucia Yoneama (Conference manager)
Pedro L. Grande
Agenor Hentz
Raul C. Fadanelli Filho
Carla E. Iochims dos Santos
Paulo Jobim
Liana A. Bouffleur
Elis S. Moura
Rafaela Debastiani
Claudia T. de Souza
Marcia A. Rizzutto (IF-USP)

FINANCIAL SUPPORT

The PIXE 2013 Organizing Committee would like to take this opportunity to thank all sponsors for their support to the PIXE 2013 conference. We are very grateful to the sponsors listed below.

CAPES – Coordenação de Aperfeiçoamento de Pessoal de Nível Superior

CNPq - Conselho Nacional de Desenvolvimento Científico e Tecnológico

FAPERGS – Fundação de Amparo à Pesquisa do Estado do Rio Grande do Sul

INES - Instituto Nacional de Engenharia de Superfície

FAPESP - Fundação de Amparo à Pesquisa do Estado de São Paulo

SBF – Sociedade Brasileira de Física

UFRGS - Universidade Federal do Rio Grande do Sul

IF-UFRGS – Instituto de Física, UFRGS

NEC - National Electrostatics Corporation

OM - Oxford Microbeams Ltd.

IAEA – International Atomic Energy Agency

ONRG – Office of Naval Research Global – GRANT NUMBER N62909-12-1-1139

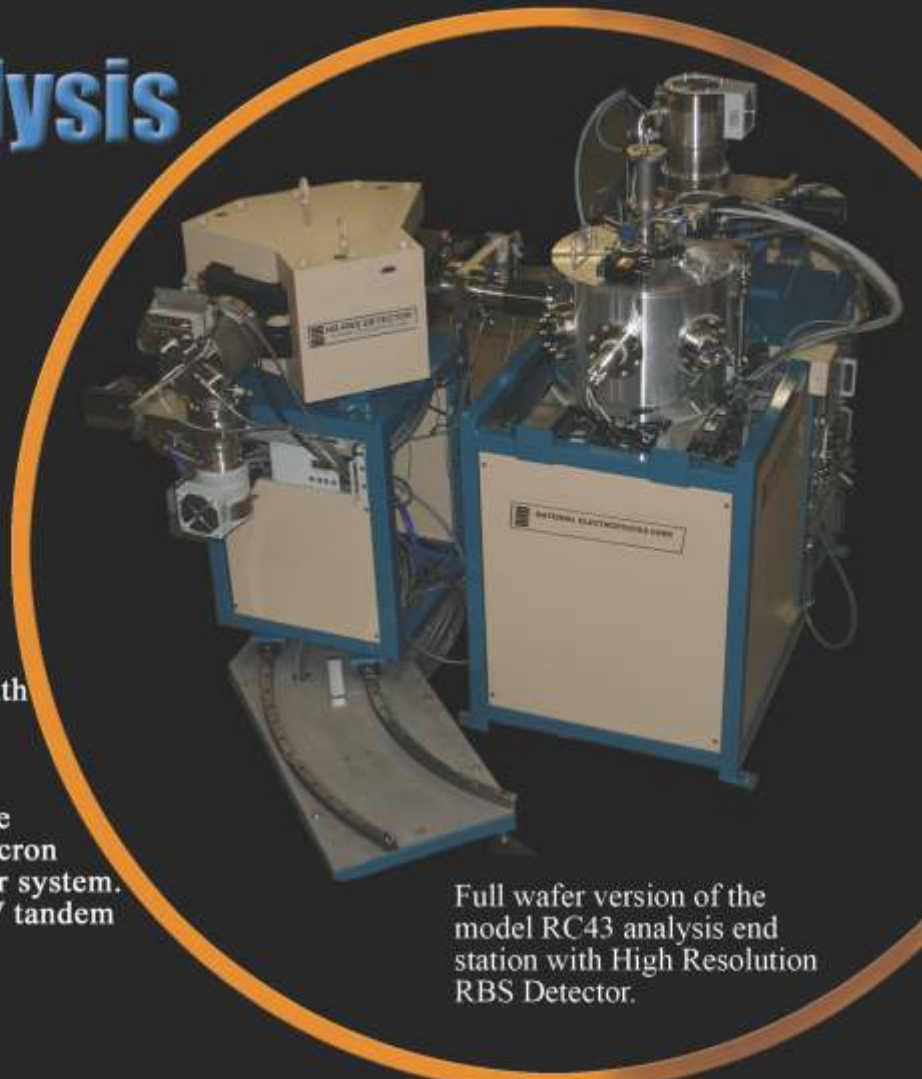
(The contents of this book do not necessarily reflect the position or the policy of the United States Government and no official endorsement should be inferred.)

MeV Beam Materials Analysis

National Electrostatics Corporation manufactures complete MeV beam materials analysis instruments capable of performing **RBS, channeling RBS, micro RBS, HR-RBS, PIXE, ERDA and Nuclear Resonance Analysis.**

These instruments are based on the Pelletron ion beam accelerator capable of providing beam energies from below 1 MeV to the 100's MeV region.

The NEC analysis systems are equipped with the Model RC43 analysis endstation, which contains a 5-axis goniometer for precision sample handling and surface barrier particle detector for forward and backscatter particle detection. Options are available for a 20 micron He⁺ beam and Ångstrom resolution detector system. Typically used with the 1.0, 1.7 and 2.0 MV tandem Pelletrons.



Full wafer version of the model RC43 analysis end station with High Resolution RBS Detector.



**Tandem Pelletrons
Equipped for Channeling
RBS, PIXE, ERD, and NRA**



National Electrostatics Corporation

For more information, visit us online at www.pelletron.com or call **608-831-7600**
E-mail: nec@pelletron.com Fax: 608-831-9591 7540 Graber Rd, P.O. Box 620310 Middleton, WI USA 53562-0310





Equipment and software for high energy ion beam applications

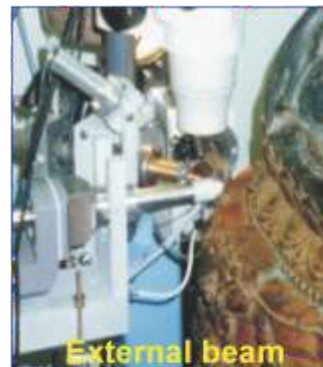
Established in 1986, Oxford Microbeams Ltd is the world's leading supplier of high energy ion microbeam equipment and software.

Applications

- Proton beam writing
- PIXE and PIXE mapping
- RBS and RBS mapping
- Channeling Contrast microscopy
- Scanning Transmission Ion microscopy
- Ion Beam Induced Charge microscopy
- Ionoluminescence mapping
- Elastic Recoil Detection Analysis
- Ion induced secondary electron images
- Ion beam modification of materials
- Heavy ion focusing
- External beams
- Single ion hits



OM2000 endstation



External beam



Vertical lens assembly

Performance of OM systems:

With the Oxford triplet configuration of OM52 miniature lenses, spot sizes of $30 \times 40\text{nm}$ have been achieved for low current applications¹, and 20nm high aspect ratio structures have been written using proton beam writing².

OM2000 endstation: $300 \times 450 \text{ nm}$ spot sizes with a 50pA , 2MeV proton beam have been demonstrated with the OM2000 system³.

¹ The Singapore high resolution single cell imaging facility, F. Watt, Xiao Chen, Armin Baysic De Vera, C. N. Udalagama, Ren Minqin, J. A. van Kan, A. A. Bettioli, Nuclear Instruments & Methods B 269 (2011) 2168-2174

² Proton Beam Writing of 3D Nanostructures in Hydrogen Silsesquioxane" JA Van Kan, AA Bettioli, and Frank Watt. Nano Letters 6 (2006) 579-582

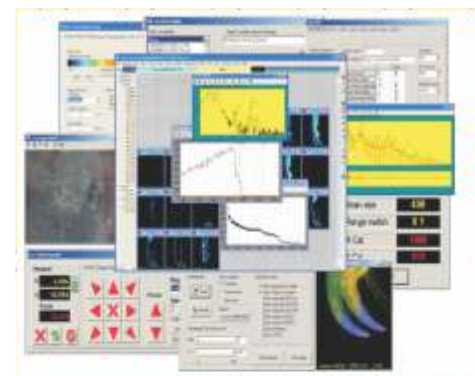
³ The Singapore high energy ion nanoprobe facility, F Watt, JA van Kan, I Rajta, AA Bettioli, TF Choo, MBH Breese and T Osipowicz, Nuclear Instruments & Methods B (2003) 210, p14-20.



OMDAQ2007

Hardware and Software package

- Microbeam data acquisition and scan control
- XYZ stage control
- Off-line spectrum analysis (PIXE and RBS)
- Listmode playback



Download a DEMO version from
<http://www.microbeams.co.uk/downloads>

Under development

All the user-friendly features of OMDAQ integrated with the fast low-level FPGA hardware developed in Singapore.

PIXE 2013

FOR TECHNOLOGY AND GLOBAL DEVELOPMENT

GENERAL INFORMATION

General Information about Gramado

Local weather

The temperature in this area during the months of March/April ranges from 16°C (~61°F) at night to 24°C (~75°F) during the day.

Currency

The Brazilian currency is the Real (symbol R\$). The currency exchange symbol for the real is BRL.

Banking hours

Most banks are open from Monday to Friday from 10:00 to 15:00 without break. Most of the ATM machines (24/7) provide international service.

Credit Cards

Most hotels, restaurants and shops in Brazil accept all major credit cards such as VISA, MasterCard, American Express, and Diners Club.

Electricity

Electricity in Brazil could be 110 V or 220 V AC. In the city of Porto Alegre the voltage is 110V while in Gramado is 220V. Please be careful.

General Information about the conference

Conference Location

Hotel Serra Azul
Rua Garibaldi, 152 CEP 95670-000 Gramado, RS – Brazil
Phone: (54) 3295 7200 Fax: (54) 32957 272

Conference Manager

Maria Lucia Yoneama
pixe2013@ufrgs.br

Conference Registration Desk

The conference registration desk will be available at the Secretariat on March 3rd, Sunday, from 17:00 to 20:00 and on March 4th, Monday from 8:00 – 8:30.

Secretariat

Opening hours: Sunday: 17:00 – 20:00
Monday to Friday: during conference hours

Internet Connection

Hotel Serra Azul has a free Wi-Fi Internet connection.

Coffee Break

Coffee break will take place in the hall close to the auditorium.

Buffet lunch

Lunch will be served at the Hotel Serra Azul restaurant around 12:30.

Presentation Guidelines

Plenary Talk

The time-frame for Invited Speaker presentations is 35 minutes. Additional 5 minutes will be allowed for follow-up questions.

Oral Presentations

Oral presentations will be limited to 15 minutes. Additional 5 minutes will be allowed for discussion.

Poster Presentations

The poster size should be 90 cm (in width) x 120 cm (in height). The background of the poster board is white. Pins are not allowed. Tape will be provided. Authors should be present at their posters sessions for discussion with attendees.

Social Program

The social program of the PIXE 2013 conference includes a welcome reception, a banquet and a day trip to Vale dos Vinhedos and a tour to Caracol National Park.

Welcome Cocktail (Monday, March 4th)

Conference participants and accompanying persons are invited to attend a Welcome Cocktail at the Hotel Serra Azul (Salão Diamante) on March 4th at 19:40.

Banquet

The conference banquet will be held at Churrascaria Zelão where a typical all-you-can-eat Brazilian barbecue will be served. Besides the meat, a variety of side dishes and salads will be served as well.

Outing

Tour at Caracol National Park – Caracol falls is a 420 feet (130 m) waterfall located about 4.35 miles (7 km) from Canela, RS, Brazil. The falls are situated between the pine forest zone of the Brazilian Highlands and the southern coastal Atlantic Forest. The base of the waterfall can be reached by a steep 927-step trail maintained by the Projeto Lobo-Guará.

Trip to Vale dos Vinhedos – A trip to Vale dos Vinhedos is planned after the tour at Caracol National Park. During the trip (approximately 2 hours long), participants will enjoy the nice landscape of the region. Upon arrival, lunch will be served at the local restaurant owned by Valduga's family (Villa Valduga restaurant). A visit to Casa Valduga winery, one of the most important Brazilian wine producers, is also planned.

Accompanying persons program

For accompanying persons, the hotel offers infrastructure for leisure, such as swimming pool, sauna, SPA and fitness room.

Those who want to enjoy Gramado and its surrounding areas may visit the site http://www.tripadvisor.com/Tourism-g303536-Gramado_State_of_Rio_Grande_do_Sul-Vacations.html for tips and information about tours, day trips and shopping. Moreover, you may also contact the tourism agency available at the Hotel Serra Azul for further information and sightseeing schedules for the period of the conference.

PIXE 2013

FOR TECHNOLOGY AND GLOBAL DEVELOPMENT

CONFERENCE SCHEDULE

March 3 rd Sunday	March 4 th Monday	March 5 th Tuesday	March 6 th Wednesday	March 7 th Thursday	March 8 th Friday	
	8:00 Registration		Outing			
	8:30 Opening			9:00 I8 Cohen		
	9:00 I1 Lapicki	9:00 I6 Mesjasz		9:40 O23 Lucarelli	9:00 I13 Sera	9:40 O30 Sugai
	9:40 O1 Miranda	9:40 O12 Olabanji		10:00 O24 Kertész	10:00 O31 Olise	10:00 O31 Olise
	10:00 O2 Mantero	10:00 O13 Mars		10:20 Coffee Break	10:20 Coffee Break	10:20 Coffee Break
	10:20 Coffee Break	10:20 Coffee Break		10:50 I9 Maenhaut	10:50 I14 Bailey	10:50 I14 Bailey
	10:50 I2 Reis	10:50 O14 Przybylowicz		11:30 O25 Yu	11:30 O32 Santos	11:30 O32 Santos
	11:30 O3 Fadanelli	11:10 O15 Kada		11:50 I10 Simon	11:50 O33 Puri	11:50 O33 Puri
	11:50 O4 Cohen	11:30 O16 Torok		12:30 Lunch	12:10 Closing	12:10 Closing
	12:10 O5 Heirwegh	11:50 O17 Grime		14:00 I11 Grime Oxford Microbeams	12:30 Lunch	12:30 Lunch
	12:30 Lunch	12:10 O18 Chaves		14:50 Poster B	14:00	14:00 Bus Departure to Porto Alegre
	14:00 I3 Pelicon	12:30 Lunch			16:00 Coffee Break	
	14:40 O6 Strivay	IAC - IHC Meeting 13:30 Poster Setup			16:30 I12 Calligaro	
	15:00 O7 Pichon	14:50 Poster A			17:10 O26 Rizzutto	
	15:20 O8 Topic				17:30 O27 Eder	
	15:40 O9 Pineda				17:50 O28 Smit	
	16:00 Coffee Break	16:00 Coffee Break			18:10 O29 Neelmeijer	
	16:30 I4 Jones	16:30 I7 Ortega				
	17:10 O10 Sortica	17:10 O19 Carmona				
	17:30 O11 Fazinic	17:30 O20 Terakawa				
		17:50 O21 Sarita	IAC Meeting 18:30			
	19:00 I5 Ishii Fukushima	18:10 O22 Harada	Poster Setup 18:30			
	19:40 Welcome Cocktail			19:50 Banquet		
Registration & Refreshments 17:00 - 20:00						

SCIENTIFIC PROGRAM

SUNDAY MARCH 3, 2013

17:00 – 20:00 Registration

MONDAY MARCH 4, 2013

8:00 – 8:30 Registration

8:30 Opening – L. Amaral

9:00 – 10:20 - Session I

Chair: J. F. Dias

9:00 **I1 Werner Brandt legacy to PIXE: past, present, and future perspective**
G. Lapicki

9:40 **O1 L-shell x-ray production cross sections of selected lanthanoids by impact of $^4\text{He}^+$, $^7\text{Li}^{2+}$, $^{10}\text{B}^{2+}$, $^{12}\text{C}^{4+}$, $^{16}\text{O}^{4+}$, and $^{19}\text{F}^{3+}$ ions with energies between 0.50 Mev/u and 0.75 Mev/u**
J. Miranda, M. Lugo, G. Murillo, B. Méndez, R.V Díaz, J. López-Monroy, J. Aspiazú, P. Villaseñor

10:00 **O2 Atomic de-excitation and PIXE in Geant4: an update**
A. Mantero, S. Incerti, V. Ivantchenko, A. Taborda, P. C. Chaves, C. Champion and M. A. Reis

10:20 Coffee Break

10:50 – 12:30 - Session II

Chair: J. Miranda

10:50 **I2 EDS high resolution PIXE and spectra fine structure**
M.A. Reis, P.C. Chaves, A. Taborda, M.L. Carvalho, J.P Marques

11:30 **O3 Coulomb heating of H_2^+ , B_2^+ and C_2^+ molecules in Si <110>**
R. C. Fadanelli and M. Behar

11:50 **O4 Key experimental M subshell line X-ray production cross sections for slow light ions on high atomic number targets compared with ECUSAR theory**
David D. Cohen, Eduard Stelcer, Jagoda Crawford, Armand Atanacio, Greg Doherty, and Gregory Lapicki

12:10 **O5 Comparison of attenuation coefficient databases used in μ -PIXE analysis – XCOM, Chantler or...?**
C. M. Heirwegh, I. Pradler, and J. L. Campbell

12:30 Lunch

14:00 – 16:00 Session III

Chair: M. Reis

14:00 **I3 Facility & Micro-PIXE on biological tissues**
P. Pelicon, P. Vavpetič, N. Grlj, N. Ogrinc, L. Jeromel, M. Kelemen, G. Kukec Mezek, P. Pongrac, K. Vogel-Mikuš, M. Regvar

14:40 **O6 X-ray production cross-sections measurements for high-energy alpha particle beam for Si, Fe and Cu**
T. Dupuis, G. Chêne, A. Marchal, F. Mathis and D. Strivay

15:00 **O7 Multi-detector and systematic imaging system designed and developed within the New AGLAE project**
L. Pichon, C. Pacheco, B. Moignard, T. Guillou, Q. Lemasson, Ph. Walter

15:20 **O8 PIXE as a Characterisation Tool in the Cutting Tool Industry**
C.S.Freemantle, N. Sacks, C.A. Pineda-Vargas, M. Topic

15:40 **O9 Microprobe Study of Ni-Ge Interactions in Lateral Diffusion Couples**
D.Chilukusha, C.A. Pineda-Vargas, R. Nemetudi, A. Habanyama, C.M. Comrie

16:00 Coffee Break

16:30 – 17:50 Session IV

Chair: S. Matsuyama

16:30 **I4 External Heavy Ion PIXE and MeV-SIMS at the Surrey Ion Beam Centre**
B. N. Jones, L. Antwis, V. Palitsin, G. Grime, and R. Webb

17:10 **O10 Structural characterization of CdSe/ZnS quantum dots using PIXE, RBS and MEIS**
M. A. Sortica, P. L. Grande, C. Radtke, L. G. Almeida, R. Debastiani, J. F. Dias, A. Hentz

17:30 **O11 Integration of XRF spectrometer for simultaneous and/or complementary use with PIXE at the external ion beam analysis setup**
S. Fazinic, D. Cosic, M. Jaksic, A. Migliori, A. G. Karydas, V. Desnica and D. Mudronja

Panel session

Chair: A. Simon

19:00 **I5 Recovery from the radioactive pollution due to Fukushima First Nuclear Power Plant Accident**

K.Ishii, A.Terakawa, S.Matsuyama, Y.Kikuchi, F.Fujishiro, A. Ishizaki, N.Osada, H.Arai, K.Sugai, K.Nagakubo and T.Sakurada

19:40 **Welcome Cocktail**

TUESDAY MARCH 5, 2013

9:00 – 10:20 - Session V

Chair: R. Ortega

9:00 **I6 Micro-PIXE in plant sciences**

J. Mesjasz-Przybylowicz and W. J. Przybylowicz

9:40 **O12 PIXE analysis of thaumatooccus danielli in Osun state of Nigeria**

S.O. Olabanji, G.A. Osinkolu, D.A. Pelemo, and A.T. Oladele

10:00 **O13 IBA and ICP-OES determination of trace elements in indigenous medicinal herbs and their extracts on the infertility in the human male reproductive system**

J.A. Mars, F. Weitz, D. Fisher, R. Henkel

10:20 Coffee Break

10:50 – 12:30 Session VI

Chair: P. Pelicon

10:50 **O14 Elemental imaging of organic matter and metal associations in ore deposits using micro-PIXE and micro-EBS**

S. Fuchs and W.J. Przybylowicz

11:10 **O15 Development of microscopic optics for high-resolution IL spectroscopy with proton microbeam probe**

W. Kada, T. Satoh, A. Yokoyama, M. Koka, and T. Kamiya

11:30 **O16 The new in-air micro-PIXE setup in Atomki, Debrecen**

Zs. Török, Zs. Kertész, R. Huszánk, I. Rajta, Z. Szikszai, L. Csedreki, A. Angyal, E. Furu, Z. Szoboszlai, Á. Z. Kiss, I. Uzonyi, and L. Palcsu

11:50 **O17 Stereoscopic PIXE imaging applied to space debris impact craters from the Hubble Space Telescope**

G.W. Grime, A.T.Kearsley, V. Palitsin, C. Jeynes, J. Colaux, and R.P. Webb

12:10 **O18 Study of a nearly pristine pyroxenite sample using low and high energy PIXE methods**

P.C. Chaves, A. Taborda, D.P.S. de Oliveira ,M.A. Reis

12:30 Lunch

13:30 **IAC - IHC Meeting**

Poster setup

14:50 - 16:00 **Poster Session A**

16:00 Coffee Break

16:30 – 18:30 Session VII

Chair: W.J. Przybylowicz

16:30 **I7 Micro-PIXE for the quantitative imaging of chemical elements in single cells**

R. Ortega

17:10 **O19 Iron quantification and distribution in 6-OHDA animal and cellular models of Parkinson's disease using micro-PIXE**

A. Carmona, L. Perrin-Verdugier, C. Carcenac, S. Roudeau, S. Bohic, D. Carrez, T.D. Wu, S. Marco, J.L. Guerquin-Kern, M. Savasta and R. Ortega

17:30 **O20 Elemental analysis of a murine solid tumor treated with a vascular disrupting agent AVE8062**

A. Terakawa, K. Ishii, S. Matsuyama, Y. Kikuchi, Y. Ito, K. Kusano, H. Sugai, M. Karahashi, Y. Nozawa, S. Yamauchi, H. Yamazaki, Y. Funaki, S. Furumoto, N. Ito, S. Wada, and K. Sera

17:50 **O21 Role of copper, zinc, and selenium in uterine cervical cancer**

P. Sarita, G. J. Naga Raju, S. Bhuloka Reddy

18:10 **O22 Microcapsular imaging of malignant tumors and radiation-induced release of liquid-core microcapsules for their treatment**

S. Harada, K. Ishii, T. Sato, K. Sera, S. Ehara, M. Enatsu, T. Kamiya, S. Goto

WEDNESDAY MARCH 6, 2013

8:00 – 17:00 **OUTING**

18:30 **IAC Meeting**

Poster Set up

THURSDAY MARCH 7, 2013

9:00 – 10:20 Session VIII

Chair: W. Maenhaut

9:00 **I8 Currents Trends in the Application of IBA Techniques to Air Pollution Source Fingerprinting and Source Apportionment**

David Cohen, Ed Stelcer, Armand Atanacio, Jagoda Crawford

9:40 **O23 The upgraded external-beam PIXE/PIGE set-up at LABEC for very fast measurements on aerosol samples**

F. Lucarelli, G. Calzolari, M. Chiari, D. Mochi and S. Nava

10:00 **O24 Complex study of indoor aerosols at a kindergarten, an elementary school and a secondary grammar school**

Z. Szoboszlai, E. Furu, A. Angyal, Zs. Török and Zs. Kertész

10:20 Coffee Break

10:50 – 12:30 Session IX

Chair: D. Cohen

10:50 **I9 A brief overview of the first twenty years (1970-1989) of aerosol analysis by PIXE and ten-year study (1995-2004) of fine aerosol at Sde Boker, Israel, using PIXE**

W. Maenhaut, with for the study at Sde Boker also A. Karnieli and M. O. Andreae

11:30 **O25 Characterization and source estimation of size-segregated aerosols during 2008-2012 in an urban environment in Beijing**

Lingda Yu, Guangfu Wang, Renjiang Zhang

11:50 **I10 Nuclear Spectrometry for Environmental Analysis and Mapping**

Aliz Simon

12:30 Lunch

14:00 – 14:50 Session X

Chair: B. Jones

14:00 **I11 Twenty five years of OMDAQ**

G.W. Grime

14:50 - 16:00 Poster session B

16:00 Coffee

16:30 – 18:30 Session XI

Chair - Szőkefalvi-Nagy

16:30 **I12 PIXE in cultural heritage studies: present role and new challenges**
T. Calligaro and J.-C. Dran

17:10 **O26 Metallic objects belonging to the first emperor of Brazil studied with PIXE technique**
V.C. Ambiel, M.A. Rizzutto, J. F. Curado, P.H.O.V. Campos, E.A.M. Kajiya and T.F.Silva

17:30 **O27 OLDAPS – Obsidian Least Destructive Analysis Provenancing System**
F.M. Eder, C. Neelmeijer, N.J.G. Pearce, J.H. Sterba, M. Bichler, S. Merchel

17:50 **O28 Analysis of archaeological precious stones from Slovenia**
Ž. Šmit, H. Fajfar, M. Jeršek, T. Knific, A. Kržič, and J. Lux

18:10 **O29 Renaissance enamels - colouring and state of preservation: Non-destructive studies by external PIXE–PIGE–RBS**
C. Neelmeijer, L. Hasselmeyer, and J. Eulitz

19:50 Banquet

FRIDAY MARCH 8, 2013

9:00 – 10:20 Session XII

Chair: K. Ishii

9:00 **I13 Influence of Heavy Elements in the Sludge Conveyed by the 2011 Tsunami upon Human Health and Recovery of the Marine Ecosystem**
K. Sera, S. Goto, C. Takahashi, Y. Saitoh, and K. Yamauchi

9:40 **O30 PIXE analysis of Cs in soil and rice plants**
H. Sugai, K. Ishii, S. Matsuyama, A. Terakawa, Y. Kikuchi, H. Takahashi, A. Ishizaki, F. Fujishiro, H. Arai, N. Osada, M. Karahashi, Y. Nozawa, S. Yamauchi, K. Kikuchi, S. Koshio, and K. Watanabe

10:00 **O31 Low energy PIXE analysis of Nigerian Flour and Bread samples**
F.S. Olise, A. Fernandes, P.C. Chaves, A. Taborda, M.A. Reis

10:20 Coffee

10:50 – 12:10 Session XIII

Chair: J. F. Dias

10:50 I14 PIXE and Ion Beam Analysis in Forensics

Melanie Bailey, John Warmenhoven, Matt Christopher, Karen Kirkby, Vladimir Palitsin, Geoff Grime, Chris Jeynes, Brian Jones and Roger Webb

11:30 O32 Characterization of elemental ammunition manufactured in Brazil

Anaí Duarte, Luiza Manfredi, Carla Eliete Iochims dos Santos, Livio Amaral, Johnny Ferraz Dias

11:50 O33 Development of particle induced x-ray emission facility at cyclotron laboratory and its prospective applications

Dr. N.K. Puri, M.L. Garg, I.M. Govil

12:10 CLOSING

12:30 Lunch

14:00 Bus Departure to Porto Alegre

PI E 2013

FOR TECHNOLOGY AND GLOBAL DEVELOPMENT

POSTER SESSIONS

Tuesday

PA01 - PA35

Thursday

Pb01 - PB40

- PA01 Investigations of metal correlation in bile, gallstones and blood of Urolithiasis patients by PIXE using a peltier cooled X-ray detector**
Daisy Joseph, Narayana Kalkur, Aslin Shameena, Arul Thanigai
- PA02 PIXE and XRF analysis of atmospheric aerosols from a site in the West area of Mexico City**
R.V Díaz, J. López-Monroy, J. Miranda, A.A. Espinos
- PA03 Challenges in understanding inner shell ionization by heavy ion impact**
N.K. Puri
- PA04 Thin and thick target PIXE analysis of the study of Cu²⁺ biosorption mechanism by the *Egeria densa***
F.R. Espinoza-Quiñones, A.N. Módenes, M.A. Rizzutto, G.H.F. Santos and C.E. Borba
- PA05 EXAFS Measurements of Nickel/Nickel Oxide Nanoparticles and its comparison with TEM and XRD results**
Arvind Agarwal, Manish Kumar Singh & Mohan Chandra Mathpal
- PA06 Comparison of mobile XRF and PIXE for geological core analysis**
D. Strivay, F.P. Hocquet, A. Beckers and A. Hubert-Ferrari
- PA07 PIXE Analysis of Cancer-Afflicted Human Bladder**
G.J.Naga Raju, P.Sarita M.Ravi Kumar, S.Bhuloka Reddy
- PA08 External-beam PIXE analysis of aerosol samples at GIC4117 tandem accelerator laboratory of Beijing Normal University**
WANG Guangfu, YU Lingda, ZHANG Renjiang, LI Xufang, WU Bingbing, AN Kun, CHU Junhan
- PA09 Specific absorbed fraction of X-ray in tissues from human organs**
H.C.Manjunatha
- PA10 Development of microscopic optics for high-resolution IL spectroscopy with proton microbeam probe**
W. Kada, T. Satoh, A. Yokoyama, M. Koka, and T. Kamiya

- PA11 Studies on Pt-Mo Intermetallics by PIXE and other Analytical Techniques with High Resolution**
M. Topic, Z. Khumalo, C.A. Pineda-Vargas
- PA12 Elemental Characterization of Ammunition and Respective GSR from Clean Range Line (CBC®)**
Luiza R. Manfredi da Silva[†], Anaí Duarte, Carla E. Iochims dos Santos, Lívio Amaral, Maria Lúcia Yoneama[†], J. F. Dias, A. A. Petersen Xavier
- PA13 Determination of elemental atmospheric concentrations by PIXE in highly loaded samples from Cape Verde**
M. Almeida-Silva, S.M. Almeida, C.A. Pio, T.Nunes, J. Cardoso, P.C. Chaves, A. Taborda, M.A. Reis
- PA14 Comparison of EDS and WDS high resolution PIXE spectra and *ab initio* atomic calculations**
A. Taborda, P.C. Chaves, M.L. Carvalho, J.P Marques, M. Kavčič, M.A. Reis
- PA15 Distribution and quantification of trace elements in natural diamonds of Juina, Brazil, using the PIXE and RBS techniques**
Rosa, L.F.S.; Plá Cid, C.C.; Jones, N.B.; Plá Cid, J.; Nardi, L.V.; Gisbert, P.E.; Homem, M.G.P.; Farenzena, L.S.; Webb, R.
- PA16 Investigation of the stopping powers of H⁺ and H₂⁺ in silicon in E<90 keV energy region by measuring the hydrogen depth profile with NRA**
T.S. Wang, J.T. Zhao, X.X. Xu, S. Zhang, K.H. Fang, X.C. Guan
- PA17 Mapping of medium and high Z elements in an agate sample using a CdTe based high energy PIXE setup**
P.C. Chaves, A. Taborda, M.A. Reis
- PA19 X-ray production cross-sections measurements for high-energy alpha particle beam for Si, Fe and Cu**
T. Dupuis, G. Chêne, A. Marchal, F. Mathis and D. Strivay
- PA20 N to K Uranium PIXE spectra obtained at the High Resolution High Energy PIXE setup**
P.C. Chaves, A. Taborda, J.P Marques, M.A. Reis

- PA21 PIXE study of aerosol samples from an iron and steel smelting company at Ile-Ife, Nigeria**
F.S. Olise, O.K. Owoade, S.M. Almeida, A. Fernandes, P.C. Chaves, A. Taborda, M.A. Reis, L.T. Ogundele, O.G. Fawole, H.B. Olaniyi
- PA22 On the evolution of silver tarnishing**
V. Corregidor, J. Cruz, P.C. Chaves, M.A. Reis, L.C. Alves
- PA23 Elemental concentrations analysis of tomato paste**
R. Debastiani, M. M. Ramos, C. E. I. dos Santos, V. S. Souza, M. L. Yoneama, L. Amaral and J. F. Dias
- PA24 Fixed and free line ratio DT2 PIXE fitting and simulation package**
M.A. Reis, P.C. Chaves, A. Taborda, J.P Marques, N.P Barradas
- PA25 Ion beam analysis of Brazilian coffee**
R. Debastiani, C. E. I dos Santos, M. M. Ramos, V. S. Souza, M. L. Yoneama, L. Amaral, J. F. Dias
- PA26 Strontium content in otoliths of common fish species in the northern Baltic Sea**
J-O. Lill, M. Himberg, L. Harju, A. Lindroos, K. Gunnelius, J-H. Smått, S-J. Heselius and H. Hägerstand
- PA27 Chemical speciation of chlorine in atmospheric aerosol samples by high resolution PIXE**
Zs. Kertész, E. Furu, and M. Kavčič
- PA28 The new in-air micro-PIXE setup in Atomki, Debrecen**
Zs. Török, Zs. Kertész, R. Huszánk, I. Rajta, Z. Szikszai, L. Csedreki, A. Angyal, E. Furu, Z. Szoboszlai, Á. Z. Kiss, I. Uzonyi, and L. Palcsu
- PA29 Variation of atmospheric aerosol components and sources during smog episodes in Debrecen, Hungary**
A.Angyal, Zs. Kertész, Z. Ferenczi, E. Furu, Z. Szoboszlai, Zs. Török, and Z. Szikszai
- PA30 PIXE analyses over a long period : a case of Neolithic variscite jewels from Western Europe (5th-3th millennium BC).**
G. Querré, Th. Calligaro, S. Domínguez-Bella and S. Cassen

- PA31 Characterization of the lapis lazuli from the Egyptian treasure of Tôd and its alteration using external μ -PIXE and μ -IBIL**
T. Calligaro, Y. Coquinot, L. Pichon, G. Pierrat-Bonnefois, P. de Campos, A. Re, D. Angelici
- PA32 PIXE-PIGE analysis of size-segregated aerosol samples from remote areas**
G. Calzolari, M. Chiari, F. Lucarelli, S. Nava, S. Becagli, C. Ghedini, F. Rugi, D. Frosini, R. Traversi and R. Udisti
- PA33 PIXE and ICP-AES comparison in evaluating the efficiency of metal extraction and analysis in aerosol samples.**
F. Rugi, S. Becagli, G. Calzolari, M. Chiari, C. Ghedini, F. Lucarelli, M. Marconi, S. Nava, M. Severi, R. Traversi and R. Udisti
- PA34 External beam milli-PIXE as analytical tool for Neolithic obsidian provenance studies**
A. Constantinescu, D. Cristea-Stan, I. Kovács and Z. Szőkefalvi-Nagy
- PA35 Improvement of the Tohoku microbeam system for nanoscopic analysis**
S. Matsuyama, K. Ishii, A. Terakawa, Y. Kikuchi, M. Fujiwara, H. Sugai, M. Karahashi, Y. Nozawa, S. Yamauchi, K. Watanabe, M. Fujisawa, M. Ishiya and T. Nagaya
- PB01 Nitrogen ionization cross section by electron impact**
A. P. L. Bertol, P. Pérez, J. Trincavelli, G. Castellano, R. Hinrichs, M.A.Z. Vasconcellos
- PB02 Iron L-shell chemical effects in iron nitride films**
A.P.L. Bertol, S.D. Jacobsen, P. Pérez, J. Trincavelli, G. Castellano, R. Hinrichs, M.A.Z. Vasconcellos
- PB03 L-shell ionization cross sections induced by protons and alpha-particles in the 0.7-2.0 MeV/amu range for Fe, Ni, Ru, and Ag**
A.P.L. Bertol, T.P. Rodríguez, A.H. Sepúlveda, J. Trincavelli, G. Castellano, R. Hinrichs, M.A.Z. Vasconcellos
- PB04 IBA analysis of TiO₂-doped nanocomposites to be used in orthodontic occlusal restoration.**
M. Abdelaziz, J. Mars, A. Atbayga, D. Gihwala
- PB05 Applications of IBA to quantify the effect of Zr on Ti-alloy wires to be used as orthodontic material**
K. Ali, J. Mars, A. Atbayga, D. Gihwala

- PB06 Comparison of IBA and ICP-OES analyses of trace elements in the serum specimens of rats fed with extracts of anti-oxidant tea to ascertain trace element absorption**
C. Kunsevi-Kilola, J.A. Mars, D. Gihwala
- PB07 Correlation of element concentrations, determined by IBA, with clinical parameters of HIV-Aids serum specimens**
M.L. Maqutu, J.A. Mars, C. Kunsevi-Kilola, M. Saayman, S. Tarr, A. Mohammed
- PB08 Application of IBA to determine the effects of Kolaviron (*Garcinia kola*) on the elemental metabolism in the rat liver and kidney**
J.A. Mars, C. Kunsevi-Kilola, D. Gihwala
- PB09 Ion-beam analysis of plasma of HIV-Aids positive individual patients and comparison to CD4 counts**
J.A. Mars, M.L. Maqutu, C. Kunsevi-Kilola, S. Tarr, A. Mohammed
- PB10 Application of IBA in environmental remediation using skins of cocoa (*Theobroma cacao*) and sweet potatoe (*Ipomoea batatas*)**
K. Sumbu, J.A.Mars, D. Gihwala
- PB11 MicroPIXE and microNRA: associated tools for materials characterization**
L.A.Bouffleur, J.F. Dias, and L. Amaral
- PB12 Application of IBA in the comparative analyses of fish scales used as biomonitors in the Matola River, Mozambique**
J.F. Guambe, J.A. Mars, J. Day
- PB13 Bremsstrahlung in low atomic number thick targets by proton incidence**
P. Pérez, T. Rodríguez, A. Bertol, M. A. Z. Vasconcellos and J. Trincavelli
- PB14 L-shell x-ray production cross section for Fe, Ni, Ru and Ag by electron incidence**
A.Sepúlveda, A. Bertol, M. A. Z. Vasconcellos, R. Hinrichs and J. Trincavelli
- PB15 Structure of the x-ray emission L spectra for Fe, Ni, Ru, Ag and Te by electron incidence**
T. Rodríguez, A. Sepúlveda, A. Bertol, G. Castellano, A. Carreras, M. A. Z. Vasconcellos and J. Trincavelli

- PB16 Self-consistent simulation of an electron beam for a new autoresonant x-ray generator**
Ana M. Herrera, Eduardo A. Orozco, and Valeriy D. Dugar-Zhabon
- PB17 Study of injuries to fish liver with PIXE and micro-PIXE**
E. M. Stori, M. L. C. F. Rocha, J. F. Dias, C. T. de Souza, L. Amaral, Johnny F. Dias
- PB18 PIXE facility at Centro Atómico Bariloche**
S. Limandri, C. Olivares, L. Rodriguez, G. Bernardi and S. Suárez
- PB19 Characterization of Ancient Metal Using Non-destructive Methods**
Hellen Santos, Nemitala Added
- PB20 Analysis of early 20th century pigments in R. Heintz's paintings using PIXE and mobile analytical systems**
C. Defeyt, H. Calvo del Castillo, A. Deneckere, F.-P. Hocquet, P. Vandenabeele and D. Strivay
- PB21 Development of a low-beam-energy PIXE analysis system based on an ion implanter**
W. Kada, A. Kishi, M. Sueyasu, F. Sato, Y. Kato, and T. Iida
- PB22 Trace Element Analysis of Fly ash Using Proton Induced X-rays Emission (PIXE)**
B K Sharma, B. P. Singh, R. Prasad
- PB23 PIXE analysis of some anti-diabetic medicinal plants in Nigeria**
S.O. Olabanji, O.R. Omobuwajo, D. Ceccato, A.C. Adebajo, M.C. Buoso, and G. Moschini
- PB24 High energy Ion beam analysis at ARRONAX**
C. Koumeir, A. Guertin, F. Haddad, V. Metivier, N. Michel, D. Ragr and N. Servagent
- PB25 Analysis of trace elements in polymers by PIXE**
C. T. Souza, L. A. Boufleur, C.E.I. dos Santos, E. M. Stori, D. V. Bauer, R. M. Papaléo, L. Amaral, J. F. Dias
- PB26 PIXE analysis of pre-colonial pottery from Sambaqui do Panaquatira**
R. A. Ikeoka, C. R. Appoloni, M. A. Rizzutto, T.F.Silva and A. M. Bandeira

- PB27 Trace Elements Level in Serum of Melanoma Patients by PIXE and HR-ICPMS**
Suene Bernardes, Manfredo Harri Tabacniks, Jorge Eduardo de Souza Sarkis, Ernesto, Talita Oliveira, Ivan Abranches Oliveira Santos, Francisco de Assis Ribas Bosco, Andrea Fernandes de Oliveira, Janaina Namba Shie
- PB28 Metallic Objects Belonging to the First Emperor of Brazil studied with PIXE Technique**
V.C. Ambiel, M.A. Rizzutto, J. F. Curado, P.H.O.V. Campos, E.A.M. Kajiya and T.F.Silva
- PB29 Optimization of PIXE Quantitative System to Assist the Traceability of Pearl and other Gemstones**
S. Murao, K. Sera, S. Goto, C. Takahashi, L. Cartier, and K. Nakashima
- PB30 Metabolomics approach regarding the effects of the treatment of undernourished rats with Shiitake mushroom (*Lentinula edodes*)**
Patrícia Molz, Joel Henrique Ellwanger, Carla Eliete Iochims dos Santos, Deivis de Campos, Marisa Terezinha Lopes Putzke, Daniel Prá, Valeriano Antonio Corbeline, Silvia Isabel Rech Franke
- PB31 External beam PIXE and ionoluminescence micro-imaging of Mesoamerican jade**
T. Calligaro, C. Andrieu, Y. Coquinot, C. Delobelle, J. Gazzola, F. Gendron, V. Gonzalez, O. Jaime-Riveron, B. Moignard, Q. Lemasson, C. Pacheco, L. Pichon, S. Ramos
- PB32 Elemental concentrations in hepatic and renal tissues of *Mugil curema* Valenciennes, 1836 in two coastal systems in southeastern Brazil**
W.S. Fernandez, J.F. Dias, L.A. Boufleur, C.E.I. dos Santos, M.L. Yoneama, J.F. Dias
- PB33 Elemental detection in muscle of flatfish *Achirus lineatus* and *Trinectes paulistanus* (Actinopterygii, Pleuronectiformes) from Santos Bay, Southeastern Brazilian coast**
Maria Luiza Chiste Flaquer da Rocha, Johnny Ferraz Dias and June Ferraz Dias
- PB34 PIXE applications to the toxicological field**
C.E.I. dos Santos, J.F. Dias, P. F. C. Jobim, L. Amaral, M. L. Yoneama, V.M. Andrade and J. da Silva
- PB35 Structural changes in quantum dots core-shell CdSe/ZnS by thermal treatment and proton irradiation**
L. G. Almeida, M. A. Sortica, P. L. Grande, C. Radtke, R. Debastiani, J. F. Dias, A. Hentz

- PB36 Swift-heavy ion-sputtered CaF₂ nanoparticles characterized by medium energy ion scattering**
M. Hatori, M. A. Sortica, J. F. Dias, P. L. Grande, W. Assmann, A. Weizmüller, M. Toulemonde, C. Trautmann
- PB37 Evaluation of radioactive transfer of soils contaminated with radioactive cesium by micro-PIXE analysis**
F. Fujishiro, K. Ishii, S. Matsuyama, H. Arai, A. Ishizaki, N. Osada, H. Sugai, K. Kusano, Y. Nozawa, S. Yamauchi, M. Karahashi, S. Oshikawa, K. Kikuchi, S. Koshio, K. Watanabe and Y. Suzuki
- PB38 Improvement of the stability of X-ray emission by the thermal excitation of pyroelectric crystals**
F. Naruse, H. Honda, Y. Nakanishi, S. Fukao, Y. Ito, Y. Sato, and S. Yoshikado
- PB39 An evaluation of the radiocesium retention ability by root-mat horizon using micro PIXE analysis**
H. Arai, K. Ishii, S. Matsuyama, K. Kusano, Y. Nozawa, S. Yamauchi, M. Karahashi, S. Oshikawa, K. Kikuchi, S. Koshio, K. Watanabe, Y. Suzuki, F. Fujishiro, A. Ishizaki, H. Sugai, A. Terakawa, Y. Kikuchi, and N. Osada
- PB40 Concentration of Cs in plants and Water for the radioactive pollution due to Fukushima first nuclear power plant disaster**
A. Ishizaki, K. Ishii, S. Matsuyama, S. Koshio, S. Yamauchi, K. Kusano, Y. Nozawa, M. Karahashi, S. Oshikawa, K. Kikuchi, K. Watanabe, S. Itoh, K. Kasahara, S. Toyama, Y. Suzuki, F. Fujishiro, N. Osada, H. Arai, A. Terakawa, Y. Kikuchi and H. Takahashi

PIXE 2013

FOR TECHNOLOGY AND GLOBAL DEVELOPMENT

ORAL SESSIONS

PIE 2013

FOR TECHNOLOGY AND GLOBAL DEVELOPMENT

ABSTRACTS

Invited talks

I1-I14

I1 Werner Brandt legacy to PIXE: past, present, and future perspectives

G. Lapicki

Department of Physics, East Carolina University, Greenville, NC 27858, USA

Universal Cross Sections for K-Shell Ionization by Heavy Charged Particles, one of the most important papers for the PIXE community, was published forty years ago [1]. This paper that originated with an introduction of the binding and Coulomb-deflection effects [2] and the papers that followed laid the foundations of the so-called ECPSSR theory [3].



Werner Brandt (1925-1983). Photo circa 1970's [from New York University archives].

While it would be impossible to review all seminal and multi-faceted contributions of Werner Brandt to physics, this talk will focus on the development of a theory for inner-shell ionization at the NYU Radiation and Solid State Laboratory in the past from my perspective as one of his last students and post-docs. The present state of this theory, since his untimely passing three decades ago, will also be addressed with some thoughts about its future.

[1] G. Basbas, R. Laubert, W. Brandt, Phys. Rev. A 7 (1973) 983-1001.

[2] W. Brandt, R. Laubert, I. Sellin, Phys. Rev. 151 (1966) 51-59

[3] W. Brandt, G. Lapicki, Phys. Rev. A 23 (1981) 1717-1729.

I2 EDS high resolution PIXE and spectra fine structure

M.A. Reis^(a,b), P.C. Chaves^(a,b), A. Taborda^(a,b), M.L. Carvalho^(b,c), J.P Marques^(b,c)

(a) IST/ITN, Instituto Superior Técnico, Universidade Técnica de Lisboa, Campus Tecnológico e Nuclear, EN10, 2686-953 Sacavém, Portugal

(b) Centro de Física Atómica da Universidade de Lisboa, Av. Prof. Gama Pinto 2, 1649-003 Lisboa, Portugal

(c) Dept. Física da Fac. Ciências da Universidade de Lisboa, Campo Grande, Edifício C8, 1749-016 Lisboa, Portugal

On January 1913, James Chadwick published the first firm observations of the emission of gamma rays induced by alpha rays, a 4% enhancement in the radiation produced by a gold shielding when compared to an aluminum shielding of an ionization chamber containing an alpha emitter. One hundred years past, we face again important even if small-sized new results on particle induced X-ray emission work. X-ray microcalorimeters spectrometers (XMS), which first generation systems emerged as commercially available in the last decade (even if there are still very few companies able to provide them), can be easily compared in breakthrough capacity to late 1960s semiconductor detectors. The main issue now being no longer a simple improvement on detection limits but instead the whole new scope of possibilities and challenges that emerge from the possibility to easily measure and resolve N, M and L lines, minor transitions and secondary effects such as multiple ionization or radiative Auger satellites, many of which carry structural and/or chemical information. Once again we face few percent effects with much added value information, not only but also because the information is now carried by radiation able to overcome significantly thick layers of matter without distortion. Furthermore, these developments have also helped in understanding the physics behind effects that defy established assumptions in X-ray spectrometry and in particular in low energy PIXE spectrometry. In this talk we will present a review of experimental evidence and achievements reached in the last decade. Some of these were pointed out in previous meetings, others are discussed in more detail at this meeting, in any case we expect to be able to expose an overview of solved and unsolved issues and make a point of what we think is the present day status of PIXE, its close future challenges and bright future perspectives if these challenges can be overcome.

13 Facility & Micro-PIXE on biological tissues

P. Pelicon^(a), P. Vavpetič^(a), N. Grlj^(a), N. Ogrinc^(a,c), L. Jeromel^(a), M. Kelemen^(a), G. Kukec Mezek^(a), P. Pongrac^(b), K. Vogel-Mikuš^(b), M. Regvar^(b)

^(a) Jožef Stefan Institute, Jamova 39, SI-1000, Ljubljana, Slovenia

^(b) Biotechnical Faculty, University of Ljubljana, Večna Pot 111, SI-1000 Ljubljana, Slovenia

^(c) LOTRIČ Metrology I.t.d., Selca 163, SI-4227 Selca, Slovenia.

By the improvements of the accelerators, ion lenses and detectors, micro-PIXE became a technique of choice for tissue elemental mapping in the cases, where high elemental sensitivity and a high lateral resolution need to be combined with a quantitative nature of the elemental analysis. As an instrumentally demanding technique, micro-PIXE is currently available to complement biomedical research together with several related techniques, such as micro-X-ray fluorescence (micro-XRF) spectroscopy at synchrotron radiation facilities and table-top method of laser ablation with inductively coupled plasma mass spectrometry (LA-ICP-MS).

Preparation of biological tissues for micro-PIXE analysis is a dedicated process, which dominantly determines the quality of the results. Shock-freezing, slicing and freeze-drying of the tissues are most frequently used in the research of processes in complex organisms. Recent results on research in a plant biology [1,2], nanotoxicology [3] and ecology at JSI will be presented.

A need for preserving intact sub-cellular morphology motivated the efforts to keep the tissue in a frozen hydrated state during the analysis. First micro-PIXE measurements on frozen hydrated tissues were reported in 2007 by iThemba group [4]. Several micro-XRF facilities at synchrotrons started to offer such sample handling for external users. We report on instrumental and methodological progress at JSI aimed to provide micro-PIXE analysis on frozen hydrated tissue for users from biomedical area.

We will elaborate on further developments of the instrumentation for micro-PIXE at JSI. In 2012, a multicusp ion source was installed at JSI, with H⁻ beam brightness of order of magnitude higher than previously used beams from duoplasmatron ion source. This is expected to introduce an availability of a sub-micrometer beam sizes for routine micro-PIXE work. The confocal PIXE [5] and stereo-PIXE [6] approaches to introduce depth dimension in micro-PIXE will be presented, as well as our involvement in the development of digital acquisition system for micro-PIXE.

[1] P. Pongrac, K. Vogel-Mikuš, M. Regvar, P. Vavpetič, P. Pelicon, I. Kreft, J. *Agricult. and Food Chem.* 59 (2011) 1275.

[2] L. Lyubenova, P. Pongrac, K. Vogel-Mikuš, G. Kukec Mezek., P. Vavpetič, N. Grlj, P. Kump, M. Nečemer, M. Regvar, P. Pelicon, P. Schroeder, *Metalomics* 4 (2012), 333.

[3] S. Novak, D. Drobne, J. Valant, Ž. Pipan-Tkalec P. Pelicon, P. Vavpetič, N. Grlj, I. Falnoga, D. Mazej and M. Remškar, *Env. Toxicol. And Chem.* 31, (2012), 1083.

[4] G. Tylko, J. Mesjasz-Przybylowicz, W.J. Przybylowicz, *Nucl. Instr. Meth. B* 260 (2007) 141.

[5] N. Grlj, P. Pelicon, M. Žitnik, P. Vavpetič, D. Sokaras, A-G. Karydas, B. Kanngießner, *Nucl. Instr. Meth. B* 269 (2011), 2237.

[6] E. Gholami Hatam, P. Pelicon, M. Lamehi-Rachti, P. Vavpetič, O. R. Kakuee, N. Grlj, M. Čekada, V. Fathollahi, *J. Anal. At. Spectrom.* 27 (2012) 834.

14 External Heavy Ion PIXE and MeV-SIMS at the Surrey Ion Beam Centre

B. N. Jones^(a), L. Antwis^(a), V. Palitsin^(a), G. Grime^(a), and R. Webb^(a)

^(a) Ion Beam Centre, University of Surrey, Guildford, Surrey, GU2 7XH, UK

In recent years, several ion beam analysis (IBA) facilities have modified their beam lines to use swift, heavy primary ion beams for time-of-flight secondary ion mass spectrometry (MeV-SIMS) [1]. MeV-SIMS uses electronic sputtering to perform imaging mass spectrometry simultaneously with other IBA techniques, such as heavy ion PIXE. Recent results show that SIMS of wet samples (Wet-SIMS [2]) is possible using 6 MeV copper primary ion beams extracted out of the vacuum system into a tenth of atmospheric pressure (i.e. above the vapor pressure of water).

As will be shown in this work, a newly built fully ambient pressure MeV-SIMS beam line at the Surrey Ion Beam Centre exploits the complementary aspects of heavy ion PIXE and MeV-SIMS. Four silicon drift detectors placed *in vacuo* behind a thin silicon nitride exit window measure X-rays induced by a 10 MeV chlorine beam, focused to a micron lateral resolution with an Oxford Microbeams Ltd. magnetic quadrupole triplet lens. This design allows the sample to be placed within a few millimeters of the exit window such that a curtain of He gas can stream across the sample's surface and transport molecular ions desorbed by electronic sputtering into the inlet of a differentially pumped mass spectrometer. The mass spectrometer, an orthogonal time-of-flight device, can operate with a continuous primary ion beam. This allows for simultaneous heavy ion PIXE and MeV-SIMS measurements to be performed with the sample kept in fully ambient pressure with short acquisition times.

We present preliminary data that shows the potential for this new combination of techniques in an effort to inspire the PIXE community to measure heavy ion cross sections so that heavy ion PIXE might be employed more reliably in the future.

[1] B. N. Jones, V. Palitsin, R. Webb, Nucl. Instrum. Methods Phys. Res., Sect. B: 19th International Conference on Ion Beam Analysis 268 (2010) 1714-1717.

[2] J. Matsuo, S. Ninomiya, H. Yamada, K. Ichiki, Y. Wakamatsu, M. Hada, T. Seki, T. Aoki, Surf. & Interface Anal., 42 (2010) 1612-1615.

15 Recovery from the radioactive pollution due to Fukushima First Nuclear Power Plant Accident

K.Ishii, A.Terakawa, S.Matsuyama, Y.Kikuchi, F.Fujishiro, A. Ishizaki, N.Osada, H.Arai, K.Sugai, K.Nagakubo and T.Sakurada

Department of Quantum Science and Energy Engineering,
Tohoku University, Sendai 980-8579, Japan

The great East Japan earthquake happened at 14:46 11th March 2011. After the earth quake, the huge tsunamis of above 16m height hit the east coast of Northeastern Japan. About 20,000 peoples died or went missing and many houses were lost. The tsunamis caused the nuclear accident of Fukushima first nuclear power plant. Three nuclear reactors hydrogen-exploded 12th, 14th and 15th March, one after another, and scattered the huge amount of radioisotopes of ^{131}I and $^{134,137}\text{Cs}$ on the prefectures in the eastern region of Japan. Especially, Fukushima prefecture where the nuclear plant is located was contaminated very much. This radiation catastrophe worried us about the internal exposure by taking contaminated foods and the external exposure by surrounding radioactivity. The radiation exposure was mainly caused by ^{131}I in the earlier stage of the accident and then by $^{134,137}\text{Cs}$. Now, the radiation doses on the asphalt or concrete places and some areas are gradually decreasing and become around a half value of the earlier one. This is well known as the weathering effect.

We found that the density of cesium radioisotopes decreases with a function of depth from the ground surface, and almost of all cesium radioisotopes were distributed in the thickness of 1cm. We washed the contaminated soil 3 times. The radioactivity of soil reduced one twenty fifth of original one. Almost all cesium radioisotopes were contained in remains liquid. Depositing muddy water, we separated clay from water. It was confirmed that the water was no radioactive. This resulted that cesium radioisotopes were not ionic in soil and water, and adhered mainly to clay on the ground. Therefore, cesium radioisotopes have not been detected in river water and city water from the early stages of the accident. The volume of clay was about one tenth of the contaminated soil. We applied this idea to decontaminate the school yards (about 7000m²) of elementary schools of Marumori town adjacent to Fukushima.

To secure the safe of foods, we have measured radioisotopes in foods produced in Miyagi prefecture and Fukushima city since March 2011. At the present, the cesium radioactivity of foods is almost less than several Bq/kg. However, the radioactivity exceeding 100 Bq/kg is very rarely detected in some foods. We applied PIXE to research the agriculture of plants without radioactive cesium but cultivated in the contaminated soil. The activity of the contaminated soil in Fukushima is very high but the quantity of radioisotopes is extremely few in comparison to other Alkali elements. It is expected that the chemical and biological processes of cesium radioisotopes in the soil is different from the case of high quantity of cesium. We cultivated plants in the soil contaminated with trace amount of natural cesium. The elemental imaging techniques of sub-millimeter-PIXE and micro-PIXE were very useful to investigate the distribution of cesium in the plant. We introduce one of our results, there were no cesium in the interior of rice grains, namely, polished rice do not contain cesium radioisotopes. Thus, the safety of rice produced in radioactive stricken areas was confirmed.

Many trials for recovery from the radioactive disaster now are in progress, and the situation improves every year.

I6 Micro-PIXE in plant sciences

J. Mesjasz-Przybylowicz^(a) and W. J. Przybylowicz^(a,b)

^(a) Materials Research Department, iThemba LABS, National Research Foundation, P.O. Box 722, Somerset West 7129, South Africa

^(b) on leave from AGH University of Science & Technology, the Faculty of Physics and Applied Computer Science, Kraków, Poland

Studies of the role played by elements in fundamental processes in physiology, nutrition, elemental deficiency and toxicity as well as environmental pollution require accurate, quantitative methods with good spatial resolution. The problem of proper measurements of elemental balances and elemental transfers between various levels of biological organisation (from abiotic to biotic systems; along the food chains; within organs and cells) becomes essential for understanding the mechanisms influencing the selection, interaction, distribution and transport of elements. Highly sensitive techniques for bulk elemental analysis are mostly used in these investigations. These techniques usually offer adequate sensitivity, but without spatial resolution. On the other hand, advanced studies of elemental distribution at a cellular level are mostly conducted using techniques with high spatial resolution, but low sensitivity. Ideally, these studies should be conducted on organs and tissues of sizes as far down as the cellular and sub-cellular level. This applies to e.g. future directions in ionomics and metallomics and opens up new, exciting possibilities of studies of trace metal role. The micro-PIXE has been applied in plant sciences for more than thirty years and has reached a high level of maturity. This is one of the few microanalytical, multielemental techniques capable of quantitative studies of elemental distribution at ppm level with with ability to perform quantitative elemental mapping and easy quantification of data extracted from selected micro-areas. Preparation of biological specimens is undoubtedly the crucial and most difficult part of analysis, and only cryotechniques are recommended presently for all types of microanalytical studies. Established sample preparation protocols will be presented. Most of results are obtained for cryofixed and freeze-dried material but analysis of samples in frozen-hydrated state brings important advantage. Recent applications in plant sciences will be presented to illustrate multidisciplinary research where close collaboration between biologists and physicists is a key to success.

17 Micro-PIXE for the quantitative imaging of chemical elements in single cells

R. Ortega^(a,b)

^(a) Univ. Bordeaux, CENBG, UMR 5797, F-33170 Gradignan, France

^(b) CNRS, IN2P3, CENBG, UMR 5797, F-33170 Gradignan, France

The knowledge of the intracellular distribution of biological relevant metals is important to understand their mechanisms of action in cells, either for physiological, toxicological or pathological processes. However, the direct detection of trace metals in single cells is a challenging task that requires sophisticated analytical developments. The aim of this seminar will be to present the recent achievements in this field using micro-PIXE analysis. The combination of micro-PIXE with RBS (Rutherford Backscattering Spectrometry) and STIM (Scanning Transmission Ion Microscopy) allows the quantitative determination of trace metal content within sub-cellular compartments. The application of STIM analysis will be more specifically highlighted as it provides high spatial resolution imaging (<200 nm) and excellent mass sensitivity (<0.1 ng). Application of the STIM-PIXE-RBS methodology is absolutely needed when organic mass loss appears during PIXE-RBS irradiation. This combination of STIM-PIXE-RBS provides fully quantitative determination of trace element content, expressed in $\mu\text{g/g}$, which is a quite unique capability for micro-PIXE compared to other micro-analytical methods such as the electron and synchrotron x-ray fluorescence or the techniques based on mass spectrometry. Examples of micro-PIXE studies for sub-cellular imaging of trace elements in the various fields of interest will be presented such as metal-based toxicology, pharmacology, and neurodegeneration [1].

[1] R. Ortega, G. Devès, A. Carmona. *J. R. Soc. Interface*, 6, (2009) S649–S658.

18 Currents Trends in the Application of IBA Techniques to Air Pollution Source Fingerprinting and Source Apportionment

David Cohen, Ed Stelcer, Armand Atanacio, Jagoda Crawford

Australian Nuclear Science and Technology Organisation,
Locked Bag 2001, Kirrawee DC, NSW, 2232, Australia

IBA techniques have been used for many years to characterise fine particle air pollution. This is not new the techniques are well established. Typically 2-3 MeV protons are used to bombard thin filter papers and up to four simultaneous techniques like PIXE, PIGE, RBS and ERDA will be applied to obtain ($\mu\text{g/g}$) concentrations for elements from hydrogen to lead. Generally low volume samplers are used to sample between 20-30 m^3 of air over a 24 hour period, this together with IBA's sensitivity means that concentrations down to 1 ng/m^3 of air sampled can be readily achieved with only a few minutes of proton irradiation. With these short irradiation times and low sensitivities for a broad range of elements in the periodic table, large numbers of samples can be obtained and analysed very quickly and easily. At ANSTO we have used IBA methods to acquire a database of over 50,000 filters from 85 different sites through Australia and Asia, each filter has been analysed for more than 21 different chemical species.

Large databases extending over many years means that modern statistical techniques like positive matrix factorisation (PMF) can be used to define well characterised source fingerprints and source contributions for a range of different fine particle air pollutants. In this paper we will discuss these PMF techniques and show how they identify both natural sources like sea spray and windblown soils as well as anthropogenic sources like automobiles, biomass burning, coal-fired power stations and industrial emissions. These data are particularly useful for Governments, EPA's and managers of pollution to better understanding pollution sources and their relative contributions and hence to better manage air pollution.

Current trends are to take these IBA and PMF techniques a step further and to combine them with wind speed and back trajectory data to better pin point and identify emission sources. We show how this is now being applied on both a local, regional and global scale with examples of local industrial pollution in urban areas and with long range air pollution being tracked from China into Vietnam.

19 A brief overview of the first twenty years (1970-1989) of aerosol analysis by PIXE and ten-year study (1995-2004) of fine aerosol at Sde Boker, Israel, using PIXE

W. Maenhaut^(a,b), with for the study at Sde Boker also A. Karnieli^(c) and M. O. Andreae^(d)

^(a)Ghent University, Dept. Analytical Chemistry, Krijgslaan 281, S12, BE-9000 Gent, Belgium

^(b)Dept. Pharm. Sci., University of Antwerp, Universiteitsplein 1, BE-2610 Antwerp, Belgium

^(c)Remote Sensing Laboratory, Jacob Blaustein Institutes for Desert Research, Ben-Gurion University of the Negev, Sde Boker Campus 84990, Israel

^(d)Biogeochemistry Dept., Max Planck Institute for Chemistry, P.O. Box 3060, D-55020 Mainz, Germany

First, a brief overview is provided of the first twenty years (1970-1989) of aerosol analysis by PIXE. PIXE and also its application to aerosol samples started with the seminal paper of Johansson et al. [1]. The potential of PIXE for aerosol analysis was soon recognized by Tom Cahill from UC Davis and Jack Winchester from Florida State University (FSU) and accelerators that were previously dedicated to nuclear physics research were from the early 1970s on also used for this new type of application. The enthusiasm of Tom and Jack stimulated many others and researchers from several other countries, including Denmark, Sweden, Finland, Belgium, Italy, Brazil, and South Africa, started with applying PIXE to aerosol analysis. Spectrum acquisition was done with energy-dispersive Si(Li) detectors, which were introduced in the second half of the 1960s, and the spectrum analysis profited from the increasing use of minicomputers and the publication of the very timely book by Bevington [2] with ready-to-use Fortran routines. Aerosol samplers with high time and/or size resolution, such as the Nelson streaker, the PIXE Int. cascade impactor, and the Davis DRUM impactor, were developed and intensively employed. The number of papers on aerosol analysis by PIXE increased steadily over the 1970-1989 period. Moreover, PIXE became the preferred aerosol analysis technique. Over the above 20-year period, its share in the total number of publications on the elemental analysis of aerosols grew from 9% in the first 5 years to as large as 65% in the last 5 years.

Secondly, results are presented from a 10-year study of fine aerosol at Sde Boker, Israel. From January 1995 through December 2004 aerosol samples were collected at this site with a Gent stacked filter unit sampler. The collections were done according to a 2-2-3 day schedule, which resulted in about 150 samples per year. The samples were analyzed for the particulate mass (PM) by weighing, for black carbon (BC) by a light reflectance technique, and for up to 46 elements by a combination of PIXE and instrumental neutron activation analysis [3]. Here, we report on the fine (PM₂) size fraction data for the PM, BC, and the following 9 anthropogenic elements S, V, Ni, Cu, Zn, As, Se, Sb, and Pb, and discuss their time trends, seasonal variation, correlations, and source areas. The largest changes in the annual medians over the 10-year period were found for S, Ni, Sb, and Pb, i.e., of -34%, -25%, +26%, and -40%, respectively. The seasonal variation was largest for S, with 1.5 times higher concentrations in summer than in the other 3 seasons. V and Ni were very highly correlated with each other ($r = 0.95$), pointing to a dominant common source, which is undoubtedly heavy oil burning. Trajectory statistics [4], using 10-day back trajectories with arrival at 300 m above ground, was applied to assess the source areas. S originated mostly from southeastern Europe (i.e., Turkey, Bulgaria, Romania, Ukraine, and southern Russia) and As from the southeastern part of European Russia.

[1] T. B. Johansson, R. Akselsson, S. A. E. Johansson, Nucl. Instrum. Methods 84 (1970) 141-143.

[2] P. R. Bevington, Data reduction and error analysis for the physical sciences, McGraw-Hill, New York, 1969.

[3] W. Maenhaut, N. Raes, W. Wang, Nucl. Instrum. Methods Phys. Res., Sect. 269 (2011) 2693-2698.

[4] A. Lupu, W. Maenhaut, Atmos. Environ. 36 (2002) 5607-5618.

110 Nuclear Spectrometry for Environmental Analysis and Mapping

Aliz Simon

International Atomic Energy Agency, Division of Physical and Chemical Sciences, Vienna International Centre P.O. Box 100, A-1400 Vienna, Austria. Phone: +43 1 2600-21706, FAX: +43 1 26007, e-mail: Aliz.Simon@iaea.org

The International Atomic Energy Agency (IAEA) helps countries to mobilize peaceful applications of nuclear science and technology. The three main pillars of the activities are: safety and security; science and technology; and safeguards and verification. As part of the science and technology pillar, the Physics Section supports Member States regarding utilization of particle accelerators and research reactors, applications of nuclear instrumentation, and controlled nuclear fusion research. Support is provided to the Member States in the form of capacity building, knowledge transfer and networking.

The IAEA's coordinated research activities are designed to contribute to this mandate, by stimulating and coordinating research in IAEA Member States in selected nuclear fields. These coordinated research activities are normally implemented through Coordinated Research Projects that bring together research institutes from both developing and developed Member States to collaborate on the research topic of interest.

The establishment of sustainable education and training programmes is fundamental for the safe, secure and efficient development of the nuclear field. The IAEA offers a wide spectrum of activities in support of education, training, human resource development and capacity building including interregional, regional and national training courses and workshops; assists visits and reviews services; initiates, formulates and runs programmes; networks managers and specialists for sharing good practices; assists in publications that compile the best international practices; supplies training materials and training tools; and supports internship programmes for the young generations of scientists and fellows.

For the developing countries, the Technical Cooperation Programme provides the necessary skills and equipment to establish sustainable technology in the counterpart country or region through training courses, expert missions, fellowships, scientific visits, and provision of equipment.

This talk gives an overview of the IAEA Physics Section activities with a special emphasis on the following activities:

- Improving the analytical performance of PIXE and other IBA techniques;
- Networking for environmental analysis;
- Radioisotope environmental mapping;
- Future perspectives for new IBA methods, especially Heavy Ion PIXE combined with MeV-SIMS.

I11 Twenty five years of OMDAQ

Geoffrey W. Grime

Oxford Microbeams Ltd.
Oxford, U.K.
omltd@microbeams.co.uk



The hardware and software package OMDAQ provides a solution to the problems of multi-channel data acquisition, hardware control and data processing in a nuclear microbeam system. First developed in the late 1980s it has subsequently been under continuous development to improve the usability and functionality. An interface to GUPIXWIN [1] provides seamless processing of PIXE spectra using 'Q-factor' normalization to the simultaneous RBS spectrum [2].

This presentation reviews the history, principles and capabilities of OMDAQ with a particular emphasis on the PIXE-related features and will discuss the envisaged directions of future development.

[1] <http://pixe.physics.uoguelph.ca/gupix/main/>

[2] G.W. Grime, "The "Q factor" method: Quantitative microPIXE analysis using RBS normalisation", Nucl. Instr. and Meths. B109. (1996) 170-174

112 PIXE in cultural heritage studies: present role and new challenges

T. Calligaro and J.-C. Dran

Centre de recherche et de restauration des musées de France, Palais du Louvre, Paris, France

The non-destructive study of artistic and archaeological objects relies on the use of a large panel of modern analytical tools. Among them, PIXE plays a prominent role due to its almost unique combination of excellent analytical features in terms of sensitivity and accuracy combined with a non-destructive and even non-invasive character. The latter advantage stems from extensive instrumental progress – like the external beam - carried out since the advent of PIXE in the 1970s to account for the precious and unique nature of artworks and archaeological artifacts that preclude any sampling or damage. The situation has however evolved in the recent years as several competing techniques providing non-destructively the chemical composition have arisen, which more or less shake the privileged status of PIXE. On one hand, analytical techniques implemented with tabletop or movable XRF instruments have been massively developed, which allow in situ analysis and represent a progress in terms of artworks safety and flexibility of analysis. On the other hand, access to synchrotron radiation facilities is becoming easier and therefore the use of the powerful X-ray absorption techniques (XANES, EXAFS), that add chemical environment information to the elemental analysis, is progressively gaining popularity. Considering these trends, it seems important to reassess the place of PIXE in the field of art and archaeology and to underline its specific assets. The aim of this article is to pinpoint the situation where PIXE is the best analytical tool with regard to the specificity of art and archaeological items and to stress the new challenges it will have to face. Case studies carried out with the AGLAE facility of the C2RMF will illustrate the situations where PIXE exhibits specific advantages:

Light element measurement. The high ionization cross section of light elements by charged particles favors the accurate measurement of sodium, magnesium, aluminum and silicon, whose concentration is, for instance, fundamental for the determination of many ancient materials like glasses, ceramics or rocks.

Seamless quantization. In general, the accurate determination of the composition of complex samples containing a 'dark matrix' - i.e. elements not appearing in the X-ray spectrum like hydrogen, carbon, oxygen - is more easily and accurately obtained using PIXE than XRF that suffers from pronounced matrix effects (critical dependency of X-ray yields with regard to the concentration of unknown elements).

Better control of excitation volume. The fact that the PIXE emission probing depth is limited by the particle range allows to better control of the depth of analysis (analysis of surface layers on top of substrates like glazes on ceramics). Furthermore, some depth information, not available using XRF, can be gained with PIXE by varying the incident particle energy.

Probe focusing and scanning. Unlike X-ray beams, particle beams are easily focused and deviated using magnetic and electrostatic fields. This provides interesting imaging capabilities in particular a fast scanning of the beam at the surface of the object to acquire compositional maps in a short time.

Simultaneous combination with other IBA techniques. During the same irradiation RBS can deliver the layer thickness in the same area, PIGE the concentration of very light elements like lithium, beryllium, boron or fluorine, and non-Rutherford BS that of carbon and oxygen.

A serious challenge is however posed by cultural heritage materials prone to damage by particle beams. It is the case of organic compounds - binder and varnish - or white lead pigments composing paint works. Since damage appears as linked to the beam fluence, a way to overcome this serious drawback is to perform PIXE using a low intensity beam spread over a large surface using fast scanning compensated by an improved detection efficiency.

113 Influence of Heavy Elements in the Sludge Conveyed by the 2011 Tsunami upon Human Health and Recovery of the Marine Ecosystem

K. Sera^(a), S. Goto^(b), C. Takahashi^(b), Y. Saitoh^(b), and K. Yamauchi^(c)

^(a)Cyclotron Research Center, Iwate Medical University

^(b)Takizawa laboratory, Japan Radioisotope Association

^(c)Division of Pulmonary Medicine, Department of Internal Medicine, Iwate Medical University

We reported the studies on bad influences of the contaminated sludge conveyed by the 2011 tsunami upon the environment in the Sanriku district [1, 2]. The tsunami brought not only huge damages but also a large amount of sludge from the bottom of the sea to the coastal lands including seaports, urban districts, farmlands and tidelands. We gathered sludge and plant samples over a wide area of Sanriku along the shore in order to investigate the effect of the sludge on the environment. It was found that the sludges piled upon the lands and also the plants growing on the attacked lands were contaminated with heavy elements. It is anticipated that they might give bad influences both on the human health and on the recovery of marine ecosystem. Inhalation of contaminated aerosols originating from the dried sludge may become worrisome for the people still living in the stricken area. In order to evaluate changes of elemental concentration in a body before and after the disaster, we collected long hairs from the suffered people and the people engaging in reconstruction and rescue works. Sludge samples were newly collected in the Miyagi and the Fukushima prefectures. Also, sludge samples were collected in October 2012 at the same places as those reported in reference 1 in order to evaluate changes of heavy-elemental concentration after one year. Hairs were analyzed by means of a standard-free method for untreated hairs that we developed [3]. We measured the hairs in 1 cm increments in order to investigate changes of elemental concentration in a body before and after the tsunami. Sludge samples were analyzed on the basis of our powdered-internal-standard method [4].

Figure shows changes of elemental concentration in the hair taken from a suffered person. Both essential and toxic elements show noticeable changes before and after the tsunami. We also analyzed the hairs taken from women belonging to Self-defending Force who were engaged in rescue works shortly after the tsunami. The results of hair analyses and those of sludge and plants analyses will be reported.

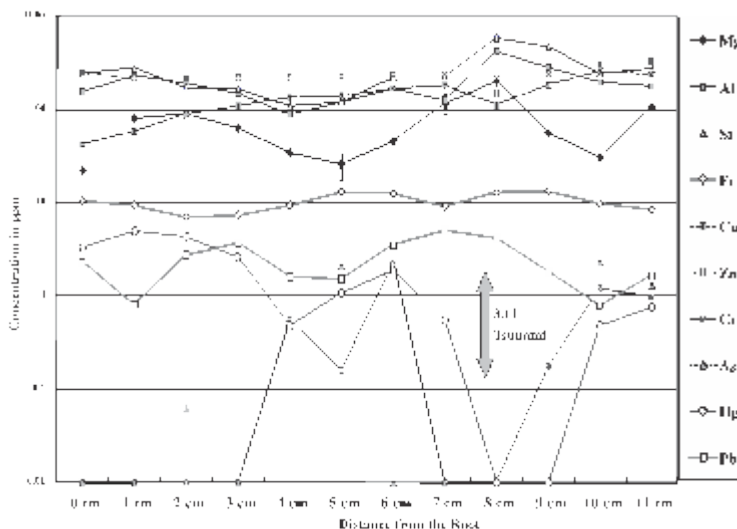


Figure. Changes of elemental concentration in hairs before and after the tsunami.

[1] Baba, F., C., Sera, K., Goto, S., Takahashi, C., and Saitoh, Y., IJPIXE, Vol.22-1-2, 231-239, (2012)

[2] Sera, K., Baba, F., Goto, S., Takahashi, C., Saitoh, Y., and Matsumasa, M., IJPIXE Vol.22- 1-2, 139-147, (2012)

[3] Sera, K., Futatsugawa, S. and Matsuda, K., Nucl. Instr. and Meth. B 150, 226-233 (1999)

[4] Sera, K., Futatsugawa, S. and Ishiyama, D., IJPIXE Vol.9-1,2, 63-81 (1999)

I14 PIXE and Ion Beam Analysis in Forensics

Melanie Bailey^(a), John Warmenhoven^(a) Matt Christopher^(b), Karen Kirkby^(b), Vladimir Palitsin^(b), Geoff Grime^(b), Chris Jeynes^(b), Brian Jones^(b) and Roger Webb^(b)

^(a)Department of Chemistry, University of Surrey, UK

^(b)Surrey Ion Beam Centre, University of Surrey, UK

The University of Surrey has, for the past four years, collaborated with police institutions from across Europe and the rest of the world to scope potential applications of ion beam analysis (IBA) in forensic science. In doing this we have consulted practitioners across a range of forensic disciplines, and critically compared IBA with conventional characterisation techniques to investigate the areas in which IBA can add evidential value.

In this talk, the results of this feasibility study will be presented, showing the types of sample for which IBA shows considerable promise. We will show how a combination of PIXE with other IBA techniques (EBS, PIGE, MeV-SIMS) can be used to give unprecedented characterisation of forensic samples and comment on the significance of these results for forensic casework. We will also show cases where IBA not appear to add any significant improvement over conventional techniques.

PIE 2013

FOR TECHNOLOGY AND GLOBAL DEVELOPMENT

ABSTRACTS

Oral contributions

01-033

O1 L-shell x-ray production cross sections of selected lanthanoids by impact of ${}^4\text{He}^+$, ${}^7\text{Li}^{2+}$, ${}^{10}\text{B}^{2+}$, ${}^{12}\text{C}^{4+}$, ${}^{16}\text{O}^{4+}$, and ${}^{19}\text{F}^{3+}$ ions with energies between 0.50 Mev/u and 0.75 Mev/u

J. Miranda^(a), M. Lugo^(b), G. Murillo^(c), B. Méndez^(c), R.V Díaz^(c), J. López-Monroy^(c), J. Aspiazú^(c), P. Villaseñor^(c)

^(a) Instituto de Física, Universidad Nacional Autónoma de México, Apartado Postal 20-364, 01000 México, D.F., Mexico, {miranda@fisica.unam.mx}.

^(b) Facultad de Química, Universidad Nacional Autónoma de México, Circuito Escolar, Ciudad Universitaria, 04510 México, D.F., Mexico, {marcelo.lugo@gmail.com}.

^(c) Instituto Nacional de Investigaciones Nucleares, Centro Nuclear “Nabor Carrillo”, Autopista México-Toluca, Salazar, Edo. Mex., Mexico.

L-subshell X-ray production cross sections from Ce, Nd, Sm, Eu, Gd, and Dy, induced by the impact of ${}^7\text{Li}^{2+}$ ions were measured, to complement previous works using ${}^4\text{He}^+$, ${}^{10}\text{B}^{2+}$, ${}^{12}\text{C}^{3+}$, ${}^{16}\text{O}^{3+}$, and ${}^{19}\text{F}^{3+}$ ions with energies in the range 0.50 MeV/u to 0.75 MeV/u [1-3]. They are compared with theoretical calculations using the ECPSSR theory (which modifies the Plane Wave Born Approximation), and related theoretical models. Several corrections, such as Multiple Ionization of the target atom (MI), Electron Capture by inner shells of the incoming ion (EC), United Atom (UA), and Intra-shell coupling (IS) theories, were added to the ECPSSR model. It was found that the theory does not describe accurately the experimental results for all cases. Furthermore, a possible universal scaling for the x-ray production cross sections of the ($L_3M_4 + L_3M_5$) line is proposed, based on a reduced velocity parameter χ_L^R . This scaling seems to be useful for all the studied projectile-target combinations analyzed in this work, suggesting that more extensive theoretical studies in this direction might be followed.

Acknowledgement

The authors acknowledge the technical assistance of J.C. Pineda. JM thanks DGAPA-UNAM for a sabbatical scholarship.

References

- [1] M. Lugo-Licona and J. Miranda, Nucl. Instr. Meth. B 219-220 (2004) 289-291.
- [2] M. Lugo-Licona and J. Miranda, J. Radional. Nucl. Chem. 262 (2004) 391-401.
- [3] M. Lugo-Licona and J. Miranda, L-subshell X-ray production cross sections from rare earth elements induced by heavy ions, in M. Budnar, (Ed.), Proc. X Int. Conf. on PIXE and its Analytical Applications, Portoroz, Slovenia, 2004, pp. 809/1-809/4.

O2 Atomic de-excitation and PIXE in Geant4: an update

A. Mantero^(a), S. Incerti^(b), V. Ivantchenko^(c), A. Taborda^(d,e), P. C. Chaves^(d,e), C. Champion^(b) and M. A. Reis^(d,e)

^(a)Istituto Nazionale di Fisica Nucleare, Sezione di Genova, via Dodecanneso 33, 16146 Genova, Italy

^(b)Université Bordeaux 1, CNRS/IN2P3, Centre d'Etudes Nucléaires de Bordeaux Gradignan, CENBG, Chemin du Solarium, BP120, 33175 Gradignan, France

^(c)Ecoanalytica, Moscow State University, 119899 Moscow, Russia

^(d)Centro de Física Atómica da Universidade de Lisboa, Av. Prof. Gama Pinto, 2, 1649-003 Lisboa, Portugal

^(e)IST/ITN, Instituto Superior Técnico, Universidade Técnica de Lisboa, Campus Tecnológico e Nuclear, EN10, 2686-953 Sacavém, Portugal

Geant4 [1,2] is a general purpose and open source C++ Monte Carlo simulation toolkit, widely used in the scientific community. It is able to simulate physical interactions of particles through matter. According to the user needs, models for electromagnetic interactions are provided in two Geant4 categories, the "Standard" electromagnetic category, well suited for a wide range of applications ranging from high energy physics to space and medical applications, and the "Low Energy" electromagnetic category, more adapted to the low energy regime (sub-keV range down to the ~eV range).

Particle Induced X-ray Emission (PIXE) is a well known and very useful technique for quantitative elemental analysis in environmental, archaeological, biological, medical and space applications. An atomic de-excitation package [3] is part of the Geant4 "Low Energy" electromagnetic category since 1999 and has been validated in the recent years [4]. PIXE simulation has been included in this category in 2001 and has been developed during the last years with regular updates including new ionization cross section models for incident protons and alphas and extension of the energy coverage [5].

In this work, we present an overview of the atomic de-excitation package of Geant4 and its recent developments, including the update of the condensed history ionization process in particular for the Livermore, Penelope and Geant4-DNA models. Verification and application examples will be presented as well.

Among the new developments, polynomial approximations were obtained to K, L and M-shell universal ionization cross-sections inferred from ECPSSR numerical integration of the form factor functions. In order to implement them in Geant4, the range of application of the polynomials was extended up to 100 MeV for protons and alphas, by modifying the polynomials obtained in previous work in the 0.1 to 10 MeV range [6].

Part of the presented developments is available in the last release of Geant4 (version 9.6, December 2012) and the full set will be included in the next public release of the Geant4 toolkit.

[1] S. Agostinelli et al., Nucl. Instrum. and Meth., A506 (2003), 250.

[2] J. Allison et al., IEEE Trans. Nucl. Sci., 53 (2006), 270.

[3] S. Guatelli, A. Mantero, B. Mascialino, P. Nieminen, M. G. Pia, IEEE Trans. on Nucl. Sci., 54 (2007), 585.

[4] S. Guatelli, A. Mantero, B. Mascialino, M. G. Pia, V. Zampichelli, IEEE Trans. on Nucl. Sci., 54 (2007), 594.

[5] A. Mantero et al, X-Ray Spectrometry, 40 (2011), 135

[6] A. Taborda, P. C. Chaves, M. A. Reis, X-Ray Spectrom. 40 (2011) 127-134

O3 Coulomb heating of H_2^+ , B_2^+ and C_2^+ molecules in Si $\langle 110 \rangle$

R. C. Fadanelli^(a), M. Behar^(a)

^(a) Instituto de Física, Universidade Federal do Rio Grande do Sul, Porto Alegre, Brasil

The interaction mechanism of molecular beams with matter clearly deviates from that related to the individual components of the molecule. For crystalline materials, ions that enter parallel to a particular axis or plane become channeled as their motion is guided by small correlated collisions with target atoms. For molecular ions, they undergo a breakup process since they lose their bonding electrons due to ionization in the first monolayers of the matter. The breakup and subsequent mutual nuclear repulsion is known as Coulomb explosion. Both combined phenomena, channeling and Coulomb explosion, lead to the so-called Coulomb heating. It can be described as the energy transferred to the projectile transverse motion due to the Coulomb explosion, increasing the interaction rate between the ions and the target atoms.

In this work, we present results for the Coulomb heating of H_2^+ , B_2^+ and C_2^+ molecular ions in the Si $\langle 110 \rangle$ channel. To this end, we have used two different ion beam techniques: Rutherford backscattering spectrometry (RBS) and particle induced x ray emission (PIXE). Once obtained the channeling $\langle 110 \rangle$ direction, for each angle, ion beam and energy, we have determined the corresponding RBS spectra and PIXE Si yields. By comparing the results of the RBS for molecular beams against the corresponding for the monoatomic ones, as well as the PIXE Si yields, it was possible to determine the Coulomb heating values. Simulations were also performed in order to understand the role of physical parameters of the molecules involved in the present experiment. This approach was previously used in order to determine Coulomb heating values for H_2^+ , B_2^+ and C_2^+ in Si $\langle 100 \rangle$ [1].

The previous [1] and the present results are shown in Figure 1. The Coulomb heating values are given as a function of the Coulomb energy stored in each molecule. A preliminary comparison shows that the slopes of both curves are different. These results are discussed during the presentation.

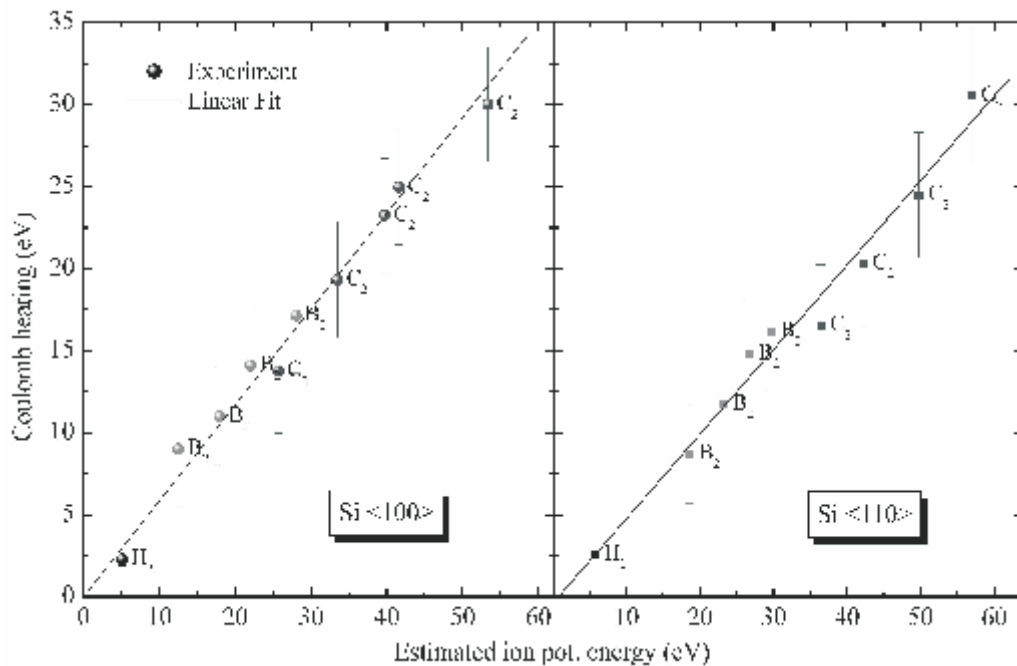


Figure 1. Coulomb heating for the $\langle 100 \rangle$ (left) and $\langle 110 \rangle$ (right) Si channels.

The Si $\langle 110 \rangle$ channel was chosen in the present work due to its larger area if compared with Si $\langle 100 \rangle$. Thus, it is expected that the Coulomb heating determination lead to a better understanding of the charge state changing of ions inside crystalline targets under channelling conditions.

[1] R. C. Fadanelli, M. Behar, and J. F. Dias, Phys. Rev. B, 81, 132101, 2010.

O4 Key experimental M subshell line X-ray production cross sections for slow light ions on high atomic number targets compared with ECUSAR theory

David D. Cohen^(a), Eduard Stelcer^(a), Jagoda Crawford^(a), Armand Atanacio^(a), Greg Doherty^(a), and Gregory Lapicki^(b)

^(a) Australian Nuclear Science and Technology Organisation, Locked Bag 2001, Kirrawee DC, NSW, 2232, Australia

^(b) Department of Physics, East Carolina University, Greenville, North Carolina 27858, USA

The x-ray production cross sections for dominant lines in each of the five M subshells have been measured for slow proton and helium ion impact on selected high atomic number targets from tungsten to uranium. Proton energies between 0.5 and 3 MeV and helium ion energies between 0.5 and 2 MeV were used providing M subshell cross sections for $0.3 < x_{Mi} < 3$, where $x_s = v_1/(q_s v_{2s})$, as defined by Brandt and Lapicki 1979, distinguishes between slow ($x_s < 1$) and fast ($x_s > 1$) collision regimes.

Ion energies and targets over these ranges cover the commonly used PIXE range for M subshell x-ray production on heavy targets across the x-ray energy range 1.3-6 keV, which has a strong overlap with key common K shell elements from Al to Fe. Hence it is important for frequently used PIXE analysis programs like GUPIX and GEOPIXE to have a consistent set of M subshell cross sections together with subshell parameters, like fluorescence yields and Coster-Kronig transition rates, which will precisely and accurately predict M shell line intensities over this low energy X-ray region of interest.

We compare our experimental x-ray production cross sections for the Ma, Mb, Mg, M2-N4 and M1-O23 lines, (together with their overlaps) representing all five M subshells with the theoretical cross sections obtained from the ECUSAR theory of Lapicki 2002. We use the DHS fluorescence yields and emission rates of Puri 2007 and the Coster-Kronig rates of Chauhan and Puri 2008 to convert the theoretical ionisation cross sections to x-ray production cross sections for each resolved x-ray line. The experiment-theory comparison was done against the velocity parameter x_{Mi} for each of the five Mi subshells. The ratios of the experimental values to the ECUSAR theoretical values (R_i) were fitted to a 5th order polynomial whose coefficients are presented for each subshell as a function of x_{Mi} .

We found for the ECUSAR comparisons with experiment; $R_{tot}=(0.96\pm 0.12)$, $R_5=(0.96\pm 0.13)$, $R_4=(0.83\pm 0.19)$, $R_3=(1.35\pm 0.23)$, $R_2=(0.91\pm 0.21)$ and $R_1=(1.03\pm 0.56)$ for reduced velocities above $x_{Mi} > 0.7$. For $x_{Mi} < 0.7$, these ratios R_i increase rapidly with decreasing collision speed for each of the 5 subshells, with the experimental values being 3 to 6 times higher than the ECUSAR predictions for these slower ions on high atomic number targets.

W. Brandt and G. Lapicki, Phys. Rev., A10 (1979) 474.

G. Lapicki, Nucl. Instrum. Meth., B189 (2002) 8.

S Puri, Atomic Data and Nuclear Data Tables 93 (2007) 730-741.

Y Chauhan and S Puri Atomic Data and Nuclear Data Tables 94 (2008) 38-49.

O5 Comparison of attenuation coefficient databases used in μ -PIXE analysis – XCOM, Chantler or...?

C. M. Heirwegh^(a), I. Pradler^(a), and J. L. Campbell^(a)

^(a) Guelph-Waterloo Physics Institute, University of Guelph, Guelph, ON Canada N1G2W1

In earlier work at Guelph [1], pure single-element standards were used to calibrate micro-PIXE analysis of a suite of fused silicate minerals and glasses, with the intent of improving the accuracy for analysis of geological materials. For Mg, Al and Si in the minerals, the resulting concentrations were in error by 6-8%. This pointed to a discrepancy in the database of one or more fundamental parameters (FP) used in computation of concentrations. We have therefore performed micro-PIXE measurements of individual elemental concentrations in several elemental oxides (MgO, Al₂O₃, SiO₂), and compared them with the corresponding concentrations in pure metals (Mg, Al and Si). Incorporation of a static (0.7 T) Nd-Fe-B magnetic device in front of the Ketek Vitus silicon drift detector eliminated spectral contamination by scattered protons. A beam blanking system was used to eliminate both pulse pile-up and the need for deadtime corrections. Element concentration estimates obtained using the GUPIX-related in-house spectra fitting routine GUFIT revealed a discrepancy of 3-4% that was somewhat less than before [1]. This estimate was arrived at using the GUPIX attenuation coefficient database, viz. XCOM [2]. The Chantler [3] attenuation coefficient database was substituted into the GUPIX fundamental parameter library in place of XCOM and a new set of metal to oxide elemental concentration ratios of ± 1 % was calculated. This suggests that the original 6-8% discrepancy was due to problems with the attenuation coefficient database being used and supports use of the Chantler attenuation coefficients, over those provided by XCOM, for low energy photons in low - Z materials.

[1] J. L. Campbell, G. K. Czamanske, L MacDonald, W. J. Teesdale, Nucl. Instrum. Meth. Phys. Res. Sect. B 130 (1997) 608-616.

[2] M. J. Berger, J. H. Hubbell, S. M. Seltzer, J. Chang, J. S. Coursey, R. Sukumar, D. S. Zucker, and K. Olsen, XCOM: Photon Cross Section Database (v. 1.5). [Online] Available: <http://physics.nist.gov/xcom> [Thursday, 11-Oct-2012 14:04:23 EDT]. National Institute of Standards and Technology, Gaithersburg, MD, USA, 2010.

[3] C. T. Chantler, K. Olsen, R. A. Dragoset, J. Chang, A. R. Kishore, S. A. Kotochigova, and D. S. Zucker, X-Ray Form Factor, Attenuation and Scattering Tables (v. 2.1). [Online] Available: <http://physics.nist.gov/ffast> [Thursday, 11-Oct-2012 13:57:22 EDT]. National Institute of Standards and Technology, Gaithersburg, MD, USA, 2005.

O6 X-ray production cross-sections measurements for high-energy alpha particle beam for Si, Fe and Cu

T. Dupuis^(a), G. Chêne^(a), A. Marchal^(a), F. Mathis^(a) and D. Strivay^(a)

^(a)Institut de Physique Nucléaire, Atomique et de Spectroscopie & Centre Européen d'Archéométrie, University of Liège (Belgium)

A new transport beam line has been developed at our CGR-520 MeV cyclotron for ion beam techniques. This facility allows us to produce proton and alpha particle beams with energies up to 20 MeV. A vacuum chamber dedicated to X-ray production and Non-Rutherford cross-section measurements has been recently constructed[1]. Measurements of the X-ray production cross-sections in the 6-12 MeV energy range have started using alpha particle beams on light element targets[2]. These experiments contribute to the filling a serious lack of experimental values for alpha particles of this particular energy range in databases. We are reporting here X-ray cross section measurements for Silicium, Iron and Copper. Experimental data are in good agreement with theoretical ECPSSR values.

[1] G. Chêne, F. Mathis, T. Dupuis, A. Marchal, M. Philippe, M. Clar, D. Strivay, H.P. Garnir
Nucl. Instr. and Meth. B, 268(11-12), 2010, 2015-2018

[2] T. Dupuis, G. Chêne, F. Mathis, A. Marchal, H.P. Garnir, D.Strivay, Nucl. Instr. and Meth. B, 269 (24), 2011, 2979-2983

O7 Multi-detector and systematic imaging system designed and developed within the New AGLAE project

L. Pichon^(a,b), C. Pacheco^(a,b), B. Moignard^(a,b), T. Guillou^(b,c), Q. Lemasson^(a,b), Ph. Walter^(b,c)

^(a)C2RMF – Palais du Louvre 14 quai F. Mitterrand 75001 Paris

^(b)FR3605 – MCC/CNRS/UPMC

^(c)LAMS – UMR8220 – CNRS/UPMC – 3 rue Galilée 94200 Ivry/Seine

The *New AGLAE* project aims to establish a world-class facility for non invasive analysis of Cultural Heritage materials. One of the objectives of the *New AGLAE* project is to increase the x-ray measurement detection, enabling to reduce the beam intensity thus the interaction with sensitive artworks by a ten. Multidisciplinary, the *New AGLAE* project will provide an exceptional and multipurpose beam line with a performance in spatial resolution, beam stability and a capability of multi-particle detection much higher than for the previous facility. The *New AGLAE* will give fundamental elements for the understanding of the structure of materials, their composition, properties, and change over time. One of the objectives of this project is to design and set up a new data acquisition system.

To reach that purpose, the surface and the number of P.I.X.E. detectors have been increased. Indeed, a 10 mm² and a 30 mm² Si(Li) detectors respectively dedicated to low and high energy measurements, were replaced by a cluster of five 50 mm² S.D.D. detectors. If this multi detector enables to decrease the intensity of the incident beam by one order of magnitude, involving less irradiation during the analysis, it can also provide large and/or fast maps.

So as to digital the preamp pulses obtained from the detectors, a custom Digital X-ray Processor provides both digital data and control signals compatible to a multiparameter multichannel system. This multiparameter system saves each event from x-ray, gamma and particle detectors and simultaneously the X, Y positions of the beam on the sample as a list file.

Furthermore, to draw several-cm-sized maps with a 20/40µm resolution, the scanning of the area originally combines a fast vertical magnetic deflection of the beam and a mechanical movement of the target.

To process the data, several homemade software have been developed or updated so as to rebuild any matrix of spectra, to re-bin maps, to process a series of single spectra by taking in account various setup of detectors, to process each pixel to obtain quantitative maps [1]. The spatial repartition of elements with selected ROIs can be visualized and spectra corresponding to selected pixels directly drawn on a map can be saved.

The first images collected on prestigious Cultural Heritage objects will be presented and commented, showing the limits and the perspectives of the technique.

[1] L. Pichon, L. Beck, Ph. Walter, B. Moignard, T. Guillou, A new mapping acquisition and processing system for simultaneous PIXE-RBS analysis with external beam, Nucl Instr and Meth B 268 (2010) 2028-2033

O8 PIXE as a Characterisation Tool in the Cutting Tool Industry

C.S.Freemantle^{a,b}, N. Sacks^a, C.A. Pineda-Vargas^{c,d}, M. Topic^c

(a) School of Chemical and Metallurgical Engineering & DST/NRF Centre of Excellence in Strong Materials, University of the Witwatersrand, Private Bag 3, Wits, 2050, Johannesburg, South Africa, email: chrfre@pilotholdings.com

(b) Pilot Tools (Pty) (Ltd), P.O. Box 27559, Benrose, 2011, South Africa

(c) iThemba LABS, National Research Foundation, P.O. Box 722, Somerset West 7129, South Africa, email: mtopic@tlabs.ac.za, Tel: +27 21 843 1161, Fax: +27 21 843 3543

(d) Faculty of Health & Wellness Sciences, CPUT, Bellville, South Africa

Tungsten carbide-cobalt (WC-Co) alloys are commercially one of the most successful powder metallurgy products, essentially aggregates of particles of tungsten carbide bonded with the cobalt metal via a sintering process. The tungsten carbide particles, which are hard and brittle, provide the hardness and wear resistance, while the cobalt phase provides the toughness. The combination of WC and metallic Co as a binder is an excellent system which combines high strength and hardness as well as toughness [1]. Because of this, hardmetals are predominantly used in the cutting tool industry. The applications range from metal and wood cutting tools, to rock drilling and coal mining.

Recycling of used tools has become a problem in industry and numerous methods have been developed to recycle these materials. The recycling process can be performed by removal of the binder metal (Co) using a selective process, leaving a finely divided carbide matrix or by chemical methods that convert the carbides into a different form, for example into oxides. The zinc process is a widely used method in which molten zinc is used, resulting in the formation of a molten alloy with the cementing agent (cobalt) and breaks the bond between the cementing agent and the tungsten carbide [2]. The zinc is pulled through the carbide scrap by a powerful vacuum. The resulting product consists of a mixture of WC-Co powder and can be re-used to manufacture new cutting tools. The major problems with recycling are the introduced impurities. In this study we used particle-induced X-ray emission (PIXE) techniques to determine the presence of impurities with particular interest placed on Zn and Fe. Fe impurities originate from processing or tool use, while the recrystallized Zn itself was studied to ascertain its reusability for multiple recycling runs. Additionally, PIXE has been used to characterize the elemental composition of typical cutting tool grades available on the market, in order to compare differences in microstructures and tool performance, and the implications of the elements present on the future recycling of these grades. The application of PIXE is relatively new to metallurgical engineering and generally, it can detect trace elements (impurities) in metals and alloys at concentration levels as low as $500 \mu\text{g}\cdot\text{g}^{-1}$ and below [3]. In this study, the content of Zn and Fe and their 2-D distribution were mapped out, as well as W, Ti, Ta, Nb, Cr, C, and O (and other impurity) maps in cutting tool grades. The PIXE results of the recycled powder investigated in this study show the presence of a number of impurities. More importantly, it has been seen that the PIXE technique can serve as an important tool for characterisation in the cutting tool industry.

References

- [1] L.J. Prakash, International Journal of Metals and Hard Materials, 13, (1995) 257-264.
- [2] P.G. Barnard, A.G. Starliper, H. Kenworthy, Reclamation of refractory carbides from carbide materials, US. Pat. 3595484 (1970)
- [3] E. Jallot, H. Benhayoune, G. Weber, G. Balossier, P. Bonhomme, J. Phys. D: Appl. Phys. 33, (2000) 321-326

009 Microprobe Study of Ni-Ge Interactions in Lateral Diffusion Couples

D.Chilukusha^(a), C.A. Pineda-Vargas^(b,c), R. Nemutudi^(b), A. Habanyama^(a), C.M. Comrie^(b,d)

^(a) University of Zambia, School of Natural Sciences, P.O. Box 32379 Lusaka 10101, Zambia

^(b) iThemba LABS, National Research Foundation, P.O. Box 722, Somerset West 7129 South Africa

^(c) Faculty of Health & Wellness Sciences, CPUT, Bellville, South Africa

^(d) University of Cape Town, Department of Physics, Private Bag, Rondebosch 7700 South Africa

Introduction: In recent years, germanium has attracted a significant amount of research interest due to its great potential to replace silicon as the semiconductor for ultra-fast nano-scale Complementary Metal Oxide Semiconductor (CMOS) transistors. Nickel germanides are viewed as the most suitable materials for use as ohmic contacts and interconnects to germanium. Implementation of germanium based technology will, however, require a thorough understanding of the solid state interactions in metal-germanium systems in order to foresee and avoid problems that may be encountered during integration. This study reports on the solid state interactions in the germanium-nickel lateral diffusion system, a system which has never been studied before.

Experimental Procedure: Thermally oxidised single crystal silicon wafers with orientation Si (100) were used as substrates. Deposition was done using Electron Beam Evaporation at high vacuum. Two sets of samples were prepared; one for thin film couples and the other for lateral diffusion couples. Lateral diffusion couples samples were prepared in two configurations viz: (i) Germanium islands on nickel thin films, and (ii) Nickel islands on germanium thin films. In both cases, the islands were of thickness 2000Å while the thin films had 500Å. After deposition, the samples were vacuum annealed at temperatures between 300 °C and 500 °C, and times ranging from 30 minutes to 16 hours. All anneals were done at pressures lower than 3×10^{-5} Pa.

Results: Nuclear microprobe (NMP) RBS and PIXE were applied to the study of thermally induced solid state interactions in Ni-Ge lateral diffusion couples. Lateral reactions were found to commence at a temperature as low as 300 °C. Outside the original thin-film/island interface, Ni_5Ge_3 phase was observed. Its growth was found to obey the $(t)^{1/2}$ law, indicating a diffusion-controlled process. Ge was found to be the dominant diffusing species (DDS) during the formation of Ni_5Ge_3 in the lateral diffusion configuration. The activation energy for the formation of Ni_5Ge_3 was determined to be 0.95 ± 0.01 eV. Inside the original thin-film/island interface, NiGe was detected. As the Ge atoms migrated from the source region into the surrounding Ni thin film, they left exposed the NiGe that had formed during the interfacial stage of the reaction. The activation energy of diffusion of Ge in NiGe was found to be 1.10 ± 0.01 eV.

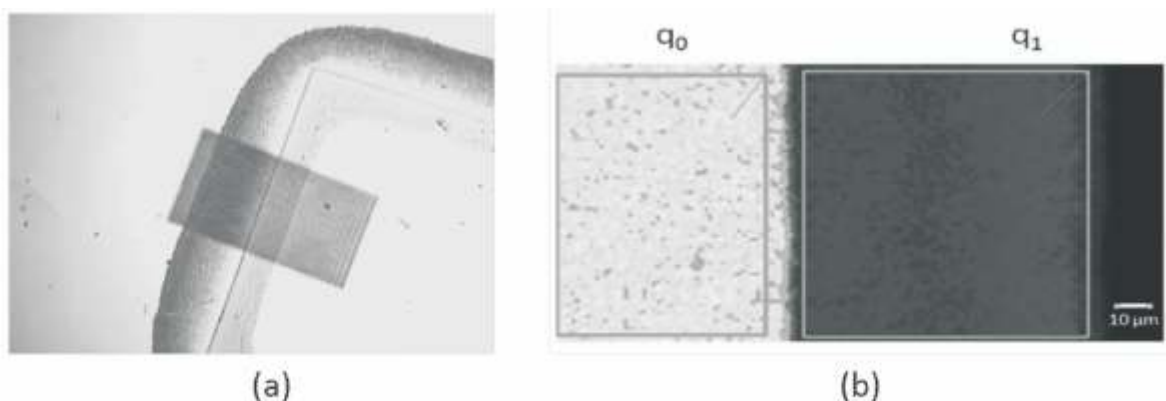


Figure : (a) Optical micrograph of sample annealed at 500 °C for 2 hours. The area that was scanned by the ion beam (rectangle) is clearly visible in the micrograph. (b) Two-dimensional micro-PIXE elemental map of the concentration of Ge atoms on the area shown in (a). The map was obtained with $L_{\alpha 1}$ X-ray lines. Two main zones, corresponding to Ni_5Ge_3 and NiGe, appear to develop. Region q_0 corresponds to the top of the Ge island.

O10 Structural characterization of CdSe/ZnS quantum dots using PIXE, RBS and MEIS

M. A. Sortica^(a), P. L. Grande^(a), C. Radtke^(b), L. G. Almeida^(a), R. Debastiani^(a), J. F. Dias^(a), A. Hentz^(a)

^(a) Institute of physics, Universidade Federal do Rio Grande do Sul (IF-UFRGS)

^(b) Institute of chemistry, Universidade Federal do Rio Grande do Sul (IQ-UFRGS)

Compound quantum dots QDs are promising materials that can be used in many fields of the technological development, but the accurate knowledge of compositional depth profiling inside of them is still a technological challenge. Medium energy ion scattering (MEIS) is an ion beam analysis technique, capable of elemental depth profiling with subnanometric depth resolution. Recently, the MEIS technique was optimized for nanostructured materials analysis [1] and became a promising tool for structural characterization inside of QDs [2,3]. In this work [4], we use the MEIS technique, combined with PIXE and RBS to characterize a core-shell nanostructure of CdSe/ZnS. The crystal size of 5.2 nm, determined by MEIS, is in good agreement with optical measurements and TEM images. The core-shell structure is resolved by the present configuration of MEIS in contrast to the present TEM measurements. The commercial CdSe/ZnS QDs has non-stoichiometric Cd and Se concentrations. The sample selected for this work have a Cd:Se ratio of 0.69:0.31. Our investigation shows that there is Cd present on the shell and the CdSe core tends to be a stoichiometric crystal. That indicates that, despite the unbalance of material, the CdSe crystal is preserved during the industrial process which allows the control of the QDs diameters. The present characterization method allows for studies of the formation and stability of the internal structure of the QDs when exposed to several kind of processes, like heating and ion irradiation.

Financial support by CNPq and PRONEX

[1] M. A. Sortica, P. L. Grande, G. Machado and L. Miotti, Journal of Applied Physics 106 (2009) 1.

[2] H. Matsumoto, K. Mitsuhashi, A. Visikovskiy, T. Akita, N. Tushima, and Y. Kido, Nuclear Instruments and Methods in Physics Research B 268 (2010) 2281.

[3] J. Gustafson, A. R. Haire, and C. J. Baddeley, Surface Science 605 (2011) 220

[4] M. A. Sortica, P. L. Grande, C. Radtke, L. Almeida, R. Debastiani, J. F. Dias, A. Hentz, Applied Physics Letters, 101 (2012) 023110.

O11 Integration of XRF spectrometer for simultaneous and/or complementary use with PIXE at the external ion beam analysis setup

S. Fazinic^(a), D. Cosic^(a), M. Jaksic^(a), A. Migliori^(b), A. G. Karydas^(b), V. Desnica^(c) and D. Mudronja^(d)

- ^(a) Laboratory for Ion Beam Interactions, Division of Experimental Physics, Rudjer Boskovic Institute, Bijenicka cesta 54, 10000 Zagreb, Croatia
- ^(b) Nuclear Spectrometry and Applications Laboratory, International Atomic Energy Agency (IAEA), 2444 Seibersdorf, Austria
- ^(c) Laboratory for Science and Technology in Art, Academy of Fine Arts in Zagreb, Ilica 85, 10000 Zagreb, Croatia
- ^(d) Natural Science Laboratory, Croatian Conservation Institute, Grskoviceva 23, 10000 Zagreb, Croatia

The Rudjer Boskovic Institute Tandem Accelerator Facility is equipped with a number of end-stations dedicated to ion beam analysis (IBA), modification of materials and nuclear physics experiments. IBA is performed at the: (i) nuclear microbeam, (ii) broad-beam in-vacuum and (iii) external beam end-stations. Several IBA techniques can be used simultaneously, Particle Induced X-ray Emission (PIXE) and Particle Induced Gamma-ray Emission (PIGE) at the external beam end-station, and additionally Rutherford Backscattering Spectroscopy (RBS) at the in-vacuum end-station.

X-ray fluorescence (XRF) analysis is a technique complementary to PIXE. Both techniques offer high analytical potential for multi-elemental investigations and material characterization. Due to different excitation mechanisms, PIXE generally exhibits higher sensitivity for lighter elements and XRF for heavier, whereas they also have different in-sample depth sensitivities. Although they use different excitation sources, both techniques can use the same data acquisition modules. With the development of miniature, low power and lightweight X-ray tubes it is possible to incorporate an X-ray source within the IBA setup and combine the two techniques for simultaneous use.

In this work, the unification of the PIXE and XRF techniques at the RBI external ion beam analysis setup has been investigated and the results are discussed. This has been done by installing a transmission miniature X-ray tube at the end-station. The tube has been properly positioned in order to irradiate the same spot on the sample as the ion beam used for PIXE/PIGE measurements. Our home made data acquisition system SPECTOR, used regularly for the IBA measurements, has been also used to acquire the XRF spectra. At first, the X-ray tube has been installed at the in-vacuum IBA station, and then to the external beam end-station. Test measurements have been carried out on various standard reference materials using both systems and the results have been analyzed. The standard PIXE and XRF spectra have been collected, as well as spectra obtained by the simultaneous ion beam and X-ray irradiation of the analyzed sample. The effects of the combined particle and X-ray induced characteristic X-ray emission have been studied and discussed. The work has been carried out with the hypothesis that when PIXE and XRF are unified into one integrated set up, their complementarities can enhance the analytical capabilities of the combined measurement system improving the quality of the obtained results.

O12 PIXE analysis of *thamatococcus danielli* in Osun state of Nigeria

S.O. Olabanji ^(*, a), G.A. Osinkolu ^(a), D.A. Pelemo ^(a), and A.T. Oladele ^(b)

^(a)Centre for Energy Research & Development (CERD), Obafemi Awolowo University (OAU), Ile-Ife, Nigeria.

^(b)Department of Pharmacognosy, Faculty of Pharmacy, Obafemi Awolowo University (OAU), Ile-Ife, Nigeria.

Thamatococcus danielli {*Marantaceae*}(Benn.) Benth [Miraculous berry] is a multi-purpose perennial herb that is widely distributed in the tropical rainforest areas of West Africa. The leaves are simple, broad with slender stems connected underground to the perennial rhizomes. Farmers grow it in pockets within cocoa (*Theobroma cacao*) and kola (*Cola nitida*) plantations in South western Nigeria, Ghana and Cameroon. Propagation is mainly by rhizomes cuttings and occasionally by the seed. *T. danielli* plays very important roles in the rural economy generating income for the peasant farmers and traders. *T. danielli* is used mainly in three ways by the people. The leaves are used in food wrapping because of its very good flavour and its preservative ability; and roof thatching while the stem is locally used as straw in weaving mats and in making baskets, bags, hats, hand fans and other artistic works. Research has shown that the fruits of *T. danielli* contain low-calorie protein named "Thaumatococcosin" which is about 2000 times as sweet as sucrose. The stems also can be processed to produce fibre industrially in addition to the industrial potential of Thaumatococcosin. Thaumatococcosin have been implicated to be suitable sweetener for diabetes patients. However, despite the great economic values, potentials and benefits of *T. danielli*, there is hardly any data on its elemental compositions. This work therefore presents the elemental composition of *T. danielli* plant's parts (leaves, stems, fruits (mesocarps), seeds and roots (rhizomes)) from six different towns in Osun State of Nigeria using the Particle Induced X-ray Emission (PIXE) technique. The 2.0 MV collimated proton beam from the NEC 1.7 MV 5SDH Tandem accelerator of the Centre for Energy Research and Development (CERD), Obafemi Awolowo University, Ile-Ife, Nigeria was employed for the measurements. The results showed the detection of elements which include K, Ca, Fe, Mn, Sr, Zn, Pb, Br, and Cl at various concentrations. These very important novel results are presented and discussed.

Keywords: PIXE, *Thamatococcus danielli*, Elemental compositions, Nigeria.

*Corresponding author. Tel. +234 803 532 1791

E-mail: skayode2002@yahoo.co.uk

O13 IBA and ICP-OES determination of trace elements in indigenous medicinal herbs and their extracts on the infertility in the human male reproductive system

J.A. Mars^(a); F. Weitz^(b), D. Fisher^(a), R. Henkel^(a)

^(a) Department of Medical Bioscience, University of the Western Cape, Private Bag X17, Bellville, 7535, South Africa

^(b) Department of Biodiversity and Conservation Biology, University of the Western Cape, Private Bag X17, Bellville, 7535, South Africa

The abnormality of infertility in humans is biologically defined (Mader, 2004; Wood, 1994; Ellison, 2001) as the inability of a species to reproduce its own kind after period of 12 month of unprotected sexual intercourse/copulation. It is however difficult when one wishes to quantify the occurrence of infertility, since it is seldomly expressed explicitly, but mostly in conjunction with population growth dynamics which include socio-economic factors.

Various plants (herbs) have been used as treatment for infertility. These plants however have not yet been scientifically analysed. In this paper we determined the major and trace element composition of *Typha capensis* (rhizome and leaves) *Cissampelos capensis* (leaves) and *Hermannia cilliata*, which were sourced from the Cape Flats Nature Reserve, Bellville, Western Cape Province, South Africa.

The trace element concentration determination are at time cumbersome, especially when destructive analytical methods such as ICP-OES are used. For our determination, the various samples were freeze-dried. Part of the freeze-dried sample was used for ICP-OES and the other for PIXE analysis. For PIXE the dried sample was pressed into a pellet, then coated with a layer of carbon and irradiated with a 3 MeV proton beam. We report on the trace element content of the various parts of the plant and comment on the applicability of the part in male infertility.

O14 Elemental imaging of organic matter and metal associations in ore deposits using micro-PIXE and micro-EBS

S. Fuchs^(a) and W.J. Przybylowicz^(b)

^(a)Earth and Planetary Science, McGill University, Montreal, H3A 2A7, Canada; e-mail: sebastian.fuchs@mail.mcgill.ca

^(b)Materials Research Department, iThemba LABS, National Research Foundation, PO Box 722, Somerset West 7129, South Africa; e-mail: przybylowicz@tlabs.ac.za

Keywords: Witwatersrand gold deposits; Au-U bearing conglomerates

Organic matter is a common constituent in many ore deposits, such as the Witwatersrand and Carlin-type gold deposits, the Zn-Pb-Cu-bearing Mississippi Valley-type deposits and the polymetallic Kupferschiefer. Genesis of most of these deposits is linked to hydrothermal processes; however, the role of organic matter in the ore-forming process is not well understood. The Witwatersrand deposits in South Africa are the biggest gold and uranium resources on earth, where up to 50% of the total gold and almost 100% of the total uranium is hosted in bituminous seams and nodules. Understanding the transport mechanisms and deposition processes helps in evaluating the economic potential of these ore deposits.

The nuclear microprobe of iThemba LABS, South Africa, was used for quantitative mapping on bituminous seams and nodules in Au-U-bearing conglomerates from the Black, Carbon Leader and Vaal Reefs. Simultaneous use of micro-PIXE and micro-EBS (elastic backscattering spectrometry) gave a more comprehensive picture of elemental distribution, including C/O ratios. Native gold with varying concentrations of Ag, Hg and Cd occurs either isolated in the organic matrix or at the grain boundaries between organic matter and small quartz veinlets. Uraninite is intergrown with gold in the carbon nodules of Black Reef. In the organic seams of the Carbon Leader Reef uraninite was grown around gold nuclei in the centre, which is replacing organic matter. Pb and Th occur together in association with uraninite, but also as native lead. C/O ratios obtained by micro-EBS allow reconstruction of the maturation path of organic matter in the deposit. The elevated homogeneous distribution of S gives the evidence for organo-sulphur species in the organic matter and can be used with C/O ratios to characterize heavy, polar bitumen fractions. REEs (e.g. Ce and Y), Ca, Ti, Al and Fe associated with hydrothermal alteration zones suggesting an interaction of a liquid aqueous and hydrocarbon phases and the formation of new minerals (sericite, brannerite, pyrophyllite). The results give strong evidence that Au and U were transported by circulating aqueous and/or insoluble organic phases and precipitated in solidified bitumen seams and nodules.

O15 Development of microscopic optics for high-resolution IL spectroscopy with proton microbeam probe

W. Kada, T. Satoh, A. Yokoyama, M. Koka, and T. Kamiya

Takasaki Advanced Radiation Research Institute, Japan Atomic Energy Agency

Combined techniques of PIXE and IL are currently investigated with proton microbeam for the precise analysis and imaging of microscopic targets [1]. Spectroscopy of IL is adaptable to simultaneous analysis with conventional in-air micro-PIXE system and able to characterize the chemical composition of the irradiation targets while the wavelength of the IL photons is strongly affected by the chemical-state of the elements [2]. However, IL was not well obtained from the targets with size of micrometers comparing to the PIXE analysis [3]. The sensitivity and the S/N ratio of IL detection are needed to be improved to perform spectroscopic analysis of the IL from such a micrometer-sized particulate targets.

In this study, we have developed a new optics for the IL measurement using confocal micro lens optics. Anti-reflection-coated convex lens was installed in a microbeam line of 3MV single ended accelerator for in-air micro-PIXE analysis system. The focal points of the lens were set on the irradiation target and input terminal of optical fiber. The effective focus area on the target was approximately $800 \times 800 \mu\text{m}$ considering chromatic aberration of the IL photons ranging 300 to 950 nm. Electrically-cooled back-thin CCD spectrometer was used for the spectroscopic analysis of IL with a wavelength resolution of 0.5 nm in the range of 200 to 950 nm. Photon counting unit was also employed for the monochromatic and panchromatic imaging of IL.

Spectroscopic observations of IL from microscopic mineral targets were performed using microbeam probe of 3 MeV H^+ with current of 1- 200 pA. Figure 1 shows an IL spectrum from an Al_2O_3 crystal with acquisition time of 15 ms. The IL spectrum had a maximum spectral resolution of 3 nm and single peak correspond to the impurity of chromium was clearly observed. The spectral analysis of IL was also applicable to the other natural mineral target and also particulate target like aerosols with different elemental and chemical compositions.

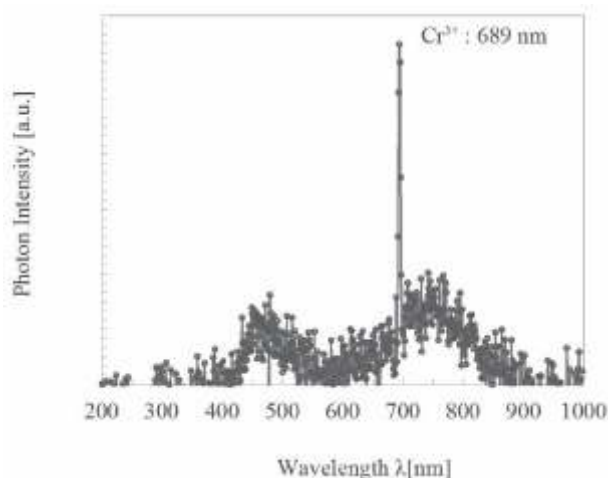


Figure 1. IL spectrum obtained from mineral sample of Al_2O_3 .

- [1] W. Kada, A. Yokoyama, M. Koka, T. Satoh, and T. Kamiya, *Int. J. of PIXE* 21 (2011) 1-11. [2] J.S. Laird, J. Wilkinson, C. Ryan, A. Bettioli, *Nuclear Inst. Meth. B*, 269 (2011) 2244-2250. [3] W. Kada, A. Yokoyama, M. Koka, T. Satoh, and T. Kamiya, *Int. J. of PIXE* 22 (2012) 21-27.

O16 The new in-air micro-PIXE setup in Atomki, Debrecen

Zs. Török^(a,b), Zs. Kertész^(a), R. Huszánk^(a), I. Rajta^(a), Z. Szikszai^(a), L. Csedreki^(a,b),
A. Angyal^(a), E. Furu^(a,b), Z. Szoboszlai^(a), Á. Z. Kiss^(a), I. Uzonyi^(a), and L. Palcsu^(a)

^(a)Institute of Nuclear Research of the Hungarian Academy of Sciences (Atomki), Laboratory of Ion Beam Applications, H-4026 Debrecen, Bem tér 18/c, Hungary

^(b)University of Debrecen, H-4032 Debrecen, Egyetem tér 1, Hungary

In this work we present a new in-air micro-PIXE measurement setup installed at the Laboratory of Ion Beam Applications of Atomki, Debrecen, Hungary. The new external measurement system was set up on the nuclear microprobe beamline.

An external beam add-on system by Oxford Microbeams was mounted on the already existing microprobe vacuum chamber. The samples are positioned by using a digital microscope, two alignment lasers and a precision XYZ stage. The measurement system is equipped with two X-ray detectors for PIXE analysis, a surface barrier detector for RBS and a HP-Ge detector for γ -ray detection. The arrangement permits the combination of these techniques either simultaneously or separately, too. The beam current is measured with a beam chopper placed in the vacuum chamber. Exit windows with different thickness and of different materials can be used according to the actual demands. At the moment kapton foils of 8 mm thicknesses and silicon nitride (Si_3N_4) films with 100 nm, 200 nm and 500 nm thicknesses are at our disposal. The thickness, density and composition of the window materials were measured by profilometry and by RBS, STIM and PIXE in order to check whether the parameters provided by the producers were real.

The capability of the new in-air micro-PIXE setup was demonstrated on standard reference materials and on geological (a stalactite) and archaeological samples.

Acknowledgement. The development of the new in-air microbeam system was partially financed by the Hungarian Academy of Sciences. This work was carried out in the frame of the János Bolyai Research Scholarship of the Hungarian Academy of Sciences and TÁMOP-4.2.2/B-10/1-2010-0024 project.

O17 Stereoscopic PIXE imaging applied to space debris impact craters from the Hubble Space Telescope

G.W. Grime^(a), A.T. Kearsley^(b), V. Palitsin^(a), C. Jeynes^(a), J. Colaux^(a), and R.P. Webb^(a)

^(a) Ion Beam Centre, University of Surrey, Guildford, GU2 7XH, UK.

^(b) Science Facilities, Natural History Museum, Cromwell Road, London, U.K.

The large information depth associated with PIXE analysis means that the analysis of thick samples with buried structures are not meaningful without additional information to constrain the depth distribution. This is particularly detrimental in micro-PIXE imaging, where in some cases the detail in the maps can be lost due to overlapping signals from different depths. This problem has been addressed in a number of ways ranging from mapping using additional techniques, such as RBS (e.g. [1]) to full computed tomography (e.g. [2]). A simple method which can reveal visually the depth structure of certain samples is stereoscopic imaging, in which two elemental maps recorded with different beam - sample angles are presented stereoscopically, e.g. as red-green anaglyphs. This can provide valuable information to help with the interpretation of complex microPIXE images.

There is growing interest in knowing the number and type of space debris particles in near earth orbits so that appropriate protection can be designed into future space craft. A collaboration [3] between the European Space Agency, NASA, the Natural History Museum, London and the Surrey Ion Beam Centre, has analysed nearly 200 space debris impacts from the external radiator panel of the wide-field planetary camera (WFPC-2) which had been recovered during a Space Shuttle mission after nearly 15 years in orbit. The majority of the analysis was carried out using EDS, but the microPIXE was used in about 20% of the cases to provide additional information in ambiguous cases. The WFPC-2 radiator was coated with a thick layer of titanium – zinc paint, so that the impacts were in the form of craters of a wide range of morphology ranging from deep narrow pits to large areas of spallation. Conventional PIXE mapping of these craters proved to be difficult to interpret, and so the samples were mounted on a rotating stage and stereoscopic was used to view the shape of the crater and so determine the three-dimensional distribution of the impact products.

This presentation will briefly review the recording and presentation of stereoscopic microPIXE image and then present examples of the use of the technique on the WFPC-2 space debris impacts.

[1] G.W. Grime et al., Nuclear Insts and Meths B, 54, (1991) 353-362.

[2] C. Habchi, et al, Nuclear Instr. and Meths B 249, (2006), 653-659.

[3] In addition to the authors, this collaboration includes the following organisations and people:
NASA Goddard Space Flight Center, Greenbelt, Maryland, USA. (T. J. Griffin and B. B. Reed)
NASA Johnson Space Center, Houston, Texas, USA (P. D. Anz-Meador, J.-C. Liou, D. Ross, G. A. Robinson and J. N. Opiela) European Space Agency, Noordwijk, The Netherlands. (L. Gerlach)

O18 Study of a nearly pristine pyroxenite sample using low and high energy PIXE methods

P.C. Chaves^(a), A. Taborda^(a,b), D.P.S. de Oliveira^(c), M.A. Reis^(a,b)

(a) Centro de Física Atómica da Universidade de Lisboa, Av. Prof. Gama Pinto 2, 1649-003 Lisboa, Portugal

(b) IST/ITN, Instituto Superior Técnico, Universidade Técnica de Lisboa, Campus Tecnológico e Nuclear, EN10, 2686-953 Sacavém, Portugal;

(c) Laboratório Nacional de Energia e Geologia (LNEG), Apartado 7586, 2611-901 Alfragide, Portugal

A sample collected from a borehole drilled in the old Pingarela concession in Carrazedo within the Bragança Chromite Field [1] located approximately 10 km ESE of Bragança – Trás-os-Montes, was analysed by standard and high energy PIXE at both CTN (previous ITN) PIXE setups. Prior to analysis, the cylindrical sample was just cut vertically and the face was polished. No additional operations were performed apart from mounting the sample in the sample-holders of each of the analytical chambers, and cleaning the surface for analysis before introducing the sample-holder in the analytical chamber. The sample is a fine-grained metapyroxenite grading to coarse-grained in the base with disseminated sulphides and fine veinlets of pyrrhotite and pyrite. Low energy PIXE was carried out in the standard PIXE setup using a 1.25 MeV proton beam to extract information on elements from Mg to Fe. In the low energy conditions, only three different spots were analysed. Matrix composition obtained in this way was then used to determine the medium and high Z elemental concentrations using the DT2 code (also present in another communication at this conference) applied to the spectra obtained in the High Resolution and High Energy (HRHE)-PIXE setup (also described at another communication in this conference) by irradiation of the sample with a 3.9 MeV proton beam provided by the CTN 3MV Tandem accelerator. In this paper we present results, discuss detection limits of the method and the eventual added value of the use of the CdTe detector in this context.



Figure 1: Greyscale photograph of the mapped region. The whole area is limited by Al tape used to mount the sample in the sample-holder. Overall the mapped area is 54x16mm² and a total of 18x4 spots of 1x3mm² in size were analysed by high energy PIXE to obtain the medium and high Z concentration maps.

[1] D.P.S. De Oliveira, H.M.C.V Santana, C.A. Meireles, F. Guimarães, in: P.J. Williams et al. (eds.), Proceedings of the 10th Biennial SGA Meeting of the Society for Geology Applied to Mineral Deposits, Townsville, Australia, 17th to 20th of August, 2009, Smart Science for Exploration and Mining (2010) 158-160

O19 Iron quantification and distribution in 6-OHDA animal and cellular models of Parkinson's disease using micro-PIXE

A. Carmona^(a,b), L. Perrin-Verdugier^(a,b), C. Carcenac^(c), S. Roudeau^(a,b), S. Bohic^(d), D. Carrez^(e), T.D. Wu^(e), S. Marco^(e), J.L. Guerquin-Kern^(e), M. Savasta^(c) and R. Ortega^(a,b)

^(a)CNRS, IN2P3, CENBG, UMR 5797, F-33170 Gradignan, France

^(b)Université de Bordeaux, CENBG, UMR 5797, F-33170 Gradignan, France

^(c)INSERM U836, Dynamique et Physiopathologie des Ganglions de la Base, Grenoble Institut des Neurosciences, Grenoble, France

^(d)INSERM U836, Rayonnement synchrotron et recherches médicales, Grenoble Institut des Neurosciences, Grenoble, France

^(e)INSERM U759, Institut Curie Recherche, Orsay, France

Ion beam microanalysis offers a unique combination of analytical methods that can be used with micrometric resolution for the determination of chemical element distributions. This work illustrates how the association of PIXE (Particle Induced X-ray Emission) and BS (Backscattering Spectrometry) allows the quantitative determination of trace element content in tissue and single cells. PIXE is used for trace element detection, while BS enables beam current normalization and local mass determination.

We investigated the role of iron in the aetiology of Parkinson's disease. The neurotoxin 6-OHDA (6-hydroxydopamine) induces neurons degeneration in the substantia nigra and is currently used in animal models to induce Parkinsonism and iron increase. However studies are contradictory about iron increase or not after 6-OHDA injection. In order to elucidate this point we determined iron distribution and quantification in animal tissues and single cells exposed to 6-OHDA. A specific cryogenic protocol for sample preparation was carried out which preserves biological structures and chemical distribution. Animals were sacrificed after 6-OHDA intracranial injection. Brains were perfused and cryofixed by immersion in cryogenic liquid. Brain sections were prepared for micro-PIXE analyses and adjacent tissue for histological identification of substantia nigra (pars compacta and pars reticulata). Brains sections were lyophilised at low temperature. On the other hand, dopaminergic cells were exposed to 6-OHDA and/or to iron in culture medium and prepared also using cryogenic methods.

The results show that no iron increase occurs in the substantia nigra pars compacta of lesioned animals with respect to non lesioned animals. In the same way no differences in iron were found between lesioned and control side of the same animals. Also no significant differences in iron content into cells treated or not to 6-OHDA were found. Moreover we found that 6-OHDA is more toxic when an excess of iron occurs previously in cells. So we conclude that 6-OHDA treated animal and cells are not a good model to reproduce iron elevation for Parkinson's disease studies.

[1] R. Ortega, P. Cloetens, G. Devès, A. Carmona, S. Bohic, PLoS ONE, 2 (2007) e925.

[2] A. Carmona, G. Devès, R. Ortega, Analytical Bioanalytical Chemistry, 390 (2008) 1585-1594.

[3] A. Carmona, G. Devès, S. Roudeau, P. Cloetens, S. Bohic, R. Ortega, ACS Chemical Neurosciences, 1 (2010) 194-203.

O20 Elemental analysis of a murine solid tumor treated with a vascular disrupting agent AVE8062

A. Terakawa^(a), K. Ishii^(a), S. Matsuyama^(a), Y. Kikuchi^(a), Y. Ito^(a), K. Kusano^(a), H. Sugai^(a), M. Karahashi^(a), Y. Nozawa^(a), S. Yamauchi^(a), H. Yamazaki^(b), Y. Funaki^(b), S. Furumoto^(c), N. Ito^(d), S. Wada^(d), and K. Sera^(e)

^(a)Department of Quantum Science and Energy Engineering, Tohoku University, Sendai, 980-8579, Japan.

^(b)Cyclotron and Radioisotope Center, Tohoku University, Sendai, 980-8578, Japan.

^(c)Tohoku University Graduate School of Medicine, Sendai 980-8575, Japan.

^(d)Kitasato University School of Veterinary Medicine, Towada 034-8628, Japan.

^(e)Cyclotron Research Center, Iwate Medical University, Tomegamori, Takizawa, 020-0173, Japan.

Therapeutic strategies targeting tumor vasculature have received a great attention in cancer treatment. Vascular disrupting agents (VDAs) are designed to cause a rapid and selective blood flow interruption in tumors leading to extensive tumor necrosis as a result of oxygen and nutrient deprivation. VDAs give rise to a catastrophic shutdown in the vascular function of the tumor. However, it has been observed that the tumor cells at the border between malignant and normal tissue survive treatment with VDAs¹. The most likely explanation for this finding is that the tumor cells at the tumor periphery are supported by oxygen and nutrients from the surrounding normal vessels and repopulate the tumor after the VDA treatment². As a result, the solid tumor treated with a VDA has the periphery of viable tumor cells surrounding the inner necrotic tissue. Therefore, it is expected that elemental distributions in tumor tissue after exposure to the VDA are presumably different from those in untreated tumor tissue. The aim of this work was to study effects on spatial distributions of elements in a solid tumor caused by a vascular disruption agent, AVE8062 (a derivative of combretastatin A-4) on the basis of particle-induced X-ray emission (PIXE) analysis using a submillimeter-sized proton beam.

NFSa fibrosarcoma cells ($5 \times 10^6/50$ mL) were transplanted into a hind limb of C3H/HeSlc male mice aged 11-14 weeks old. When tumor diameters reached around 10mm, AVE8062 was injected i.p. at a single dose of 40 mg/kg to the mice. The mice were sacrificed by cervical dislocation 24 hours after AVE8062 administration, and the tumors were excised and immediately frozen with powdered dry ice. We obtained tissue section samples for PIXE analysis by cutting the frozen tumors in a cryostat.

Spatial distributions of principal elements in the the control and treated tumors have been obtained from the submilli-PIXE analysis at Tohoku University. It was found that AVE8062 treatment made significant differences in their spatial distributions between the untreated and treated tumors. Although the principal elements appear to be distributed uniformly in the tissue section of the control tumor, potassium and sulfur concentrations can be seen at the periphery of the treated tumor. In addition, a ring of calcium concentration has been found just inside the periphery of the treated tumor. It is suggested that the ring-shaped distribution of calcium observed just inside the tumor periphery is related to hypoxia-induced response.

[1] P. Hinnen and FALM Eskens, "Vascular disrupting agents in clinical development", *British Journal of Cancer* 96 (2007) 1159-1165.

[2] Dietmar W. Siemann, David J. Chaplin, Michael R. Horsman, "Vascular-Targeting Therapies for Treatment of Malignant Disease", *CANCER*, 100 (2004) 2491-2499.

O21 Role of copper, zinc, and selenium in uterine cervical cancer

P. Sarita^a, G. J. Naga Raju^a, S. Bhuloka Reddy^b

^aDepartment of Physics, Institute of Technology, GITAM University, Visakhapatnam-530 045, India.

^bSwami Jnanananda Laboratories for Nuclear Research, Andhra University, Visakhapatnam-530 003, India.

The objective of this study was to evaluate the levels of trace elements in blood sera of uterine cervix cancer patients, analyze their alteration with respect to healthy controls, ascertain the role played by them in the initiation, promotion and inhibition of cancer, and identify the best predictors amongst these for disease occurrence and progression. Moreover, the variation of trace elemental content in the sera of cervix cancer patients with the clinical stage of disease and with therapy was also studied. Particle induced X-ray emission (PIXE), a well established method for elemental analysis, was used in this work to identify and quantify trace elements in the blood sera of uterine cervix cancer subjects and healthy control subjects. The PIXE measurements were carried out using 2.5 MeV collimated proton beam from the 3 MV Tandem Pelletron Accelerator at Ion Beam Laboratory, Institute of Physics, Bhubaneswar, India. Among all the trace elements identified in this work, statistically significant alterations in serum levels of copper, zinc, and selenium were observed among the various studied groups. The observed alterations are discussed with respect to the possible mechanisms by which these elements might influence the carcinogenic process.

O22 Microcapsular imaging of malignant tumors and radiation-induced release of liquid-core microcapsules for their treatment

S. Harada^(a), K. Ishii^(b), T. Sato^(c), K. Sera^(d), S. Ehara^(a), M. Enatsu^(c), T. Kamiya^(c), S. Goto^(e)

^(a)Department of Radiology, School of Medicine, Iwate Medical University, 19-1 Uchimaru, Morioka, Iwate 020-8505 Japan.

^(b)Department of Quantum Science and Energy Engineering, School of Engineering, Tohoku University, 6-6, Aramaki Aza Aoba, Aoba-ku, Sendai, Miyagi 980-8579, Japan.

^(c)Takasaki Advanced Radiation Research Institute, Japan Atomic Energy Agency, 1233 Watanuki, Takasaki, 370-1292 Gunma Japan.

^(d)Cyclotron Center, Iwate Medical University, 348-58 Tomegamori, Takizawa, 020-0173 Iwate Japan.

^(e)Nishina Memorial Cyclotron Center (NMCC), Japan Radioisotope Association, 348-58 Tomegamori, Takizawa, 020-0173 Iwate Japan.

Purpose:

Basing on the study of PIXE and Micro PIXE camera, microcapsules of 2 types were designed: (1) CT-detectable anti- $\alpha\beta 3$ ($E[c(RGDfK)]_2$) microcapsules containing P-selectin and P-selectin glycoprotein ligand-1 (PSGL-1) to observe malignant tumors via $\alpha\beta 3$ -antigen-antibody accumulation, and (2) malignant tumors-treating microcapsules that release anticancer drug on irradiation and have a high affinity to P-selectin. To test the ability of these microcapsules for imaging malignant tumors and for treating them, we subject C3He/N mice with MM48 tumor to 2 radiotherapy sessions.

Methods and Materials.

For the first session, microcapsules were prepared by spraying a mixture of 4.0% alginate, 3.0% hyaluronic acid, and $1\ \mu\text{g}$ $E[c(RGDfK)]_2$ ($\alpha\beta 3$ antibody) into 0.5 mmol FeCl_2 , supplemented with $1\ \mu\text{g}$ P-selectin. Microcapsules for the second session were produced by spraying the above-mentioned mixture with 5mg carboplatin into 0.5 mol/L FeCl_2 containing 0.1 $\mu\text{mol/L}$ of PSGL-1 and the FcSv antibody against P-selectin [1]. In the first session, the microcapsules were intravenously injected, and 6 h later, the incipient metastatic foci were observed using CT. Subsequently, a 10- or 20-Gy ^{60}Co γ -radiation dose was administered. In the second session, 1×10^{10} microcapsules were intravenously injected 1 h before P-selectin expression peaked; the microcapsules were allowed to interact with P-selectin for 1–6 h after irradiation in order to deliver sufficient microcapsules. The second session was conducted in a similar manner to the first. The releasing of P-selectin or carboplatin were imaged using micro PIXE camera. The amount of carboplatin (Pt containing anticancer drug) were quantified, using PIXE.

Results.

The capsule and liquid core sizes (φ) were $2.3 \pm 0.92\ \mu\text{m}$ and $1.6 \pm 0.6\ \mu\text{m}$, respectively. The injected anti- $\alpha\beta 3$ $E[c(RGDfK)]_2$ microcapsules accumulated in the vascular endothelium of the incipient metastasis, and their kinetics and accumulation could be detected by CT. These accumulated microcapsules released P-selectin and PSGL-1 in response to the first irradiation. P-selectin, which was released from the microcapsules and whose expression was induced by the first irradiation, showed peak expression 6 h after irradiation: it was $78.2 \pm 3.4\%$ with the 10-Gy radiation dose and $86.3 \pm 4.6\%$ with the 20-Gy radiation dose. The microcapsules for radiosensitizing the metastasis were injected 5 h after the first session. Their accumulation was maximum at 3 h after the injection. After the second session, the microcapsules released carboplatin, which increased significant regression of tumors.

Thus, better diagnosis and treatment of incipient metastasis are possible with our microcapsules.

[1] S. Harada, S. Ehara, K. Ishii, et.al. Int. J. Radiat. Oncol. Biol. Phys. 75 (2) (2009) 455-462

O23 The upgraded external-beam PIXE/PIGE set-up at LABEC for very fast measurements on aerosol samples

F. Lucarelli^(a), G. Calzolai^(a), M. Chiari^(a), D. Mochi^(a) and S. Nava^(a)

^(a) Department of Physics, University of Florence and INFN, Florence, Italy

Particle Induced X-ray Emission (PIXE) technique has been widely used since its birth for the study of the aerosol composition, and for a long time it has been the dominating technique for its elemental analysis. However now it has to compete with other techniques, like Induced Coupled Plasma and detection by Atomic Emission Spectroscopy (ICP-AES) or Mass Spectrometry (ICP-MS) or Synchrotron Radiation XRF (SR-XRF). To remain competitive, a proper experimental set-up is important to fully exploit PIXE capabilities. At LABEC, an external beam line is fully dedicated to PIXE-PIGE measurements of atmospheric aerosols [1]. Recently SDD (Silicon Drift Detectors) have been introduced for X-ray detection thanks to their better resolution with respect to Si(Li) detectors and the possibility of managing high counting rates (up to 50 kHz at 0.5 msec shaping time). This implies, in turn, the possibility of using very high beam currents thus drastically reducing the measurement time. However their use for a complete characterization of X-rays was limited by the small thickness and surface areas available. Now SDD with a thickness of 500 nm and 80 mm² area have been introduced in the market. We have therefore replaced the Si(Li) detector used so far for the detection of medium-high Z elements with such a SDD. A comparison of the two detectors has been carried out; PIXE minimum detection limits (MDLs) at different proton beam energies have been studied to find out the best energy for PIXE measurements on aerosol samples collected on different substrata, namely Teflon, Kapton, Nuclepore and Kimfol, used for daily or hourly sampling or for cascade impactors. In particular in the case of Teflon filters, the production of g-rays by F in the Teflon filter limits the current which may be used and the Compton g-ray background worsens the MDLs. Due to the lower thickness of the SDD detector with respect to a typical Si(Li) detector, these problems are reduced; therefore beam currents 10 times higher or more may be used and consequently measuring time as low as 1 minute per sample can be attained and MDLs are improved. Similar improvements are obtained in the analysis of filters collected with the streaker sampler, with measuring times which become comparable to the ones used with SR-XRF (every hourly spot can be analyzed in times down to the minute). Obviously the higher the currents the shorter the life time of the 7.5 mm thick Uplex extraction, forcing several precautional changes of the window during a day of measurements. Therefore we have implemented a 500 nm thick Si₃N₄ membrane as new and durable extraction window. Some example of applications with this upgraded set-up will be presented.

[1] G. Calzolai, M. Chiari, I. García-Orellana, F. Lucarelli, A. Migliori, S. Nava and F. Taccetti, *Nucl. Instr. & Meth.* 2006; B249, 928.

O24 Complex study of indoor aerosols at a kindergarten, an elementary school and a secondary grammar school

Z. Szoboszlai^(a), E. Furu^(a,b), A. Angyal^(a), Zs. Török^(a,b) and Zs. Kertész^(a)

^(a)Institute of Nuclear Research of the Hungarian Academy of Sciences (ATOMKI), H-4001 Debrecen, P.O.Box 51, Hungary

^(b)University of Debrecen, H-4010 Debrecen, Egyetem tér 1, Hungary.

It is well known that exposure to particulate matter during school-age, when children are in their gowning stage, can have lifelong adverse effects on their health. Because most of the children spend at least 30 % of their time in educational institution, it is particularly important to better investigate these microenvironments.

In our previous study [1], which was carried out in the heating season in three urban educational institutions (a kindergarten, an elementary school and a secondary grammar school) in Debrecen, we found high concentration of coarse aerosols and showed that the concentration increased in the lower educational levels. The goal of present study was to characterize and compare the mass concentration, elemental composition and mass size distribution of particle matter sampled in a heating and non-heating season in these three schools. The coarse and fine fractions of particulate matter were characterized by gravimetry, particle-induced X-ray emission (PIXE) and in some cases by micro-PIXE and scanning electron microscopy (SEM). In the non-heating season, we found that the concentrations followed the trend which was observed in the non-heating season ($C_{\text{kind.g.}} > C_{\text{elem. sch.}} > C_{\text{sec.gr.sch.}}$) but the amount of the PM concentration was lower than in the heating season (Figure 1.). We also found that the concentrations of coarse aerosols were higher inside the institutions than in outdoor in the non-heating season. On the basis of elemental concentration, we observed that most part of the PM mass inside the institutions was originated from the crust and transported from outdoors through the windows and foot transport in all seasons. Other significant part of the PM was derived from local indoor sources such as detergents, chalk, building materials, magnesia powder, and chemical reactions from the chemistry laboratory. On the basis of the obtained data, the total and regional deposition efficiencies of the different types of particles within the human respiratory system were also calculated by using a stochastic lung deposition model.

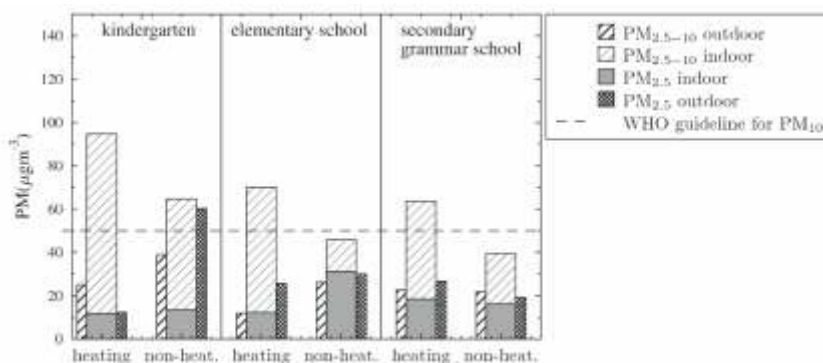


Figure 1. PM_{2.5} and PM_{2.5-10} average concentrations in a heating and non-heating season in the three educational institutions.

Acknowledgement

The work was supported by the TÁMOP-4.2.2/B-10/1-2010-0024 project and co-financed by the European Union and the European Social Fund. This work prepared in the frame of the János Bolyai Research Scholarship of the Hungarian Academy of Sciences.

[1] Z. Szoboszlai, E. Furu, A. Angyal, Z. Szikszai Zs. Kertész, Investigation of indoor aerosols collected at various educational institutions in Debrecen, Hungary X-RAY SPECTROMETRY 40:(3) (2011) 176-180.

O25 Characterization and source estimation of size-segregated aerosols during 2008-2012 in an urban environment in Beijing

Lingda Yu^a, Guangfu Wang^{a,c,*}, Renjiang Zhang^b

^aKey Laboratory of Beam technology and Materials Modification of Ministry of Education, College of Nuclear Science and Technology, Beijing Normal University, Beijing 100875, China

^bKey Laboratory of Regional Climate-Environment Research for Temperate East Asia (RCE-TEA), Institute of Atmospheric Physics, Chinese Academy of Science, Beijing 100029, China

^cBeijing Radiation Center, Beijing 100875, China

During 2008-2012, size-segregated aerosol samples were collected using an eight-stage cascade impactor at Beijing Normal University (BNU) Site, China. These samples were analyzed using particle induced X-ray emission (PIXE) analysis for concentrations of 21 elements consisting of Mg, Al, Si, P, S, Cl, K, Ca, Ti, V, Cr, Mn, Fe, Ni, Cu, Zn, As, Se, Br, Ba and Pb. The size-resolved data sets were then analyzed using the positive matrix factorization (PMF) technique in order to identify possible sources and estimate their contribution to particulate matter mass. Nine sources were resolved in eight size ranges (0.25 ~ 16 μ m) and included secondary sulphur, motor vehicles, coal combustion; oil combustion, road dust, biomass burning, soil dust, diesel vehicles and metal processing. PMF analysis of size-resolved source contributions showed that natural sources represented by soil dust and road dust contributed about 57% to the predicted primary particulate matter (PM) mass in the coarse size range (>2 μ m). On the other hand, anthropogenic sources such as secondary sulphur, coal and oil combustion, biomass burning and motor vehicle contributed about 73% in the fine size range (<2 μ m). The diesel vehicles and secondary sulphur source contributed the most in the ultra-fine size range (<0.25 μ m) and was responsible for about 52% of the primary PM mass.

*Corresponding author. Tel.: +86 10 62208271; fax: +86 10 62208271.

E-mail address: guangfu_w@bnu.edu.cn (G. Wang)

O26 Metallic objects belonging to the first emperor of Brazil studied with PIXE technique

V.C. Ambiel^(a), [M.A. Rizzutto](mailto:rizzutto@if.usp.br)^(b), J. F. Curado^(b), P.H.O.V. Campos^(b), E.A.M. Kajiya^(b) and T.F.Silva^(b)

(

^{a)}*Museu de Arqueologia e Etnologia da Universidade de São Paulo, Av. Prof. Almeida Prado, 1466, São Paulo, SP, Brasil;*

^(b)*Instituto de Física da Universidade de São Paulo; Rua do Matão, Travessa R, 187, São Paulo, SP, Brasil, rizzutto@if.usp.br*

First Emperor of Brazil, D. Pedro I is one of the main personalities in the history of Brazil and was responsible for the formation of the 'Brazilian nation', in September 7. With the death of King D. João VI in 1826, was acclaimed King Pedro IV in Portugal, however, held the office for a week and abdicated in favor of her daughter, Maria da Gloria. Due to political problems he also abdicated the Brazilian throne, in 1831, in favor of his son Pedro II. D. Pedro died on September 24 of 1834 at the Palace of Queluz, in Cintra and was buried in the Pantheon of the Royal House of Bragança, in Lisbon, Portugal. However in 1972, during celebrations of the 150th anniversary of the Independence of Brazil, his remains were moved to the Imperial Chapel in Monument Ipiranga installed in the city of São Paulo, Brazil. In the year 2012, was initiated a study in the Emperor including the exhumation, the inventory associated with it and several physical-chemical studies. The analyses have been performed with non-destructive techniques such as X Ray Fluorescence (XRF) in various classes of objects, including bones, tissues and metals and also Particle Induced X-Ray Emission (PIXE) in the metal objects. This article presents the PIXE results obtained for the set of metallic artifacts such as cufflinks and medals that show a wide variation in chemical composition with alloys formed mainly of copper and zinc and also made of alloys containing silver and gold. It was also verified the presence of lead and calcium, probably due to contamination suffered in the environment in which materials were found, particularly the remains were originally kept in a coffin of lead. The analyses also indicate some degree of deterioration of these objects.

O27 OLDAPS – Obsidian Least Destructive Analysis Provenancing System

F.M. Eder^(a,b), C. Neelmeijer^(b), N.J.G. Pearce^(c), J.H. Sterba^(a), M. Bichler^(a), S. Merchel^(b)

^(a) Atominstitut, Vienna University of Technology, Stadionallee 2, 1020 Vienna, Austria

^(b) Helmholtz-Zentrum Dresden-Rossendorf (HZDR), D-01314 Dresden, Germany

^(c) Institute of Geography and Earth Sciences, Aberystwyth University, SY23 3BD, Wales, UK

The natural volcanic glass obsidian is one of the classical objects of archaeometric analyses. Reliable provenancing by means of the highly specific chemical composition, the “chemical fingerprint”, can provide information about trading routes, extension of territory, long-distance contacts and the mobility of prehistoric people.

Since the pioneer work of Cann and Renfrew in 1964 [1] various analytical methods have been employed on obsidian samples in order to locate their provenance. The existing data already offers important knowledge about long-distance interactions between prehistoric human populations. However, most applied techniques just show a small part of the element spectrum. Latest studies showed that published results gained by different analytical methods are not consistent due to systematic errors [2-3].

Therefore, the application of three complementary analytical techniques on the same set of raw material samples allows both a better characterization of obsidian sources and a comparison and validation of analytical results. The aim of this multi-methodical approach is to apply in particular:

- Ion Beam Analysis (IBA) comprising of Particle Induced X-ray Emission (PIXE) and Particle Induced Gamma-ray Emission (PIGE),
- Instrumental Neutron Activation Analysis (INAA),
- Laser Ablation-Inductively Coupled Plasma-Mass Spectrometry (LA-ICP-MS)

to detect a maximum element spectrum and to compare element concentrations determined with at least two analytical techniques. This approach should check the accuracy and reliability of analytical results and should show a maximum of compositional differences between European obsidian sources to reveal the most characteristic “chemical fingerprint” composed of more than 40 elements.

These investigations are part of a new multi-methodical analytical database called the “Obsidian Least Destructive Analysis Provenancing System” (OLDAPS). This novel scientific approach for provenancing obsidian artefacts found in archaeological contexts contributes to both conservation and prehistoric research by ensuring a minimum of destruction to gain a maximum of information. Besides, it enables to assess analytical accuracies of our archaeometric elemental analyses

For this study, IBA, INAA and LA-ICP-MS measurements have been applied to the most relevant obsidian sources in central and southern Europe. IBA studies have been carried out using the external 4 MeV proton beam of the 6 MV Tandem accelerator of the Ion Beam Centre of HZDR. INAA investigations have been performed in the TRIGA Mark II 250 kW research reactor of the Atominstitut in Vienna. LA-ICP-MS measurements have been taken with the Thermo Element 2 ICP-MS coupled to an ArF gas Excimer laser system at the Aberystwyth University.

[1] J.R. Cann, C. Renfrew, Proc. Prehist. Soc. 30, (1964) 111-131.

[2] R.G.V. Hancock, T. Carter, J. Archaeol. Sci. 37, (2010) 243–250.

[3] G. Poupeau et al., J. Archaeol. Sci. 37, (2010) 2705-2720.

O28 Analysis of archaeological precious stones from Slovenia

Ž. Šmit^(a,b), H. Fajfar^(b), M. Jeršek^(c), T. Knific^(d), A. Kržič^(e), and J. Lux^(f)

^(a)Faculty of Mathematics and Physics, University of Ljubljana, Jadranska 19, SI-1001 Ljubljana, Slovenia

^(b)Jožef Stefan Institute, Jamova 39, SI-1000 Ljubljana, Slovenia

^(c)Slovenian Museum of Natural History, Prešernova 20, SI-1000 Ljubljana, Slovenia

^(d)National Museum of Slovenia, Prešernova 20, SI-1000 Ljubljana, Slovenia

^(e)Higher Vocational Centre, Kraška ul. 4, 6210 Sežana, Slovenia

^(f)Institute for the Protection of Cultural Heritage of Slovenia, Metelkova ul. 6, SI-1000 Ljubljana, Slovenia

Precious stones have been attractive pieces of jewelry since ancient times. However, due to their limited sources of origin, the quality of applied items mainly depended on long-range commercial relations, but also on fashion. In Antiquity and Late Antiquity, stones much used and sought for were emeralds and garnets. In Slovenia, emeralds are typically related to the early Roman period and are incorporated in the finds of gold jewelry from the graves. Emerald is generally beryl colored by admixture of chromium, though green colors can also be due to admixtures of iron or vanadium. Garnets were increasingly used by various nations of the People Migration period, and mounted in gilded silver or gold objects by 'cloisonné' or 'en cabochon' techniques. In Slovenia, numerous jewelry items containing garnets were found in the graves and in post-Roman fortified settlements. Geologically, according to the admixtures of metal ions, the garnets are divided into several species, while the most common among archaeological finds are almandines and pyropes and their intermediate types. It is also common to divide garnets into five groups, the first two originating from India, the third from Ceylon and the fifth from Czech Republic.

The measurements involved presumed emeralds from Roman jewelry finds in Slovenia and comparative samples of beryls from Siberia and Habachtal in Austria. The analysis determined the coloring ions and showed relations between particular stones. For garnets, ten samples from brooches, earrings and rings were selected for the analysis on the basis of previous micro Raman examination. The analysis was performed by a combined PIXE-PIGE technique using proton beam in air. The light elements of Na, Mg, Al were determined according to the emitted gamma rays, while X-rays were used for the elements heavier than silicon. Two X-ray spectra were measured in each measuring point, soft and hard X-ray; the latter was obtained using an additional absorber of 0.1 mm aluminum and a more intense proton current. In spite of the small sampling number, the results from analysis showed that the garnets of type 2 were the most numerous, which is different from the situation in France and Belgium with the predominance of type 1. Surprisingly, garnets from the Czech Republic were not found, in spite of quite close geographic distance.

O29 Renaissance enamels - colouring and state of preservation non-destructive studies by external PIXE–PIGE–RBS

C. Neelmeijer^(a), L. Hasselmeyer^(b), and J. Eulitz^(b)

^(a)Helmholtz-Zentrum Dresden-Rossendorf, POB 510119, D-01314 Dresden, Germany

^(b)Staatliche Kunstsammlungen Dresden, Mathematisch-Physikalischer Salon, Residenzschloss, Taschenberg 2, D-01067 Dresden, Germany

The work mechanism of the orbit clock, a masterpiece of Eberhard Baldewein in the 1560s [1] and permanent exhibit in the Math.-Phys. Salon of Dresden, houses in a fire-gilded brass body carrying rich silver-made ornamental strips plus decorative ornaments of coloured enamel. Recently, this unique object of art was under general restoration. PIXE analysis of dismount metal pieces searched for differences in composition possibly revealing former coaction of several workshops. Substantial studies of enamels used PIXE, PIGE and RBS simultaneously at the external 3.85 MeV proton beam in He-atmosphere, allowing both the detection of elements $Z \geq 5$ and, in particular by RBS, the identification of surface deterioration [2].

The detailed enamel artworks show opaque but also translucent layers lying upon another for achieving visual depth effects or being singly arranged on/between gold (sometimes silver) ornamentation. Chromaticity of the vitreous materials was induced due to embedding of specific metallic ions. In accordance with ref. [3] the enamels under analysis – red, green, brown, blue, black, white – show the corresponding accompanying elements – Cu, Cu plus Fe, mainly Fe, Co plus Cu, Mn plus Fe, Pb plus Sn – respectively. Enamel composition analysis (wt% of elemental oxides) took place in consideration of small adjacent gold or silver filigrees casually hidden by the proton beam. Maximum MnO concentration of 9% was obtained for black enamel improved by 1% CoO. The translucent red material (~2% CuO) includes ~1% MnO for plastic shading effects. Tints of green enamel were tuned by the addition of both ~10% Cu- and ~6% Fe-oxide. A brown-orange detail shows 22% Fe₂O₃ plus 0.4% CuO. Just about 1% CoO proves quite enough for blue enamel colouration, shaded by adding ~6% CuO.

For blue, black and green enamels the concentrations of the glass network former SiO₂ are in the order of 60% or above, just sufficient for resistance to humidity (hydrolysis, leaching) [2]. High concentration of 10-20% Na₂O (fluxing agent) along with only 2-8% K₂O (network modifier) contribute to the enamel long-term stability. These criteria, ensuring durability, are diminished in case of the red material characterized by C_{SiO₂} < 60% and C_{K₂O} > 16%. Therefore, conservation activities should mainly concentrate on decorations made from red enamel. Altogether, not one of the RBS spectra identifies oxygen enrichment in the vicinity of the enamel surface as a characteristic signal of progressing leaching effects [2].

Two positions were found pointing to potential earlier restoration work. The small blackish detail of a complex ornamentation shows 1% MnO only but nearly twice of the current concentrations for both Fe₂O₃ and CoO. In addition, the RBS spectrum shows a striking carbon surface-signal reflecting probably carbon containing material for blackening. On a peculiar opaque detail of CuO-based light blue enamel Co is missing and Pb originates from potential lead white pigment.

[1] http://www.tschirnhaus-gesellschaft.de/e_g_mps.html

[2] M. Mäder, C. Neelmeijer, Nucl. Instrum. Methods Phys. Res., Sect. B 226 (2004) 110-118.

[3] K. H. Wedepohl, Die Herstellung mittelalterlicher und antiker Gläser, F. Steiner, Akademie der Wissenschaften und der Literatur, Mainz, Stuttgart, 1993

O30 PIXE analysis of Cs in soil and rice plants

H. Sugai, K. Ishii, S. Matsuyama, A. Terakawa, Y. Kikuchi, H. Takahashi, A. Ishizaki, F. Fujishiro, H. Arai, N. Osada, M. Karahashi, Y. Nozawa, S. Yamauchi, K. Kikuchi, S. Koshio, and K. Watanabe

Department of Quantum Science and Engineering, Tohoku University,
6-6-01-2Aza-Aoba, Aramaki, Aoba-ku, Sendai 980-8579, Japan

A huge earthquake and a huge tsunami, which is called the Great East Japan Earthquake, hit Northeastern Japan on 11 March, 2011. Especially it caused the Fukushima first nuclear plant's accidents, a great deal of radioactive materials were scattered around Northeastern Japan. Among the scattered radioactive materials, radioactive isotopes ^{134}Cs and ^{137}Cs have not-so-short half lives. Since about 70% of fallout Cs is strongly bound to clay in soil [1], most of fallout Cs don't transfer to plants. However it has become a problem that some plants absorb radioactive Cs well. To solve such a problem, how radioactive Cs distribute in soil and plants may become a clue.

Since behaviors of radioactive Cs and stable ^{133}Cs in plants should be identical, the distribution of stable Cs in plants which were grown in a stable Cs-added soil may be regarded as that of radioactive Cs. Meanwhile, concentration of radioactive Cs in soil is very low. From these points of view, we added a small quantity of Cs_2CO_3 as stable Cs to soil, and grew rice plants in the soil. After cultivation, we investigated the distribution of stable Cs in soil and rice plants by means of PIXE. The PIXE experiments were conducted with a submilli-beam line and a micro-beam line at the Fast Neutron Laboratory, Tohoku University. Figure 1 shows a typical X-ray spectrum of soil sample (left side) and elemental maps of Fe and Cs obtained by PIXE analysis (right side). Although concentration of Cs is low, it seems that Fe and Cs distribute in the same way in soil. In this presentation, we will report results of analyses of stable Cs in soil and rice plants mainly.

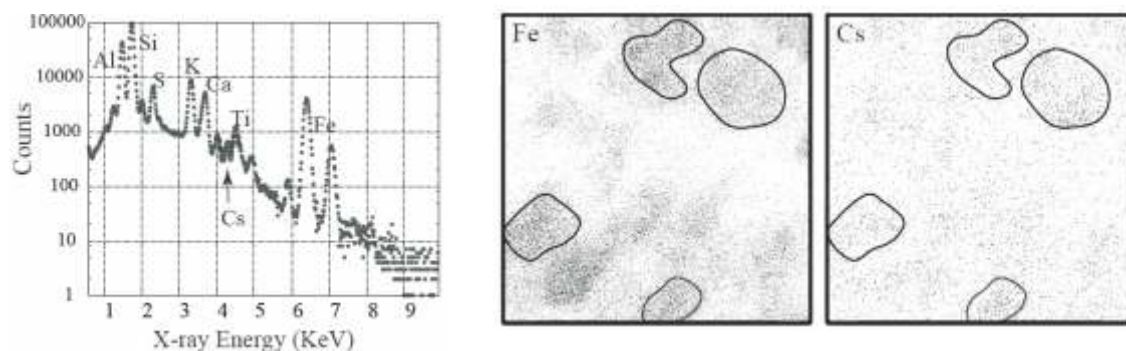


Figure 1. (Left side) A typical X-ray spectrum of soil sample. (Right side) Elemental maps of Fe and Cs obtained by PIXE analysis.

[1] Hirofumi Tsukada, Akira Takeda, Shun'ichi Hisamatsu, Jiro Inaba, Journal of Environmental Radioactivity, Vol. 99, 6 (2008) 875-881.

O31 Low energy PIXE analysis of Nigerian Flour and Bread samples

F.S. Olise^(a), A. Fernandes^(c), P.C. Chaves^(c), A. Taborda^(b,c), M.A. Reis^(b,c)

(a) Department of Physics, Obafemi Awolowo University, Ile-Ife, 220005, Nigeria;

(b) IST/ITN, Instituto Superior Técnico, Universidade Técnica de Lisboa, Campus Tecnológico e Nuclear, EN10, 2686-953 Sacavém, Portugal;

(c) Centro de Física Atómica da Universidade de Lisboa, Av. Prof. Gama Pinto 2, 1649-003 Lisboa, Portugal

The reported usage of potassium bromate in baking bread resulted in few authors reporting some chemical methods of determining its levels in the Nigerian popular staple food. In order to examine the potentials of PIXE, we analyzed twenty samples of flours, dough and bread in a production batch as well as breads on sale for consumption at Ile-Ife, Southwestern Nigeria. The samples were collected from five different outlets with the flour air-dried while the dough was freeze dried at about -16°C . The samples were then homogenized in an agate mortar and subsequently pelletized. Samples were analysed using two proton beam energies, namely 1.25 MeV and 2.15 MeV at the standard PIXE setup of CTN. In some samples significant concentration of bromine were found. In the present work we present possible origins for the presence of this eventually dangerous contamination in the bread flour samples.

[1] Baker, J. T., (2009). Potassium Bromate. Environmental Health and Safety, material safety data sheet (MSDS), U.S.A, MSDS No. P5576.

[2] Ekop A.S., Obot, I. B. and Kpatt, E. N., (2008). Anti-Nutritional factors and potassium Bromate content in Bread and flour sample in Uyo metropolis, Nigeria. E- Journal of chemistry, 5(4), 736-741.

[3] Emeje E.O., Ofoefule, S.I., Nnaji, A. C., Ofoefule, A. U. and Brown, S. A., (2010). Assessment of Bread Safety in Nigeria: Quantitative determination of potassium bromate and lead. African Journal of food science, 4(6), 394-397.

O32 Characterization of elemental ammunition manufactured in Brazil

Anaí Duarte^(a), Luiza Manfredi^(a,b), Carla Eliete Lochims dos Santos^(a), Livio Amaral, Johnny Ferraz Dias^(a)

^(a) Physics Institute, Federal University of Rio Grande do Sul, CP 15051, CEP 91501-970, Porto Alegre, RS, Brazil.

^(b) Instituto Geral de Perícias, Av. Princesa Isabel, 1056, CEP 90230-010, Porto Alegre, RS, Brazil.

When a firearm is discharged, microscopic particles of this weapon (GSR - Gunshot Residues) are deposited in the body of the shooter, contaminating hands, skin, clothes and hair.^{1,2} These particles stem from the condensation reaction at high pressure which occurs when a gun is fired and are composed of material from the primer, projectile, case and gun itself. Therefore, its composition varies according to the type of weapon and ammunition employed.

The largest ammunition company in Brazil is Companhia Brasileira de Cartuchos (CBC)³, which maintains monopoly in the country and export to several countries. Indeed, it has consolidated markets in America, Europe and Latin America.

This work aims to obtain the elemental characterization of ammunition produced by the CBC. The samples of ammunition used in this work were provided by the Ballistics Section of the Department of Criminalistics (Instituto General de Perícias - IGP) located in Porto Alegre. The ammunition under study is the 38 SPL caliber, ogival lead type (CHOG), which was chosen with the criterion of being one of the most widely used both by police and by criminals. The analysis were carried out with PIXE (Particle-Induced X-ray Emission) employing 2.0 MeV Protons. The qualitative results are shown in **Figure 1a** and **Figure 1b**.

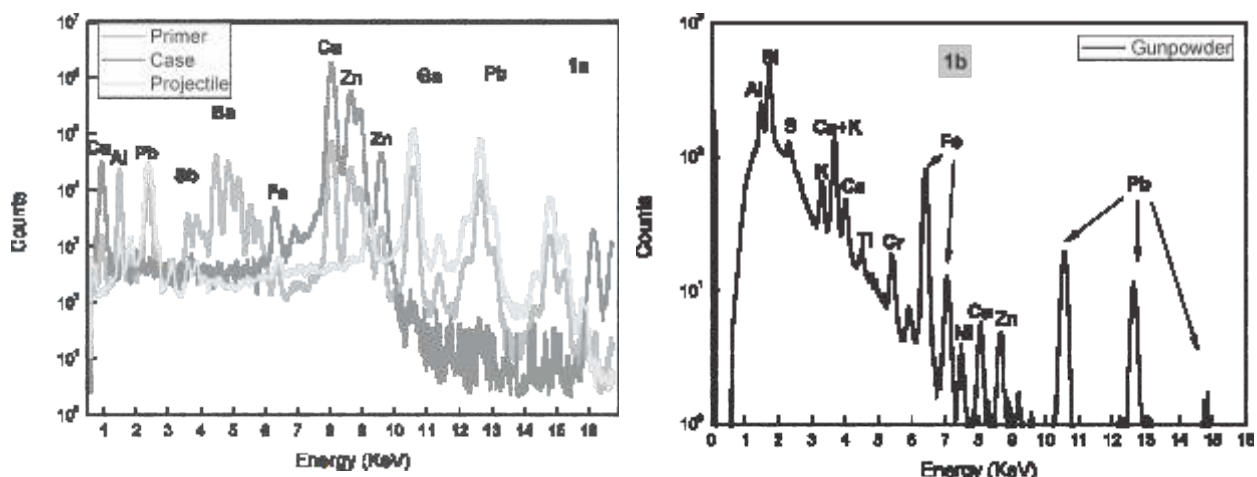


Figure 1a. Qualitative PIXE spectra obtained from samples of the .38 SPL CHOG ammunition type (case, primer and projectile). **Figure 1b.** Qualitative PIXE spectrum obtained from samples of the .38 SPL CHOG ammunition type (gunpowder). Counts were normalized by the total charge of each irradiation.

We can observe in **Figure 1a** that the primer is composed of aluminum, antimony (antimony trisulfide), barium (barium nitrate), lead (lead estifinato), copper, zinc and iron (enclosure). The case consists of copper, zinc (brass) and iron, and the projectile is basically composed of lead, antimony and gallium. In **Figure 1B** are the elements present in the gunpowder are aluminum, silicon, sulfur, potassium, calcium, titanium, chrome, iron, nickel, copper, zinc and lead.

As a next step, we intend to carry out tests of shooting with this ammunition, and then the residues will be collected and analyzed with micro-PIXE.

[1] M.J. Bailey, K. J. Kirkby and C. Jeynes. X-Ray Spectrometry (2009) 190–194.

[2] M.J. Bailey and C. Jeynes. Nuclear Instruments and Methods in Physics Research B. 267 (2009) 2265–2268.

[3] <http://www.cbc.com.br/>, accessed in 27/08/2012.

O33 Development of particle induced x-ray emission facility at cyclotron laboratory and its prospective applications

Dr. N.K. Puri^(a), M.L. Garg^(b), I.M. Govil^(c)

^(a) Assistant Professor, Department of Applied Physics, Delhi Technological University (Formerly Delhi College of Engineering, DCE), Delhi, India, 110042

^(b) Professor, Department of Bio-Physics, Panjab University, Chandigarh, India

^(c) Emeritus Professor, Department of Physics, Panjab University, Chandigarh, India

We are presenting here a description of modifications in the Variable Energy Cyclotron (VEC) Chandigarh along with the installation of Proton Induced X-ray Emission (PIXE) setup. The installation of new main magnet power supply of 400A/125V out put with 10 ppm stability (model 853 M/S Danfysik, Denmark) and a new stabilized solid state power supply for RF oscillator gave the beam characteristics substantially good enough for PIXE work. A new chamber [1] was designed to cater for Proton Induced Gamma Emission (PIGE) and Rutherford Back Scattering (RBS) analysis along with PIXE measurements. The HPGe x-ray detector, the Ge(Li) -ray detector and a Silicon Surface Barrier (SSB) detector could be mounted simultaneously in the chamber. A Turbo-Molecular vacuum pump was provided to produce a clean vacuum of the order of 10^{-7} torr in PIXE chamber. A remotely controlled stepper motor could move the 12/24-position target holder. Beam size optimization along with the minimization of background was done with the help of graphite collimators, thus making the setup suitable for practical applications. We attempted to address some of the limitations using PIXE facility of Institute of Physics (IOP), India [2] and incorporated modifications (e.g. chamber design, sample holder etc.) in our set-up. Preliminary experiments for the PIXE analysis of aerosol samples, gunshot residues samples and bone samples were presented. The aerosol samples were collected using aerosol sampling kit which involves Millipore diaphragmatic vacuum pump and Sequential Filter Unit (SFU) with coarse pored Nucleopore polycarbonate filter in such a manner that the particles passing through the 8m pore size filter were collected on the 0.4m pore size filter. Two different pistols viz. 7.65mm Indian made and 7.63mm Germany made were used to fire at a filter paper target with card board and cotton wool backing from a distance of 3 feet. Two sheets of Whatman filter paper were used to form the target. The GSR were deposited on the front filter paper, while the back filter paper protects the front one from any contamination's due to the backing material. The proton beam was bombarded on the contact ring on the front filter paper and the PIXE spectrum was taken. To see the variation of metal composition, three bone species (normal, demineralized and deproteinized) along with graphite material were run. The graphite material was used as a binder and making the targets conducting. Bone is composed of 40% organic material and the rest is mineral. From the bone spectra we could state that K is observed only in the deproteinised bone sample. The Mn to Fe ratio was more in the demineralised bone as compared to normal and deproteinised bone. This PIXE facility is fully functional and we are working on low energy X-ray spectroscopy and analytical applications for medical, archaeological, geological, aerosol, GSR samples etc.

[1] K.Malmquist et. al. J. Radioanal. Chem., 74, (1982) 125

[2] N.K. Puri et. al. IJPIXE, vol. 13, Nos. 3 & 4 (2003) 149-161

PI X E 2013

FOR TECHNOLOGY AND GLOBAL DEVELOPMENT

POSTER SESSION A

Tuesday

PA01 - PA35

PA01 Investigations of metal correlation in bile, gallstones and blood of Urolithiasis patients by PIXE using a peltier cooled X-ray detector

Daisy Joseph^a, Narayana Kalkur^b, Aslin Shameena^b, Arul Thanigai^b

(a) Nuclear Physics Division, BARC, Trombay, Mumbai-400706

(b) Anna University, Chennai

Investigations was carried out on 50 samples consisting of bile, gall stones, urinary stones, to obtain correlation of trace elements with severity of Urolithiasis diseases in patients from Hospitals in Chennai using PIXE. Urolithiasis is the condition where stones are formed in the urinary tract. In India it has affected million of people every year and the recurrence rate is more than 50%. The main component of urinary calculi includes Calcium Oxalate, Phosphate, Uricacid, Magnesium, Ammonium Phosphate (struvite) and cystine. A Proton beam of 3.5 Mev and a current of 20 nA from the Folded tandem ion Accelerator (FOTIA) was used for generating the Characteristic X-rays from the targets which were detected by a Peltier cooled detector and stored in PCA for off-line analysis. The main objective of this study was to identify the impact of toxic substance on human health in particular with crystal deposition diseases and also to find the epitaxial relationship between various crystalline components found in biological fluids Varying amounts of K, Ca, Cr, Mn, Fe, Sr, Zr were detected in the samples. Analysis and interpretation are on for a definite conclusion regarding the status of the diseases.

PA02 PIXE and XRF analysis of atmospheric aerosols from a site in the West area of Mexico City

R.V Díaz^(b), J. López-Monroy^(b), J. Miranda^(b), A.A. Espinosa^(b)

^(b) Instituto Nacional de Investigaciones Nucleares, Centro Nuclear "Nabor Carrillo", Autopista México-Toluca, Salazar, Edo. Mex., Mexico, {raul.diaz@inin.gob.mx; jose.lopezm@inin.gob.mx}

^(b) Instituto de Física, Universidad Nacional Autónoma de México, Apartado Postal 20-364, 01000 México, D.F., Mexico, {miranda@fisica.unam.mx, albertoe@fisica.unam.mx }.

The pollution by atmospheric aerosols in the Metropolitan Area of Mexico City (MAMC) is still presenting issues that require deeper studies. Because of geographical factors, most of the MAMC features, on average, very similar characteristics. These include height above the sea level, climate, wind speed and direction, resulting in very uniform pollution levels in most of the traditionally studied sites. A site with different characteristics with respect to them, Cuajimalpa de Morelos, was selected for the present work. It is located to the West of the MAMC at 2,760 m above sea level (a.s.l.), in contrast to other sites (2,240 m a.s.l.); sub-humid area with lush vegetation, influenced by the forest of the "Desierto de los Leones" National Park. Here, the wind for most part of the day is directed towards the center of the MAMC, joining flows that run from North to South. This prevents the site from receiving influence of pollutants generated in the Northern industrial zone, Xalostoc or Naucalpan. Thus, it is expected that this area should present lower concentration of pollutants than the rest of the MAMC. Therefore, the present work is aimed to study the elemental composition of coarse ($PM_{10-2.5}$) and fine ($PM_{2.5}$) fractions of atmospheric aerosol samples collected in Cuajimalpa. The sampling period covered the cold-dry season in 2004-2005 (December 1st, 2004, to March 31, 2005), exposing polycarbonate filters with a Stacked Filter Unit (SFU) of the Gent design along 24 h, every two days. The samples were then analyzed with PIXE and X-ray Fluorescence (XRF), to obtain elemental concentrations. The EPA code *UNMIX* was used to determine the number of possible influencing polluting sources, which were then identified through back-trajectory simulations with the *HYSPLIT* modeling software. Four sources (mostly related to soil) were found for the coarse fraction, while the fine fraction presented three main sources (fuel oil, industry, and biomass burning).

Acknowledgement

The authors acknowledge the technical assistance of P. Villaseñor.

PA03 Challenges in understanding inner shell ionization by heavy ion impact

Dr. N.K. Puri

Assistant Professor, Department of Applied Physics, Delhi Technological University (Formerly Delhi College of Engineering, DCE), Delhi, India, 110042

L X-ray production cross sections have been measured for thin solid targets ($\sim 50 \mu\text{g}/\text{cm}^2$) of $_{57}\text{La}$, $_{58}\text{Ce}$, $_{60}\text{Nd}$ and $_{62}\text{Sm}$ for 35–60 MeV C^{4+} and O^{5+} ions. There is an increase in these cross sections with the increasing projectile energy and the ratio of its atomic number to the atomic number of the target nucleus (Z_1/Z_2). The measured L x-ray production cross sections have been compared with the predicted values of the first Born approximation (FBA) and of the ECPSSR theory that accounts for the projectile energy loss and Coulomb deflection and the perturbed stationary-state and relativistic nature of the L-shell. For C^{4+} ions, there is a reasonable agreement with the ECPSSR predicted values for the higher Z elements (Nd and Sm), while for the lower Z elements (La and Ce), the FBA is in a better accord with the data. For O^{5+} ions, the FBA gives a better agreement for all the elements than the ECPSSR theory.

The extensive research on X-ray Production cross-sections have been carried out all over the world on understanding the basics of ion atom interaction in last few decades. Still, more fundamental approach is needed to do experimental measurements and theoretical calculations of inner shell ionization by heavy ions. More precisely, the impact of ions heavier than protons, which involve numerous processes (e.g. multiple ionization, electron capture etc.), are not explained by experimentalists due to their complexity and therefore, it is still a challenging task before the scientists [2]. As far as L X-ray production cross-sections (e.g. rare earth targets with heavy ions, C and O, ions with different charge states) are concerned, our experimental results have shown us a need for more rigorous study and experiments which would result in addressing the problems associated with the HPGe efficiency in the difficult range of 3–8 keV spectra for better match with the theoretical predications. The other parameter is anisotropy (in the emission of photons) which should be taken into consideration for the the exact measurements of L X-ray production cross-sections [2,3].

[1] R. Mehta, N.K. Puri et al. NIMB, vol. 241, Issues 1-4, (2005), 63-68

[2] J. Miranda et al. Rev. Mex. Fis. S 53 (3) (2007) 29-32

[3] O.G. de Lucio and J. Miranda Rev. Mex. Fis. 50 (2004) 319

PA04 Thin and thick target PIXE analysis of the study of Cu²⁺ biosorption mechanism by the *Egeria densa*

F.R. Espinoza-Quiñones^(a), A.N. Módenes^(a), M.A. Rizzutto^(b), G.H.F. Santos^(a) and C.E. Borba^(a)

^(a) Department of Chemical Engineering- Postgraduate Program, West Parana State University, Campus of Toledo, rua da Faculdade 645, Jd. La Salle, 85903-000, Toledo, PR, Brazil.

^(b) Physics Institute, University of São Paulo, Rua do Matão s/n, Travessa R 187, 05508-900 São Paulo, SP, Brazil

In this work the PIXE technique was used to study of metal sorption mechanism by dead biomass. As biosorbent particulates of *Egeria densa* biomass was chosen in order to remove divalent copper from an aqueous solution. Several batch copper-sorption experiments were performed by using 0.3 g of *Egeria densa* dry biomass into 50 mL of aqueous solution containing 127 mgL⁻¹ Cu²⁺ at pH 5. PIXE measurements were performed in thick and thin target samples, which were prepared from treated *Egeria densa* biosorbents and aqueous solutions, respectively. Element concentration in thick target samples was determined by the Clara software. Based on the mass balance among the major elements in the biosorbent and aqueous solution before and after Cu-removal experiments, ion exchange process is suggested as the main mechanism.

PA05 EXAFS Measurements of Nickel/Nickel Oxide Nanoparticles and its comparison with TEM and XRD results

Arvind Agarwal, Manish Kumar Singh & Mohan Chandra Mathpal

Department of Physics, M. N. National Institute of Technology, Allahabad 211004 INDIA

We have synthesized the nickel nanoparticles by pulsed laser ablation. The nickel disc in sodium dodecyl sulfate (SDS) with surfactant concentration of 10mM and 20 mM. was used with the focused output of fundamental harmonic from Nd:YAG laser operating at the first harmonic ($\lambda = 1064 \text{ nm}$). The laser power was fixed at 35 mJ/pulse with 10 ns pulse width and 10 Hz repetition rate and was used for the ablation for 60 minute. Nickel oxide nanoparticles were synthesized by chemical method for different concentration of surfactant Cetyltrimethylammonium bromide (CTAB). The surfactant was used to provide favourable site for the growth of the particulate assemblies, which influences the formation process, including nucleation, growth, coagulation and flocculation. The materials used for synthesis were nickel chloride hexahydrate, sodium hydroxide (NaOH) and Cetyltrimethylammonium bromide (CTAB). UV-Visible absorption, X-ray diffraction, and Transmission Electron Microscopy techniques were used for the characterization of produced nanoparticles. The powder samples were characterized by XRD measurements using Cu-K α radiation at 40 KV with wavelength 1.5405 \AA . The EXAFS studies of pure nickel foil and for the synthesized nanoparticles with concentration 10mM of SDS show similar structures. The position of the main peak is same. The only difference was observed in the reduction of the amplitude, which can be attributed to the coordination number. The nearest neighbor distance was similar as for pure nickel foil. The Debye-Waller factor was also similar on comparison. There was no trace of oxide and hydroxide in the EXAFS data which suggest that the synthesized nanoparticles contain only nickel metal. The extended X-ray absorption fine structure (EXAFS) studies of calculated FEFF of nickel oxide and the synthesized nanoparticles with different concentration of CTAB show similar structures. In comparison to standard NiO spectra the reduction of the amplitude and a slight shift in peak position is observed, which can be attributed to the disordered system. The Fourier transform spectra reveal that the peaks of the synthesized samples and the reference are in very similar position, and the nearest neighbor distance is also similar. Study shows CTAB plays an important role in the growth process of NiO nanoparticles. An increase in surfactant concentration resulting in the decrease of crystal size, which is attributed to the selected adsorption of ions and their respective counter ions on the crystal faces during the growth of nanoparticles.

PA06 Comparison of mobile XRF and PIXE for geological core analysis

D. Strivay^(a), F.P. Hocquet^(a), A. Beckers^(b) and A. Hubert-Ferrari^(b)

^(a)Institut de Physique Nucléaire, Atomique et de Spectroscopie & Centre Européen d'Archéométrie, University of Liège (Belgium)

^(b)Geology department, University of Liège (Belgium)

Sediment cores provide fundamental information in environmental research studies like global climate change or pollution assessment. Several laboratory instruments based on X-ray fluorescence spectrometry have been developed these last years to analyze their elemental composition directly on the cores without any sampling.

We have improved our XRF mobile system [1,2] to allow analysis of this kind of samples by adding a fully-automatic scanning system and a specific software for data acquisition. Helium flux was also improved to allow better analysis of light element. This system is then now able to analyze by 1mm step 1 meter long cores in one time with detection of elements from Na to U.

At the same time, we have developed a similar system on the PIXE system installed on the extracted beamline of the IPNAS cyclotron. The cores are analyzed by a 3 MeV proton beam and X-rays are detected by two detectors, the first one with a filter for trace element analysis, the second with a helium flux to detect low energy X-rays. A specific translation system and data acquisition have also been developed.

In order to evaluate the advantages and disadvantages of both systems, we have analyzed a core coming from lake Hazar (Turkey) that was previously analyzed with an XRF Avaatech system. The results will be compared and discussed.

[1] F.-P. Hocquet, H.-P. Garnir, A. Marchal, M. Clar, C. Oger, D. Strivay, *X-ray Spectrometry* 37 (4), 2008, 304

[2] F.-P. Hocquet, H. Calvo del Castillo, A. Cervera, C. Bourgeois, C. Oger, A. Marchal, M. Clar, S. Rakkaa, E. Micha, D. Strivay, *Analytical and Bioanalytical Chemistry* 399 (9), 2011, 3109

PA07 PIXE Analysis of Cancer-Afflicted Human Bladder

G.J.Naga Raju^a, P.Sarita^a M.Ravi Kumar^a, S.Bhuloka Reddy^b

^aDepartment of Physics, institute of Technology , GITAM University, Visakhapatnam- 530 045, India

^bSwami Jnanananda Laboratories for Nuclear Research, Andhra University, Visakhapatnam-530 003, India.

The proton induced x-ray emission (PIXE) technique was used for analysis of trace elements in small quantities of biological samples. Both the biological samples of normal and cancer-afflicted human bladder tissues were studied. The present experiment was performed using a 3 MV pelletron accelerator at the Institute of Physics in Bhubaneswar, India. A proton beam of 3 MeV energy was used to excite the samples. NIST SRM 1577b Bovine Liver Tissue was used as external standards for the determination of trace element concentration in the biological tissue samples. The elements Cl, K, Ca, Ti, Cr, Mn, Fe, Ni, Cu, Zn, and Se were identified and their concentrations were estimated. The concentrations of Ti and Zn are lower ($p < 0.005$) and that of Cr, Mn, Fe, Ni, and Cu are significantly higher ($p < 0.001$) in cancerous tissues than that in normal tissues. The deficiency or excess of different trace elements observed in the cancer tissues relative to the normal tissues of bladder are correlated to the pathology of cancer.

PA08 External-beam PIXE analysis of aerosol samples at GIC4117 tandem accelerator laboratory of Beijing Normal University

WANG Guangfu^(a,b), YU Lingda^(a), ZHANG Renjiang^(c), LI Xufang^(a), WU Bingbing^(a),
AN Kun^(a), CHU Junhan^(a)

^(a)Key Laboratory of Beam Technology and Materials Modification of Ministry of Education, College of Nuclear Science and Technology, Beijing Normal University, Beijing 100875;

^(b)Beijing Radiation Center, Beijing 100875;

^(c)Key Laboratory of Regional Climate-Environment Research for Temperate East Asia (RCE-TEA), Institute of Atmospheric Physics, Chinese Academy of Sciences, Beijing 100029

The external-beam facility at GIC4117 tandem accelerator laboratory of Beijing Normal University for PIXE analysis has been introduced. The influence of different aerosol sampling membrane filters on the beam current measurement with a homemade Faraday cup was studied by analysis of a Mn($44.0\mu\text{g}/\text{cm}^2$) MicroMatter standards sample with different filters behind it. Average and the lowest of the external-beam PIXE analysis compared with in-vacuum PIXE over about 360 aerosol samples. External-beam PIXE analysis results of PM_{2.5} aerosol fractions collected on Teflon filters on daily basis over 2010 at south campus of Beijing Normal University also were shown.

PA09 Specific absorbed fraction of X-ray in tissues from human organs

H.C.Manjunatha^{(a),*}

^(a)Department of Physics, Government College for Women, Kolar, Karnataka, India.

X-rays are widely used in medical imaging and radiation therapy. The user of radioisotopes must have knowledge about how radiation interacts with matter, especially with the human body, because when photons enter the medium/body, they degrade their energy and build up in the medium, giving rise to secondary radiation. Calculations of the energy absorbed in a medium include not only the contribution of the uncollided photons from the source, but must also include the contributions from collided and secondary photons. In practice, this is done by multiplying the contribution of the uncollided photons by the energy absorption buildup factor. An accurate absorbed dose calculation needs specific absorbed fraction of energy. Geometric progression (GP) fitting method has been used to compute energy absorption build-up factor of Human organs such as Brain, Breast, Eye lens, GI track, Heart, Kidney, Liver, Lung, Lymph, Ovary, Pancreas, Testis and Skeleton-femur. The computed absorption build-up factor is used to estimate specific absorbed fraction of energy. The thickness of the medium up to 10mm and with penetration depth up to 40 mean free paths considered.

The dependence of specific absorbed fraction of energy on incident photon energy, penetration and the thickness of the medium have also been studied. The specific absorbed fraction of energy increases up to the E_{pe} and then decreases. Here E_{pe} is the energy value at which the photo electric interaction coefficients matches with Compton interaction coefficients for a given value of effective atomic number (Z_{eff}). The variation of specific absorbed fractions with energy is due to dominance of photoelectric absorption in the lower end and dominance of pair production in the higher photon energy region. In the lower energy end photoelectric absorption is dominant photon interaction process; hence specific absorbed fractions values minimum. As the energy of incident photon increases, Compton scattering overtakes the photoelectric absorption. It results multiple Compton scattering events which increases the value of specific absorbed fractions up to the E_{pe} and becomes maximum at E_{pe} . Thereafter (above E_{pe}), pair production starts dominating which reduces the value of specific absorbed fractions to minimum. The specific absorbed fraction of energy increases with penetration depth. With increase in penetration depth, thickness of the interacting material has been increased which results in increasing the scattering events in the interacting medium. Hence it results in large specific absorbed fraction of energy values. The computed specific absorbed fractions of energy values are more accurate than the data available in the literature because the variation of an effective atomic number with energy is also considered in the calculation.

PA10 Development of microscopic optics for high-resolution IL spectroscopy with proton microbeam probe

W. Kada, T. Satoh, A. Yokoyama, M. Koka, and T. Kamiya

Takasaki Advanced Radiation Research Institute, Japan Atomic Energy Agency

Combined techniques of PIXE and IL are currently investigated with proton microbeam for the precise analysis and imaging of microscopic targets [1]. Spectroscopy of IL is adaptable to simultaneous analysis with conventional in-air micro-PIXE system and able to characterize the chemical composition of the irradiation targets while the wavelength of the IL photons is strongly affected by the chemical-state of the elements [2]. However, IL was not well obtained from the targets with size of micrometers comparing to the PIXE analysis [3]. The sensitivity and the S/N ratio of IL detection are needed to be improved to perform spectroscopic analysis of the IL from such a micrometer-sized particulate targets.

In this study, we have developed a new optics for the IL measurement using confocal micro lens optics. Anti-reflection-coated convex lens was installed in a microbeam line of 3MV single ended accelerator for in-air micro-PIXE analysis system. The focal points of the lens were set on the irradiation target and input terminal of optical fiber. The effective focus area on the target was approximately $800 \times 800 \mu\text{m}$ considering chromatic aberration of the IL photons ranging 300 to 950 nm. Electrically-cooled back-thin CCD spectrometer was used for the spectroscopic analysis of IL with a wavelength resolution of 0.5 nm in the range of 200 to 950 nm. Photon counting unit was also employed for the monochromatic and panchromatic imaging of IL.

Spectroscopic observations of IL from microscopic mineral targets were performed using microbeam probe of 3 MeV H^+ with current of 1- 200 pA. Figure 1 shows an IL spectrum from an Al_2O_3 crystal with acquisition time of 15 ms. The IL spectrum had a maximum spectral resolution of 3 nm and single peak correspond to the impurity of chromium was clearly observed. The spectral analysis of IL was also applicable to the other natural mineral target and also particulate target like aerosols with different elemental and chemical compositions.

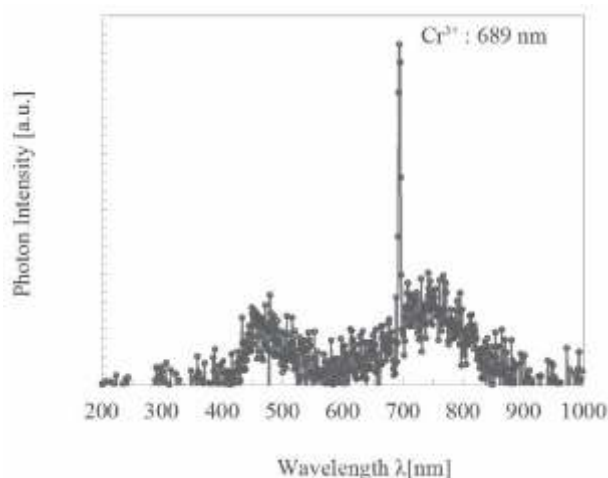


Figure 1. IL spectrum obtained from mineral sample of Al_2O_3 .

- [1] W. Kada, A. Yokoyama, M. Koka, T. Satoh, and T. Kamiya, *Int. J. of PIXE* 21 (2011) 1-11. [2] J.S. Laird, J. Wilkinson, C. Ryan, A. Bettiol, *Nuclear Inst. Meth. B*, 269 (2011) 2244-2250. [3] W. Kada, A. Yokoyama, M. Koka, T. Satoh, and T. Kamiya, *Int. J. of PIXE* 22 (2012) 21-27.

PA11 Studies on Pt-Mo Intermetallics by PIXE and other Analytical Techniques with High Resolution

M. Topic^a, Z. Khumalo^{a,b}, C.A. Pineda-Vargas^{a,c}

^(a) iThemba LABS, National Research Foundation, P.O. Box 722, Somerset West 7129, South Africa, email: mtopic@tlabs.ac.za, Tel: +27 21 843 1161, Fax: +27 21 843 3543

^(b) University of Cape Town, Physics Department, Private Bag X3, Rondebosch 7701, South Africa

^(c) Faculty of Health and Wellness Sciences, Cape Peninsula University of Technology, Belville, South Africa

The platinum group metals (PGMs) and their intermetallic compounds received particular attention in high temperature applications, in precipitation-strengthened alloys and because of their analogy with the nickel-based superalloys [1]. In addition to jewellery and glass industry, the ordered Pt-based intermetallic phases are of significant importance due to their enhanced electrocatalytic activity and magnetic characteristics. As such they are often used as catalysts or semiconductors [2,3].

In this study, the Pt-Mo coated system was used as a model system to investigate the formation of Pt-based intermetallics and their effects on physical, chemical and mechanical properties of coatings. A thin platinum layer of 0.2 microns was deposited by electron-beam deposition method on molybdenum substrate. The coated systems were afterwards annealed at different temperature and time conditions. The effects of elevated temperature on elemental distribution, coating morphology and phase transformation have been investigated by several analytical techniques with high resolution: (i) micro-PIXE (proton-induced X-ray emission), (ii) SEM (scanning electron microscopy with EDX) and (iii) X-ray diffraction (XRD).

The micro-PIXE and SEM/EDX results of the sample annealed at 1050 °C for 24 hours show the “island-type morphology”, increased surface roughness and a presence of areas having different Pt content. For micro-PIXE experiments, the region of 125 µm x 125 µm was scanned with a proton beam with energy of 3 MeV. A scan size using 128 x 128 pixels to construct the mapping content was used to ensure sufficient resolution for mapping visualisation. The concentration of Pt in the “islands” varied between 40 wt.% and 60 wt.% while approx. 20 wt% Pt was detected in surrounding areas. The EDX analyses were performed in different regions and spatial variations in chemical composition were obtained by area-chemical analyses. The spectrums (acquired in the backscattering mode) show app. 50 wt.% Pt : 50 wt.% Mo in the “white” regions and 40 wt.% Pt : 60 wt.% Mo in “grey” regions. These results indicate the presence of Pt-Mo phases with different stoichiometry. The X-ray diffraction analyses show the presence of two phases, PtMo and Pt₂Mo₃.

Based on the results obtained by the complementary techniques (PIXE, SEM, XRD) it appears that the kinetics of the present phenomena is possible through intermetallic compound formation at the interface between substrate and coating layer and the surface tension as a driving force.

In summary, an experimental condition was established for the formation of particular intermetallic compounds, which can be used to tailor the properties of coated systems depending on the required application.

[1] I.M. Wolf, Intermetallic Compounds—Principles and Practice, Ed. by J. H. Westbrook, R. L. Fleischer, John Wiley & Sons, Ltd. (2002) 3 (4)

[2] D. Lj. Stojic, T.D. Grozdic, M.P. Marceta Kaninski, V.D. Stanic, Int. J. of Hydrogen Energy 32 (2007) 2314 (2007)

[3] H. Ocken, J.H.N. van Vucht, J. of the Less Common Metals 15, (1968) 193

PA12 Elemental Characterization of Ammunition and Respective GSR from Clean Range Line (CBC ®)

Luiza R. Manfredi da Silva^(a,b), Anaí Duarte^(a), Carla E. Iochims dos Santos^(a), Lívio Amaral^(a), Maria Lúcia Yoneama^(a), J. F. Dias^(a), A. A. Petersen Xavier^(b)

^(a)Physics Institute, Federal University of Rio Grande do Sul, Av. Bento Gonçalves, 9500, CEP 91501-970, Porto Alegre (RS), Brazil.

^(b)General Institute of Forensic of Rio Grande do Sul

The presence of GSR (Gun Shot Residues) in the hands or clothes of an individual is of great interest as far as criminal investigation is concerned. These particles are formed when a shot is produced, from the condensation at high temperature and pressure of the compounds of the ammunition, consisting of material from the initiator mixture (primer), from the bullet, from the gunpowder and the from the cartridge case [1]. While the characteristics of the GSR generated by shots with conventional ammunition were already well known [2], the study of residues generated from the so-called "clean ammunition" or "nontoxic" is scarce.

Clean ammunition were developed aiming to produce less harmful residues to the environment and especially to the health of shooters who practice indoor shooting. The residues produced by this ammunition have been studied in the last years, but so far there was no technique able to identify them, since its characteristics were not yet well known.

Although the clean ammunition is not yet commercially available in Brazil, it is produced and commercialized by Brazilian Company of Cartridges (CBC) in Europe and in the U.S.A. since the 90s, and it is only a matter of time to this line of product become available for purchasing in Brazil too. Therefore, this project aims to analyze the components of CBC's Clean Range Line ammunition, as well as their GSR, in order to characterize them. To that end, PIXE is employed for the elemental characterization, while micro-PIXE is used to determine the correlation of elements present in a single particle cluster.

For the first round of measurements, 20 non-toxic ammunition cartridges belonging to the CBC's Clean Range line (.38 SPL gauge, brass jacketed bullet, cartridge case and fuse of brass) from the same lot were disassembled and their components were analyzed separately. The PIXE experiments were carried out at the Ion Implantation Laboratory (Physics Institute – UFRGS) with 3.0 MeV proton beams and typical currents of about 10 pA. The beam size was of the order of 1 mm². The qualitative results showed the presence of Ba in the samples of gunpowder and Sb in those of primer. These elements could be detected due to the high sensitivity of PIXE and has not been identified by the techniques previously applied [3].

[1] M. J. Bailey, K. J. Kirkby and C. Jeynes, X-Ray Spectrometry 38 (2009) 190–194.

[2] M.J. Bailey and C. Jeynes, Nuclear Instruments and Methods in Physics Research B 267 (2009) 2265–2268.

[3] A. Martiny, A. P.C. Campos, M. S. Sader, A. L. Pinto, Forensic Science International 177 (2008) 9–17.

PA13 Determination of elemental atmospheric concentrations by PIXE in highly loaded samples from Cape Verde

M. Almeida-Silva^(a), S.M. Almeida^(a), C.A. Pio^(b), T.Nunes^(b), J. Cardoso^(b,c), P.C. Chaves^(d), A. Taborda^(d),
M.A. Reis^(a,d)

(a) IST/ITN, Instituto Superior Técnico, Universidade Técnica de Lisboa, Campus Tecnológico e Nuclear, EN10, 2686-953 Sacavém, Portugal;

(b) CESAM, University of Aveiro, 3810-193 Aveiro, Portugal;

(c) University of Cape Verde, Praia, 279, Santiago, Cabo Verde

(d) Centro de Física Atómica da Universidade de Lisboa, Av. Prof. Gama Pinto 2, 1649-003 Lisboa, Portugal

Mineral dust produced from windblown soils and deserts is one of the largest contributors to the global aerosol loading and has a strong impact on the regional and global climate, as well as, on the marine and terrestrial ecosystems. Sahara Desert is the most important source of mineral dust, responsible for almost half of all the Aeolian material provided to the world's oceans [1] and contributing more than 1900 million tons per year [2]. The project CV-Dust aims to increase the knowledge on the impacts of Saharan dust by performing a set of measurements in the Cape Verde Island of Santiago. Cape Verde is located offshore of Western Africa coast, directly into the route of Saharan dust transport to the Atlantic, being an optimum place to study the African Aeolian aerosol. Within this project Particulate Matter with diameter lower than 10µm (PM₁₀) was collected with a Tecora sampler on Nuclepore® polycarbonate filters and element concentrations were determined by PIXE and INAA. Due to aerosol characteristics at this sampling site, PIXE data in various samples cannot be handled in traditional ways by assuming that we are in presence of thin films. The DATTPIXE [4,5] capabilities to determine X-rays equivalent thicknesses and to handle half-thick samples were used to determine elemental concentrations in high loaded samples. In this paper, both the discussion about this procedure as well as on the results achievable by using it, instead of a simple erroneous thin films approach, are discussed.

[1] R. Miller, I. Tegen, J. Perlwitz. *Journal of Geophysical Research*, 109D (2004).

[2] A. Goudie. *Journal of Environmental Management*, 90 (2009) 89-94.

[3] M.A. Reis, L.C. Alves, *Nucl. Instrum. Methods Phys. Res. B* 68 (1992), 300.

[4] M.A. Reis, L.C. Alves, A.P. Jesus. *Nucl. Instrum. Methods Phys. Res. B* 109/110: (1996) 134.

PA14 Comparison of EDS and WDS high resolution PIXE spectra and *ab initio* atomic calculations

A. Taborda^(a,b), P.C. Chaves^(a,b), M.L. Carvalho^(a,c), J.P. Marques^(a,c), M. Kavčič^(d), M.A. Reis^(a,b)

(a) Centro de Física Atómica da Universidade de Lisboa, Av. Prof. Gama Pinto 2, 1649-003 Lisboa, Portugal

(b) IST/ITN, Instituto Superior Técnico, Universidade Técnica de Lisboa, Campus Tecnológico e Nuclear, EN10, 2686-953 Sacavém, Portugal;

(c) Dept. Física da Fac. Ciências da Universidade de Lisboa, Campo Grande, Edifício C8, 1749-016 Lisboa, Portugal

(d) J. Stefan Institute, F-2, Jamova 39, P.O. Box 3000, SI-1001 Ljubljana, Slovenia

High resolution Si PIXE spectra were obtained using two different high resolution detection systems: the microcalorimeter EDS detector at IST/ITN [1] and the WDS spectrometer at J. Stefan Institute [2], with 1.0 MeV H⁺ ion beams. Spectra were compared with theoretical transition energies corresponding to the diagram lines in the X-ray spectra, but also corresponding to satellite structures associated with multi-ionisation and radiative Auger effect. The transition energies were obtained from *ab initio* relativistic calculations, using the Dirac-Fock method [3]. The energy calibration of the collected spectra was performed using both the experimental energies values (calib 1) and the theoretical energies values (calib 2) in the NIST X-ray energies database [4]. Clear differences between the two methods of calibration are observed. Differences observed, consequences of these differences and conclusions drawn from this comparison are presented and discussed.

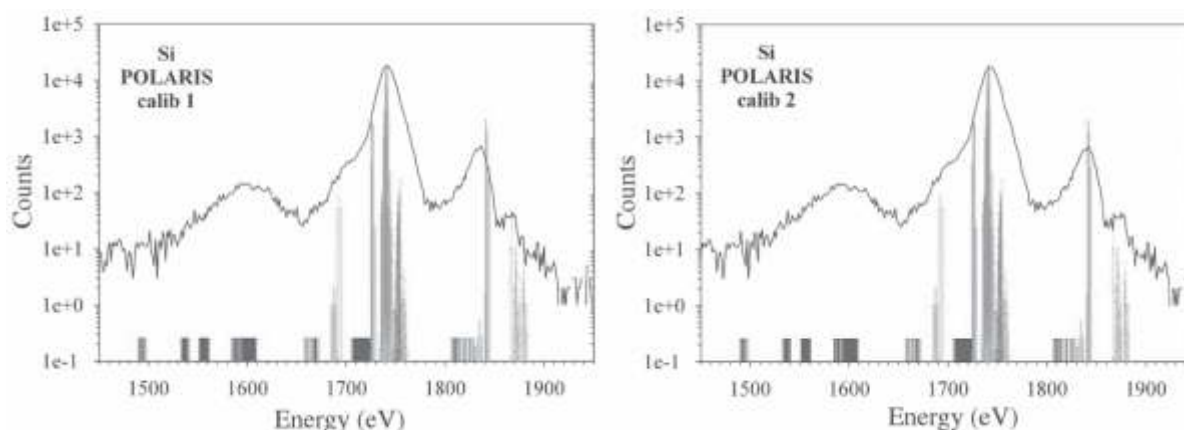


Figure 1: Overlap of the Si spectrum collected with the EDS detection system (POLARIS) and the calculated transition energies for the main and satellite lines. Left-hand side spectrum: the energy calibration was performed using the experimental energy values from NIST. Right-hand side: the energy calibration was performed using the theoretical energy values from NIST [3].

[1] P. C. Chaves, A. Taborda, M. A. Reis, Nucl. Instrum. Meth. B 268 (2010) 2010-2014

[2] M. Kavčič, M. Budnar, A. Mühleisen, F. Gasser, M. Žitnik, K. Bučar, and R. Bohinc. Sci. Instrum. 83 (2012) 033113

[3] J. P. Desclaux and P. Indelicato. MCDFGME - a MultiConfiguration Dirac-Fock and General Matrix Elements program, 2005. <http://dirac.spectro.jussieu.fr/mcdf>.

[4] R. D. Deslattes, E. G. Kessler Jr., P. Indelicato, L. de Billy, E. Lindroth, J. Anton, J. S. Coursey, D. J. Schwab, C. Chang, R. Sukumar, K. Olsen, and R. A. Dragoset. X-ray transition energies (version 1.2). National Institute of Standards and Technology, Gaithersburg MD. Online: <http://physics.nist.gov/XrayTrans>, 2005.

PA15 Distribution and quantification of trace elements in natural diamonds of Juína, Brazil, using the PIXE and RBS techniques

Rosa, L.F.S.^(a); Plá Cid, C.C.^(b); Jones, N.B.^(c); Plá Cid, J.^(d,e); Nardi, L.V.^(d); Gisbert, P.E.^(f);
Homem, M.G.P.^(b); Farenzena, L.S.^(b); Webb, R.^(c)

^aInstituto de Física, Universidade Federal do Rio Grande do Sul, Porto Alegre, RS, Brazil.

^bDepartamento de Física, Universidade Federal de Santa Catarina, Florianópolis, SC, Brazil.

^cUniversity of Surrey, Ion Beam Centre, Surrey GU2 7XH, UK

^dIGEO, Universidade Federal do Rio Grande do Sul, Porto Alegre, RS, Brazil.

^eDepartamento Nacional de Produção Mineral, Florianópolis, SC, Brazil.

^fFacultad de Geología, Universidad de Barcelona, Barcelona, Spain.

The diamonds from Juína region, Mato Grosso, Brazil, are considered the natural minerals known formed at higher pressures (> 670 km; > 22 GPa). Physical and chemical characteristics of these diamonds provide information on the composition of deep Earth, the Transition Zone and Lower Mantle [1]. Originally, the diamonds studied are irregulars, with size varying from 7 and 10 mm, brown yellowish (samples JU-01F and JU-02F) and colorless (sample JU-03). To determine the distribution and contents of trace elements (N, O, F, Si, Cl and Fe) in these diamonds, PIXE and RBS techniques were used. Images associated with the presence of these elements in the three samples were obtained by PIXE spectra acquired using a microprobe of proton of 3MeV in Surrey IBC[2], with a spot around 20 microns and 3nA of current. Preliminary results show that F, Si, Cl and Fe are punctually distributed, which suggest that these elements form aggregates in the diamond structure. The RBS technique was used to check the absolute contents, to estimate the absolute concentrations was used SIMNRA: ≈ 320 ppm for N, ≈ 2.860 ppm for O, ≈ 126 ppm for F, ≈ 550 ppm for Si, ≈ 440 ppm for Cl and ≈ 150 ppm for Fe. N values are comparable to those obtained for Juína diamonds in other studies [3]. And there are traces of elements like S (≈ 420 ppm) and Rb (≈ 120 ppm), but we need more measures to confirm these contents.

Keywords: PIXE, RBS, diamonds.

[1] M.T. Hutchison, Thesis, University of Edinburgh, U.K., 1997.

[2] A. Simon, C. Jeynes, R. P.Webb, R. Finnis, Z. Tabatabaian, P. J. Sellin, M. B. H. Breese, D. F. Fellows, R. van den Broek, R. M. Gwilliam, Nucl. Instrum. Methods Phys. Res., Sect. B, 405, pp. 219–220, 2004.

[3] M.T. Hutchison, P. Cartigny, J.W. Harris, Proceedings of the VIIth International Kimberlite Conference, v.I, pp. 372-382, 1999.

PA16 Investigation of the stopping powers of H^+ and H_2^+ in silicon in $E < 90$ keV energy region by measuring the hydrogen depth profile with NRA

T.S. Wang, J.T. Zhao, X.X. Xu, S. Zhang, K.H. Fang, X.C. Guan

School of Nuclear Science and Technology, Lanzhou University, Lanzhou, 730000, China

Stopping power data of ions are essential for ion-solid interaction. However, the experimental measurement of ions' stopping power in keV energy region is a challenge work. Thus, the uncertainty of existed experimental stopping power data is rather large in keV energy region.

In this work, the stopping power of proton (H^+) and hydrogen molecular ion (H_2^+) have been obtained from the depth profile of H^+ and H_2^+ in silicon. The H^+ and H_2^+ ions with energies of 10, 25, 35, 80 and 90 keV/amu were implanted into silicon with a fluence of 1×10^{17} p/cm², the hydrogen depth profiles in implanted samples were measured by $H(^{15}N, \alpha)^{12}C$ resonance Nuclear Reaction Analysis (NRA). The projected ranges of implanted ions are therefore obtained from the depth profiles. A code based on the Projected Range Algorithm given by Biersack, Andersen and Ziegler [1] has been developed to extract the stopping power data. In this code, the nuclear stopping power of protons is the same as that from SRIM. The best coefficients have been obtained by fitting the experimental range data. As a result, the stopping power of proton in silicon is larger than the data used in SRIM, a maximum difference reaches to 10% at energies less than 10 keV/amu.

The projected ranges of H^+ and H_2^+ ions with the same velocity were different. This difference is energy dependent. The projected ranges of H^+ is less than that of H_2^+ at energies less than 80 keV/amu, but this trend changes when energies $E \geq 90$ keV/amu. This means that the stopping power per nuclei of H_2^+ before dissociation is less than that of protons with the same velocity. The result agrees qualitatively with that predicted by MELF-GOS dielectric function theory. Therefore, the range difference could only be originated from the velocity dependence of lifetime of H_2^+ . There is a critical velocity for the dissociation of H_2^+ . The lifetime of H_2^+ has been calculated based on the stopping power given by MELF-GOS dielectric function theory [2].

[1] J.F. Ziegler, J.P. Biersack, U. Littmark, *The Stopping and Range of Ions in Solids*, (Pergamon Press, New York, 1985).

[2] C.C. Montanari, J.E. Miraglia, Santiago Heredia-Avalos, Rafael Garcia-Molina, Isabel Abril, *Phys. Rev. A* 75,022903 (2007).

PA17 Mapping of medium and high Z elements in an agate sample using a CdTe based high energy PIXE setup

P.C. Chaves^(a,b), A. Taborda^(a,b), M.A. Reis^(a,b)

(a) Centro de Física Atómica da Universidade de Lisboa, Av. Prof. Gama Pinto 2, 1649-003 Lisboa, Portugal

(b) IST/ITN, Instituto Superior Técnico, Universidade Técnica de Lisboa, Campus Tecnológico e Nuclear, EN10, 2686-953 Sacavém, Portugal;

The CTN (previous ITN) high resolution high energy PIXE setup facility presents excellent conditions to study samples having medium and high Z elements. The automated X-Y positioning system, installed in the X-Y-Z sampling support unit, represents an important advance allowing for the possibility to make macroscopic mapping of geological samples. In the present paper, the study of an agate sample, previously studied using a low beam energy and the XMS high-resolution capabilities [1], was extended, by mapping medium and high elements using the CdTe detector. The agate sample mapping is based on a total of 33 spectra obtained by irradiating the sample with H⁺ beams of 4.0 MeV from the CTN 3.0 MV Tandatron accelerator. The complete description of the high resolution high energy PIXE setup can be found in other work presented in this conference. Elemental concentrations were obtained using the DT2 code (also presented in another communication at this conference). Optical analysis and compositional analysis will be discussed in the present work.

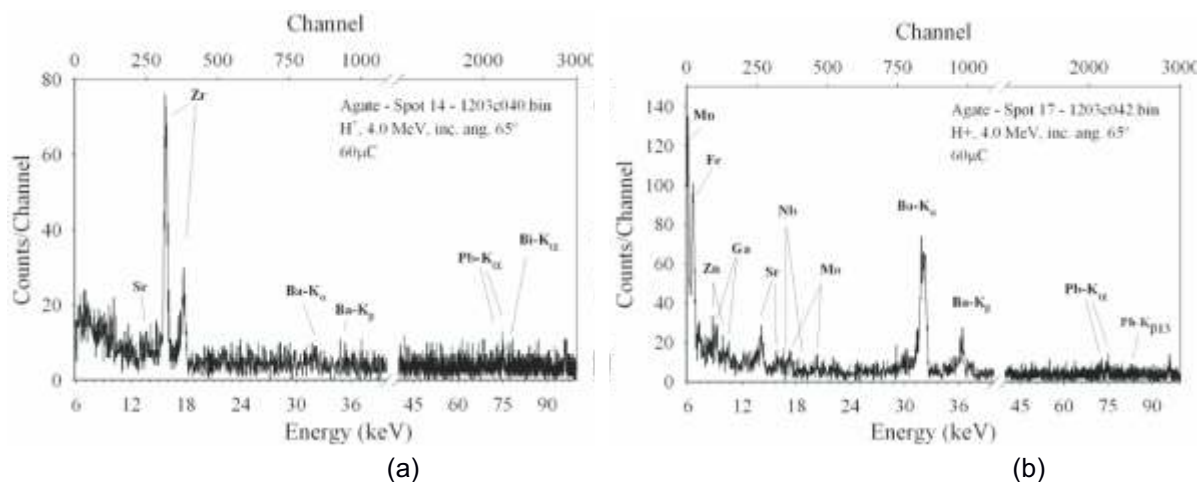


Figure 1(a,b): K X-ray spectra from agate sample. Differences between these two spots, separated by 6 mm, are clearly seen, and will be discussed in this work.

[1] M. A. Reis, P. C. Chaves and A. Taborda, X-Ray Spectrom. 2011, 40, 141–146.

PA18 Compositional characterization of GaInSb grown by LEC method

M. Streicher^(a,b), V. Corregidor^(b,c), L.C. Alves^(b,c), E. Alves^(b,c), E. M. Costa^(a), B.A. Dedavid^(a)

^(a) Pontifícia Universidade Católica do Rio Grande do Sul, Av. Ipiranga, 6681 – Porto Alegre/RS Brasil

^(b) IST/ITN, Instituto Superior Técnico, Universidade Técnica de Lisboa, Campus Tecnológico e Nuclear, EN 10, 2686-953 Sacavém, Portugal

^(c) CFNUL, Av. Prof. Gama Pinto, 2, 1649-003 Lisboa, Portugal

$\text{Ga}_{1-x}\text{In}_x\text{Sb}$ is a III-V semiconductor with a wide range of applications, the possibility of adjusting the lattice constant and the band gap energy through the variation of In content (x) make these alloys very attractive for the semiconductors modern industry [1]. The $\text{Ga}_{0.93}\text{In}_{0.07}\text{Sb}$ ingot was obtained by Liquid Encapsulated Czochralski growth method using GaSb and InSb as starting materials [2].

Three different parts were cut from the ingot (from the top, middle and bottom) and were mechanically polished with colloidal silica and sodium hypochlorite. Elemental composition characterization was done by means of IBA techniques (RBS and PIXE) in order to have information about segregation behavior along the growth direction [3], using a 2 MeV He^+ beam at IST/ITN. Moreover, electrical measurements were performed using Van der Pauw method employing indium as electrical contact.

The samples exhibited n-type conductivity as determined by the electrical measurements, which it is probably associated to the presence of In atoms in the Ga sites of the lattice or due to possible existence of other impurities. The 2D PIXE maps obtained for the three parts show the In heterogeneity distribution (figure 1), being the In concentration higher in the top than in the bottom part of the ingot. This behavior is not expected, since the segregation coefficient for In is close to unity. It was also possible to identify Sb segregation in the central region of the ingot, which can be related with the thermal variations during the growth.

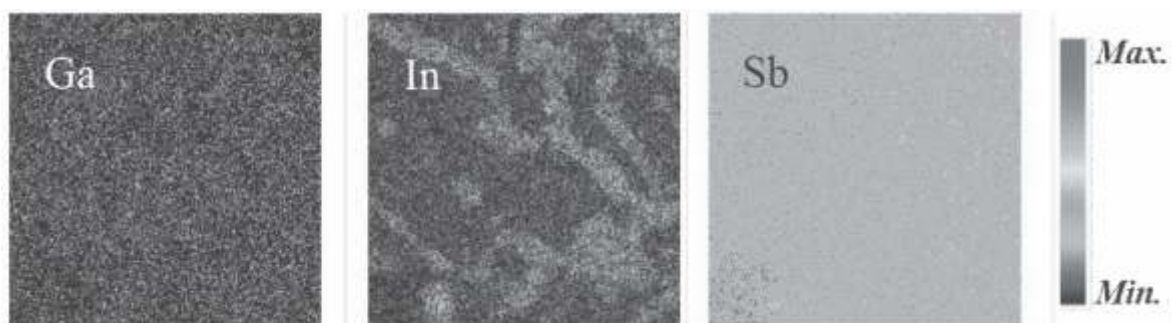


Figure 1. 2D elemental distribution of Sb, In and Ga from PIXE spectra. ($1320 \times 1230 \mu\text{m}^2$).

References

- [1] H.J. Kim, A. Chandola, R. Bhat, P.S. Dutta. *J Cryst Growth*, 289 (2006) 450-457.
- [2] M. G. Hönnicke, I. Mazzaro, J. Manica, E. Berine, E. M. Costa, B. A. Dedavid, C. Cusatis, X. R. Huang. *J Electron Mater* (2010) 1-5.
- [3] A. Mitric, T. Duffar, V. Corregidor, L.C. Alves, N.P. Barradas, *J Cryst Growth*, 310, (2008) 1424-1432.

Acknowledgments

This work was carried out within the contract CAPES Proc. No. 026612-4 together with IST/ITN. V. Corregidor acknowledges the funding support from the FCT - Ciência 2008 program.

PA19 X-ray production cross-sections measurements for high-energy alpha particle beam for Si, Fe and Cu

T. Dupuis^(a), G. Chêne^(a), A. Marchal^(a), F. Mathis^(a) and D. Strivay^(a)

^(a)Institut de Physique Nucléaire, Atomique et de Spectroscopie & Centre Européen d'Archéométrie, University of Liège (Belgium)

A new transport beam line has been developed at our CGR-520 MeV cyclotron for ion beam techniques. This facility allows us to produce proton and alpha particle beams with energies up to 20 MeV. A vacuum chamber dedicated to X-ray production and Non-Rutherford cross-section measurements has been recently constructed[1]. Measurements of the X-ray production cross-sections in the 6–12 MeV energy range have started using alpha particle beams on light element targets[2]. These experiments contribute to the filling a serious lack of experimental values for alpha particles of this particular energy range in databases. We are reporting here X-ray cross section measurements for Silicium, Iron and Copper. Experimental data are in good agreement with theoretical ECPSSR values.

[1] G. Chêne, F. Mathis, T. Dupuis, A. Marchal, M. Philippe, M. Clar, D. Strivay, H.P. Garnir Nucl. Instr. and Meth. B, 268(11–12), 2010, 2015-2018

[2] T. Dupuis, G. Chêne, F. Mathis, A. Marchal, H.P. Garnir, D.Strivay, Nucl. Instr. and Meth. B, 269 (24), 2011, 2979-2983

PA20 N to K Uranium PIXE spectra obtained at the High Resolution High Energy PIXE setup

P.C. Chaves^(a,b), A. Taborada^(a,b), J.P Marques^(a,c), M.A. Reis^(a,b)

(a) Centro de Física Atómica da Universidade de Lisboa, Av. Prof. Gama Pinto 2, 1649-003 Lisboa, Portugal

(b) IST/ITN, Instituto Superior Técnico, Universidade Técnica de Lisboa, Campus Tecnológico e Nuclear, EN10, 2686-953 Sacavém, Portugal;

(c) Dept. Física da Fac. Ciências da Universidade de Lisboa, Campo Grande, Edifício C8, 1749-016 Lisboa, Portugal

The CTN (previous ITN) high resolution high energy PIXE setup facility was set in operation on July 2008 and upgrades were being implemented until late in 2011. The study of a pure UO_2 sample and the mappings of geological samples are the first results where the whole range of possibilities have been exploited, namely the possibility of obtaining simultaneous spectra covering a very wide energy range of more than 100 keV. At low beam energy, high resolution PIXE of low energy lines (starting at 800 eV) is possible using a X-ray microcalorimeter spectrometer (XMS). In this case, if proton beams are used, energies of less than 1.1 MeV are needed to prevent particles from entering the XMS and destroy the superconductor sensor system that provides a better than 2% resolution at this energy range. When high beam energies are used, to efficiently ionise the K shells of heavier elements, say up to 4.0 MeV proton beams, then a thick low Z material filter is used in front of the XMS. This, although cutting out the possibility to study low energy X-rays, does not exclude the XMS utility since it is able to measure X-rays up to 20 keV with relative energy resolutions close to 0.2%. In these conditions, the CdTe detector can be used simultaneously and K X-rays of all elements up to Uranium are detectable, as well as some low energy γ -rays from nuclear reactions such as the 110 keV from the $^{19}\text{F}(p,p'\gamma)^{19}\text{F}$ reaction or the 62 keV from the $^{49}\text{Ti}(p,n)^{49}\text{V}$ reaction. In this paper, the full N-shell to K-shell spectra of Uranium is presented and discussed, as well as the details on the characteristics and capacities of the setup, including the automated X-Y positioning systems installed in the X-Y-Z sampling support unit, which allows for the possibility of making macroscopic mappings of geological samples (discussed in other works presented at this conference). As for the N-shell lines in the XMS spectrum, due to the lack of data, transition energies were determined using *ab initio* calculations assuming a closed shell U^{4+} electronic structure for Uranium prior to the ionisation by proton impact. Besides the simplicity reason underneath this choice, the fact that a UO_2 target was used further supports this as a good approach, thus the whole spectrum was calculated *ab initio* and conclusions are discussed.

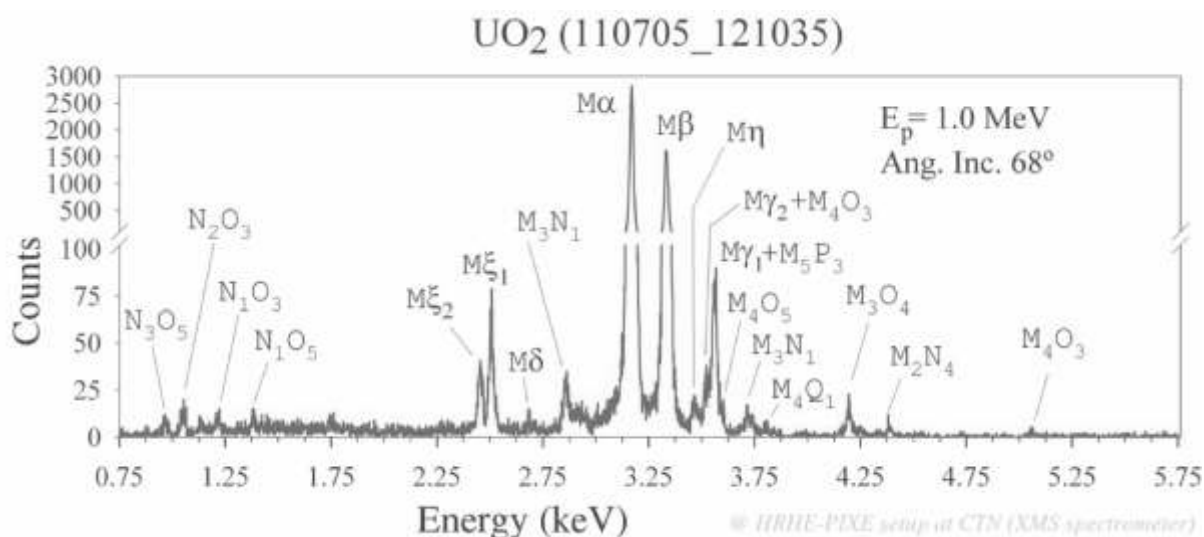


Figure 1: Uranium N- and M-shell PIXE spectrum from a pure UO_2 sample collected with the XMS spectrometer installed at the CTN HRHE-PIXE setup.

PA21 PIXE study of aerosol samples from an iron and steel smelting company at Ile-Ife, Nigeria

F.S. Olise^(a), O.K. Owoade^(a), S.M. Almeida^(b), A. Fernandes^(c), P.C. Chaves^(c), A. Tabora^(b,c), M.A. Reis^(b,c), L.T. Ogundele^(a), O.G. Fawole^(a), H.B. Olaniyi^(a)

(a) Department of Physics, Obafemi Awolowo University, Ile-Ife, 220005, Nigeria;

(b) IST/ITN, Instituto Superior Técnico, Universidade Técnica de Lisboa, Campus Tecnológico e Nuclear, EN10, 2686-953 Sacavém, Portugal;

(c) Centro de Física Atómica da Universidade de Lisboa, Av. Prof. Gama Pinto 2, 1649- 003 Lisboa, Portugal

PM₁₀ and PM_{2.5} aerosol samples were collected on Nuclepore[®] polycarbonate filters of 47 mm diameter, using Gent samplers at 15 – 17 l/min air flux. The sampling campaign took place between May 2011 and March, 2012 in the University Town of Ile-Ife, Nigeria, within and outside a new iron and steel company. Two samplers were simultaneously deployed within the factory between May and July 2011, each central to the two furnaces at each side of the casting section. The same set of samplers was deployed up – and down – wind outside the factory to monitor emissions irrespective of wind directions between August, 2011 and March, 2012. All sampling lasted continuously for 8 to 12 hours durations. Samples were analyzed using proton induced x-ray emission (CTN standard PIXE setup) and a total of sixteen chemical elements were determined. Since it was difficult to control the absolute parameters for all samples, data analysis was carried out based on a relative concentration study. In this work we present and discuss differences between samples collected within and outside the factory and compare these to published data from other local and regional aerosol studies.

[1] R. Miller, I. Tegen, J. Perlwitz. *Journal of Geophysical Research*, 109D (2004).

[2] A. Goudie. *Journal of Environmental Management*, 90 (2009) 89-94.

[3] M.A. Reis, L.C. Alves, *Nucl. Instrum. Methods Phys. Res. B* 68 (1992), 300.

[4] M.A. Reis, L.C. Alves, A.P. Jesus. *Nucl. Instrum. Methods Phys. Res. B* 109/110: (1996) 134.

PA22 On the evolution of silver tarnishing

V. Corregidor^(a,b), J. Cruz^(b,c), P.C. Chaves^(d), M.A. Reis^(a,d), L.C. Alves^(a,b)

^(a) IST/ITN, Instituto Superior Técnico, Universidade Técnica de Lisboa, Campus Tecnológico e Nuclear, EN10, 2686-953 Sacavém, Portugal

^(b) CFNUL, Av. Prof. Gama Pinto, 2, 1649-003 Lisboa, Portugal

^(c) Departamento de Física, Faculdade de Ciências e Tecnologia, Universidade Nova de Lisboa, 2829-516 Caparica, Portugal

^(d) Centro de Física Atómica da Universidade de Lisboa, Av. Prof. Gama Pinto 2, 1649-003 Lisboa, Portugal

Silver is one of the noble metals, jointly with gold, used since ancient times to produce several kinds of objects. But, contrasting with the gold, silver tends to react with several elements (mainly sulfur and chlorine) and forms the tarnish. Tarnish is a thin layer of corrosion, a consequence of the chemical reaction of the atoms from the first layers of the metal with external elements. This thin corrosion layer, in some cases, seals and protects the bulk, but the characteristic luster of silver is lost over time if cleaning procedures are not done regularly. On the other hand, the cleaning process, besides removing the tarnish, also removes silver atoms and introduces small scratches on the surface.

Most of the objects made of silver have also copper, intentionally added and in different concentration in order to obtain a harder alloy, since the silver itself is very soft to manufacture objects. If we consider ancient silver objects, the concentration of other elements is also important, and in some cases, they allow to identify the ore provenance.

Although these elements are not usually considered, they can also react with the elements from the environment and may eventually interfere in the tarnishing process. Because of that both, recent silver objects, containing a pure alloy of Ag/Cu, and old silver objects were considered in this work. PIXE and RBS measurements were performed over one year, in order to measure the evolution of the patina layer. Along this period, they were maintained in contact with the atmosphere, which in Lisbon has an average humidity level of 60-80% and temperatures of 14-30°C. The measurements were performed using a 2 MeV proton beam with 3x4 mm² dimensions at the microprobe beam line of the Van de Graaff accelerator located at IST/ITN (Lisbon).

Combining scan and point measurements it was possible to extract information about the elemental distribution over the surface and thickness of the patina layer (figure 1). The results point out the relationship between the film thickness (not homogeneous) and the distribution of the main constituents of the alloy.



Figure 1. 2D PIXE maps: Ag and S. RBS spectra recorded in different points of the maps.

V. Corregidor acknowledges the FCT-Ciência 2008 program.

PA23 Elemental concentrations analysis of tomato paste

R. Debastiani, M. M. Ramos, C. E. I. dos Santos, V. S. Souza, M. L. Yoneama*, L. Amaral, and J. F. Dias

Physics Institute, Federal University of Rio Grande do Sul, Av. Bento Gonçalves, 9500, CEP 91501970, Porto Alegre (RS), Brazil.

Tomato paste is the result of healthy and mature tomatoes *Solanum lycopersicum* submitted to an industrial processing without undergoing fermentation [1]. World production in 2000 was about 27 million ton(s), being Brazil one of the largest producers [2]. Epidemiological studies have shown that consumption of tomatoes and tomato-based products are associated with reduced risk of developing chronic diseases such as cancer and cardiovascular diseases. Tomatoes are a rich source of vitamins (folic acid, vitamins C and E), minerals (potassium), carotenoids (beta-carotene and lycopene) and flavonoids [3]. However, a number of factors such as geographic origin, cultivation practices and use of particular pesticides have a strong influence in the elemental composition of the final product. Some of these elements can be bio-accumulative metals, which are not easily expelled by the metabolism of living organisms. In order to check these issues, we carried out an elemental characterization of tomato paste made using PIXE (Particle-Induced X-ray Emission) and RBS (Rutherford Backscattering Spectrometry) techniques. Parameters like brand, storage time and packing (cans, Tetra Pak cartoons and glassware) were evaluated in the present study.

In total, four brands were analyzed. For each brand, more than one kind of packing was investigated, and it was possible to compare, for same storage time, the influence of different packings. The storage time ranged between 6 and 81 months.

The average organic composition consisted of 72.4% carbon, 12.4% nitrogen and 15.2% oxygen. The elements determined with PIXE were Na, Mg, Al, Si, P, S, Cl, K, Ca, Ti, Mn, Fe, Cu, Zn, Br, Rb and Sr.

One of the brands analyzed showed that chlorine and potassium are the elements with higher concentration. Cans are composed mainly of Fe. For the same storage time, tomato paste from glassware showed less iron than those stemming from in cans. Iron in tomato paste from cans has an exponential behavior as a function of time, reaching about 2×10^4 ppm.

[1] ANVISA – Agência Nacional de Vigilância Sanitária

[2] Embrapa

(<http://sistemasdeproducao.cnptia.embrapa.br/FontesHTML/Tomate/TomateIndustrial/importancia.htm>)

[3] Embrapa

(http://www.cnph.embrapa.br/paginas/imprensa/artigos/beneficios_tomate_para_saude.htm)

PA24 Fixed and free line ratio DT2 PIXE fitting and simulation package

M.A. Reis^(a,b), P.C. Chaves^(a,b), A. Taborda^(a,b), J.P Marques^(b,c), N.P Barradas^(a)

(a) IST/ITN, Instituto Superior Técnico, Universidade Técnica de Lisboa, Campus Tecnológico e Nuclear, EN10, 2686-953 Sacavém, Portugal

(b) Centro de Física Atómica da Universidade de Lisboa, Av. Prof. Gama Pinto 2, 1649-003 Lisboa, Portugal

(c) Dept. Física da Fac. Ciências da Universidade de Lisboa, Campo Grande, Edifício C8, 1749-016 Lisboa, Portugal

In the end of the 1980s decade when the PIXE technique was being installed at Sacavém, what is presently CTN, a home based PIXE software package, started to be developed. Its full extent, DATTPIXE, would become operational in 1992 [1] and since then it has been largely used both in academic research but also in standard analysis work. Developments of a new PIXE setup which include an EDS high resolution detector, in parallel with fundamental physics questions related to relative yields determination, raised the need for a deep revision of the software used to fit PIXE spectra and interpret data. The first steps towards this were given in 2007 by developing a new fitting code based on a proven Bayesian inference routine [2]. Still, the deepening of knowledge about the fundamental processes associated to PIXE spectra, which become more important and evident in X-ray microcalorimeter spectrometers (XMS) high resolution EDS spectra [3], made clear that an almost a full new code was necessary to provide the proper answers to all or most of all newly identified problems. Although using some of the routines developed in DATTPIXE, the new DT2 package is written in Fortran 2003 instead of Pascal, and includes both the fitting and data handling codes. DT2 is now designed to be able to deal with diagram lines as well as with satellite lines. Radiative Auger Emission (RAE) and multi-ionization satellites, but also chemically shifted lines can now be included in the fitting model and dealt with in simulation of thick target yields. In this communication we present the new DT2 package and discuss its new features, such as the possibility of fixing or leave free the relative intensity of spectra lines, even if they belong to transitions to the same shell.

[1] M.A. Reis, L.C. Alves, Nucl. Instrum. Methods Phys. Res. B 68 (1992), 300.

[2] M.A. Reis, P.C. Chaves, L.C. Alves, N.P. Barradas, X-ray Spectrom. 37 (2008), 100

[3] M.A. Reis, P.C. Chaves, A. Taborda, X-ray Spectrom. 40 (2011), 127

PA25 Ion beam analysis of Brazilian coffee

R. Debastiani, C. E. I dos Santos, M. M. Ramos, V. S. Souza, M. L. Yoneama*, L. Amaral, J. F. Dias

Physics Institute, Federal University of Rio Grande do Sul, Av. Bento Gonçalves, 9500, CEP 91501970, Porto Alegre (RS), Brazil.

Coffee is one of the most popular and consumed beverages worldwide. Consumers can make the beverage from different types of coffee such as ground coffee, instant coffee or grinding roasted coffee beans. Each type of coffee leads to different characteristics in flavor and scent. The aim of this work is to perform an elemental analysis of ground coffee and roasted coffee beans. To that end, eight popular Brazilian ground coffee brands have been chosen to make a comparative study among brands. One of these brands was selected for a complete study of the beverage preparation process. This same brand offers packages of roasted coffee beans, which allowed the elemental comparison between ground coffee and roasted coffee beans. Roasted coffee beans were ground with a pestle and mortar. The beverage was prepared using a typical coffee pot. The spent and liquid coffees were submitted to a heat treatment and subsequently homogenized and pressed into pellets. The filters used in the coffee pot were analyzed as well. For micro-PIXE studies, coffee beans were cut in different parts for analysis.

Samples of ground coffee and roasted coffee beans (grinded) were analyzed by PIXE, while light elements like C, O and N were analyzed by RBS (Rutherford Backscattering Spectrometry). The roasted coffee beans were analyzed by micro-PIXE to check the elemental distribution in the beans.

The elements found in powder coffee were Mg, Al, Si, P, S, Cl, K, Ca, Ti, Mn, Fe, Cu, Zn and Rb. Potassium is the element with higher concentration, while Ti and Zn are trace elements. Al, Si and Ti showed the same concentration for all brands. Potassium and chlorine have high solubility, and about 80% of their concentration is transferred from the powder to the beverage during the infusion. Mg, P, Cl, K, Mn, Fe, Zn and Rb showed significant variation between ground coffee and roasted coffee beans. The elemental maps show that potassium and phosphorus are correlated, and iron appears in particular clusters in different structures. Elements like Zn and Rb appear as trace element without any correlation with other elements.

*Fellowship PDS CNPq n 158137/2011-6

PA26 Strontium content in otoliths of common fish species in the northern Baltic Sea

J-O. Lill^(a), M. Himberg^(b), L. Harju^(c), A. Lindroos^(d), K. Gunnelius^(e), J-H. Smått^(e), S-J. Heselius^(a)
and H. Hägerstand^(b)

^(a)Accelerator Laboratory, Turku PET Centre, Åbo Akademi University, Porthansg. 3, FI-20500 Turku, Finland

^(b)Cell Biology, Department of Biosciences, Åbo Akademi University, Artillerig. 6, FI-20520 Turku, Finland

^(c)Analytical Chemistry, Department of Chemical Engineering, Åbo Akademi University, Biskopsg. 8, FI-20500 Turku, Finland

^(d)Geology and Mineralogy, Department of Natural Sciences, Åbo Akademi University, Domkyrkotorget, FI-20500 Turku, Finland

^(e)Physical Chemistry, Department of Natural Sciences, Åbo Akademi University, Porthansg. 3, FI-20500 Turku, Finland

The salinity of water in the northern Baltic Sea forms a gradient as it receives fresh water from several large rivers in the north and salty water by infrequent inflows of North Sea water in the south. The salinity of brackish water in the north-south direction (700 km) changes from about 3 to 7‰. In an attempt to use the salinity gradient to study migration patterns, sagittae otoliths were collected from common fish species caught at different locations along the Finnish west coast. Otoliths from fishes caught in fresh-water lakes in Finland and Estonia were also included in the study for comparison. Part of the otoliths was grinded and the powder was pressed to pellets which were irradiated in air with an ion beam from the Åbo Akademi cyclotron and the emitted X-rays were measured. Other otoliths were embedded in epoxy and polished to reveal the ring structure. These prepared otoliths were irradiated with the ion beam to determine elemental profiles. Furthermore, XRD was applied to study the crystal structure and to identify the minerals in the otoliths.

The strontium level of water is usually related to its salinity, and as the strontium ions are able to replace calcium ions in fish otoliths [1], the strontium content in fish otoliths from the same locations is expected to be very similar. However, the PIXE analyses revealed large differences in the strontium content between otoliths from different species of fish caught at the same locations. The strontium concentration in otoliths of perch and pike from the Åland Islands was about 1600 µg/g and of common whitefish 3600 µg/g. The strontium concentration in perch otoliths from the Oravais archipelago, about 400 km north of the Åland Islands, was 1400 µg/g. Corresponding concentration in otoliths of perch and pike caught in fresh-water lakes was 200 µg/g and of common whitefish from Saadjärve 400 µg/g and from Lake Inari 1000 µg/g. Otoliths of perch contained no detectable amounts of zinc (lower than 10 µg/g) but the otolith of pike and common whitefish contained 30 µg/g and 65 µg/g (RSD 28%, n=8) of zinc, respectively.

The strontium concentration in fish otoliths can be used to locate spawning habitats with different salinities of a fish population. For the supposed anadromous whitefish caught during spawning in the rivers of Kokemäki and Tornio the values were 3200 µg/g and 3000 µg/g, i.e. ~20% lower than for whitefish caught at the Åland Islands. This is an interesting observation indicating that the Ca/Sr ratio of otoliths may be used to estimate the ratio of the two populations of common whitefish, the sea-spawning and the anadromous river-spawning fishes, in sympatric populations.

[1] S.E. Campana, Mar Ecol Prog Ser 188(1999)263-297.

PA27 Chemical speciation of chlorine in atmospheric aerosol samples by high resolution PIXE

Zs. Kertész^(a), E. Furu^(a,b), and M. Kavčič^(c)

^(a)Institute of Nuclear Research of the Hungarian Academy of Sciences (Atomki), Laboratory of Ion Beam Applications, H-4026 Debrecen, Bem tér 18/c, Hungary

^(b)University of Debrecen, H-4032 Debrecen, Egyetem tér 1, Hungary

^(c)Jožef Stefan Institut, Microanalytical Center, Jamova 39, P. O. Box 3000 SI-1001 Ljubljana, Slovenia

Urban atmospheric aerosol pollution is one of the leading environmental problems in the world. In order to work out effective mitigation strategies the knowledge of particulate matter (PM) sources is essential. Chemical characterization of PM has primary importance in source determination.

At the Institute of Nuclear Research in Debrecen, the characterization of atmospheric aerosol sources is done by following the hourly evolution of elemental components, single particle microscopy and statistical analysis. Despite the few thousand km distance from the oceans chlorine was found to be a major constituent of particulate matter in Hungarian cities; in some cases even 10-20% concentrations were measured. Single particle analysis using ion and electron microscopy was proved to be a good tool to determine the sources of coarse fraction chlorine [1]. However, in the case of the fine fraction (particles with aerodynamic diameter less than 2.5 μm) the above mentioned methods did not provide any useful additional information about the chemical composition of chlorine.

In this work the chemical characterization of fine fraction Cl was done using wavelength dispersive PIXE at the high resolution X-ray spectrometer of the Microanalytical Center at the Jozef Stefan Institute, Ljubljana [2]. The high resolution $K\alpha$ and $K\beta$ proton induced spectra were of five reference materials and 2 aerosol samples were recorded. Pure compounds were used as reference materials. The chemical shift of the $K\alpha$ lines can be used to determine the oxidation state of an element. However, the oxidation state of Cl is practically always -1, thus there were only very minor differences in the measured $K\alpha$ spectra. On the contrary of this the $K\beta$ spectra exhibited high sensitivity to the chemical environment of Cl. The differences in the $K\beta$ spectra of the reference compounds were significant enough to enable the chemical analysis. Using this method the Cl in two fine fraction aerosol samples collected during a 2010 winter campaign in Budapest was clearly identified as NaCl.

Acknowledgement. This work was carried out in the frame of the János Bolyai Research Scholarship of the Hungarian Academy of Sciences and the Hungarian Research Fund OTKA and the EGT Norwegian Financial Mechanism Programme (contract no. NNF78829). This work has been supported by the European Community as an Integrating Activity «Support of Public and Industrial Research Using Ion Beam Technology (SPIRIT)» under EC contract no. 227012.

[1] A. Angyal, Zs. Kertész, Z. Szikszai, Z. Szoboszlai: Nucl. Instrum. Methods Phys. Res. B 268 (2010) 1:2211-2215.

[2] M. Kavcic, A. Karydas, Ch. Zarkadas, Nucl. Instrum. Methods Phys. Res., B 222, (2004), 601-608.

PA28 The new in-air micro-PIXE setup in Atomki, Debrecen

Zs. Török^(a,b), Zs. Kertész^(a), R. Huszánk^(a), I. Rajta^(a), Z. Szikszai^(a), L. Csedreki^(a,b), A. Angyal^(a),
E. Furu^(a,b), Z. Szoboszlai^(a), Á. Z. Kiss^(a), I. Uzonyi^(a), and L. Palcsu^(a)

^(a)Institute of Nuclear Research of the Hungarian Academy of Sciences (Atomki), Laboratory of Ion Beam Applications, H-4026 Debrecen, Bem tér 18/c, Hungary

^(b)University of Debrecen, H-4032 Debrecen, Egyetem tér 1, Hungary

In this work we present a new in-air micro-PIXE measurement setup installed at the Laboratory of Ion Beam Applications of Atomki, Debrecen, Hungary. The new external measurement system was set up on the nuclear microprobe beamline.

An external beam add-on system by Oxford Microbeams was mounted on the already existing microprobe vacuum chamber. The samples are positioned by using a digital microscope, two alignment lasers and a precision XYZ stage. The measurement system is equipped with two X-ray detectors for PIXE analysis, a surface barrier detector for RBS and a HP-Ge detector for γ -ray detection. The arrangement permits the combination of these techniques either simultaneously or separately, too. The beam current is measured with a beam chopper placed in the vacuum chamber. Exit windows with different thickness and of different materials can be used according to the actual demands. At the moment kapton foils of 8 mm thicknesses and silicon nitride (Si_3N_4) films with 100 nm, 200 nm and 500 nm thicknesses are at our disposal. The thickness, density and composition of the window materials were measured by profilometry and by RBS, STIM and PIXE in order to check whether the parameters provided by the producers were real.

The capability of the new in-air micro-PIXE setup was demonstrated on standard reference materials and on geological (a stalactite) and archaeological samples.

Acknowledgement. The development of the new in-air microbeam system was partially financed by the Hungarian Academy of Sciences. This work was carried out in the frame of the János Bolyai Research Scholarship of the Hungarian Academy of Sciences and TÁMOP-4.2.2/B-10/1-2010-0024 project.

PA29 Variation of atmospheric aerosol components and sources during smog episodes in Debrecen, Hungary

A. Angyal^(a), Zs. Kertész^(a), Z. Ferenczi^(b), E. Furu^(a,c), Z. Szoboszlai^(a), Zs. Török^(a,c), and Z. Szikszai^(a)

^(a)Institute of Nuclear Research of the Hungarian Academy of Sciences (Atomki), Laboratory of Ion Beam Applications, H-4026 Debrecen, Bem tér 18/c, Hungary

^(b)Hungarian Meteorological Service, H-1675 Budapest, P. O. Box 39, Hungary

^(c)University of Debrecen, H-4032 Debrecen, Egyetem tér 1, Hungary

Atmospheric particulate matter (APM) pollution is one of the leading environmental problems in densely populated urban environments. In most cities all around the world high aerosol pollution levels occurs regularly. Debrecen, an average middle-European city is no exception. Every year there are several days when the aerosol pollution level exceeds the alarm threshold value (100 mg/m³ for PM10 in 24- hours average). When the PM10 pollution level remains over this limit value for days, it is called “smog” by the authorities.

In this work we studied the variation of the elemental components and sources of PM10, PM2.5 and PMcoarse and their dependence on meteorological conditions in Debrecen during two smog episodes occurred in November 2011.

Aerosol samples were collected with 2-hours time resolution with a PIXE International sequential streaker in an urban background site in the downtown of Debrecen. In order to get information about the size distribution of the aerosol elemental components 9-stage cascade impactors were also employed during the sampling campaigns. The elemental composition ($Z \geq 13$) were determined by Particle Induced X-Ray Emission (PIXE) at the IBA Laboratory of Atomki. Concentrations of elemental carbon were measured with a smoke stain reflectometer. On this data base source apportionment was carried out by using the positive matrix factorisation (PMF) method.

Four factors were identified for both size fractions, including soil dust, traffic, domestic heating, and oil combustion. The time pattern of the aerosol elemental components and PM sources exhibited strong dependence on the mixing layer thickness. We showed that domestic heating had a major contribution to the aerosol pollution.

Acknowledgement. This work was carried out in the frame of the János Bolyai Research Scholarship of the Hungarian Academy of Sciences and TÁMOP-4.2.2/B-10/1-2010-0024 project.

PA30 PIXE analyses over a long period: a case of Neolithic variscite jewels from Western Europe (5th-3th millennium BC)

G. Querré^(a), Th. Calligaro^(b), S. Domínguez-Bella^(c) and S. Cassen^(d)

^(a)Laboratoire Archéosciences, UMR 6566 CReAAH, Université de Rennes 1. Rennes - France.
guirec.querre@univ-rennes1.fr

^(b)Centre de recherche et de restauration des musées de France. Palais du Louvre - Paris - France.

^(c)Departamento de Ciencias de la Tierra. Universidad de Cádiz - Spain.

^(d)Laboratoire de recherches archéologiques, UMR 6566 CReAAH. Nantes - France.

The provenance and the circulation of variscite - a precious stone resembling turquoise - that was employed for ornaments of Early Neolithic to Chalcolithic periods represent a main archeological issue. This question has motivated two research programs in Spain and France that were undertaken simultaneously and independently in the 1990. The first results obtained using LA-ICP-MS and PIXE showed that the variscite (an hydrated aluminum phosphate with iron traces) of the studied artefacts from Western France Neolithic graves were mined from Iberian deposits [1,2]. It was however necessary to extend this work to a larger number of archeological artifacts and geological references samples to confirm this hypothesis and to establish on statistically significant grounds the origin of each bead and pendant from all archeological sites [3]. It was decided to further analyze samples from France and Spain using the transnational access to the AGLAE facility of the C2RMF because of its high analytical performance, central location and secure environment.

The delays required to 1) organize the transport to the C2RMF of precious artefacts from museums and archaeological deposits in Spain, Portugal and France, 2) complete field missions in Western Europe variscite deposits to collect geological references and 3) regularly apply to call for proposals to the transnational access explain the long duration of this program. Overall, more than thousand analysis of major, minor and trace elements in variscite were carried out in 14 runs from one to four days each distributed over 13 years. Almost all Neolithic beads and pendants from France were analyzed, a large number of archeological artifacts from Iberian Peninsula as well as variscite references from archeological mines and geological outcrops identified in Western Europe.

During that period, the AGLAE external beam line underwent experimental and spectrum processing transformations. The initial Si(Li) detectors used have been repaired and eventually replaced by SDD detectors, various GUPIX versions have been used to process the spectra, and the measuring strategy has evolved through time. In this paper, we present how this long term evolution has been integrated using geochemical international standards and reference variscite to obtain a coherent geochemical database. For instance, the response of the X-ray detectors to phosphorus X-rays, varying with the detector silicon dead layer, appeared a critical parameter to achieve the precision and repeatability required to distinguish the very small differences in major elements composition (aluminum, phosphorus) and trace elements fingerprints (chromium, arsenic, uranium, etc.) of the variscite sources.

[1] S. Domínguez-Bella. Slovak Geological Magazine, 1-2. (2004) 151-158.

[2] G. Querré, F. Herbault, T. Calligaro. X-ray Spectrometry, 37, 2 (2007) 116-120.

[3] G. Querré, S. Domínguez-Bella, S. Cassen, Circulations à longues distances de matériaux emblématiques, in: G. Marchand, G. Querré, Roches et Sociétés de la Préhistoire, PUR, Rennes, 2012, pp. 307-315.

PA31 Characterization of the lapis lazuli from the Egyptian treasure of Tôd and its alteration using external μ -PIXE and μ -IBIL

T. Calligaro^(a), Y. Coquinot^(a), L. Pichon^(a), G. Pierrat-Bonnefois^(b), P. de Campos^(c), A. Re^(d), D. Angelici^(d,e)

^(a) Centre de Recherche et de Restauration des musées de France, Palais du Louvre, Paris, France

^(b) Musée du Louvre, Département des Antiquités Égyptiennes, Paris, France

^(c) Institute of Physics, University of São Paulo, São Paulo, Brazil

^(d) Istituto Nazionale di Fisica Nucleare (INFN), Sezione di Torino, Italy

^(e) Università di Torino, Dipartimento di Fisica e Dipartimento di Scienze della Terra, Torino, Italy

e-mail: thomas.calligaro@culture.fr

Lapis lazuli is among the earliest and most prized ornamental stone worked to produce carvings, beads and inlays. The first lapis lazuli workshop excavated in Pakistan was dated from the 4th millennium BC and the use of this gem is attested since the 3rd millennium BC in Mesopotamia and Ancient Egypt. Lapis lazuli is a heterogeneous metamorphic rock composed of minerals of the sodalite group like lazurite ($\text{Na}_3\text{Ca}(\text{Si}_3\text{Al}_3\text{O}_{12}\text{S})$) - to which it owes its blue color - intermixed with other minerals like calcite, diopside and pyrite. The only proven source of Lapis lazuli in Antiquity is Badakshan in Afghanistan while there are sources in Tajikistan and Russia.

This work focuses on the lapis-lazuli of the Egyptian treasure of Tôd, dating from Amenemhat II (1911-1876 BC.), third king of the 12th dynasty, that was excavated in 1936 from the basement of a temple at Thebes and now conserved in the Louvre museum, Paris. The treasure contains thousands of blocks of raw lapis lazuli, minute fragments, beads and carvings stylistically dated to various periods. After with the corpus of lapis lazuli objects found in the royal tombs at Ur, it constitutes the largest set of ancient lapis left. The treasure of Tôd first raises the question of the use of lapis lazuli in ancient Egypt and of the relations with Mesopotamia and the producing countries, because there is no source of lapis in Egypt. In addition, most of Tôd artefacts show today a dull, whitish and stained appearance. It is important to understand the alteration process that has affected those elements during their burial in their copper chests, in order to help their preservation and possibly restore their initial appearance.

A series of samples from the treasure were selected to be analysed using the 30 μm -size new external microbeam line of the AGLAE facility at the C2RMF. The system relies upon five fast counting SDD X-ray detectors coupled with an original scanning system combining vertical magnetic beam steering and horizontal target translation that allows to acquire PIXE maps (e.g. 200 x 200 pixels) on the entire artefacts within a short time (<30 min) [1]. The GUPIX-based processing of the raw maps yielded quantitative element maps that permitted to identify the mineral phases (lazurite, sodalite, pyrite, diopside, calcite, etc.) and their corresponding trace elements (Ba, Ti, As, Ni, etc). The ionoluminescence spectrum recorded for each pixel using a 200-900 nm fiber optic spectrometer provided an additional fingerprint of the luminescent mineral phases. The first objective was to identify the alteration products observed on the Egyptian artefacts, many deriving from the decomposition of the pyrite FeS_2 , whose nature was confirmed using μ -XRD and Raman spectroscopy. The second goal was to compare the chemical fingerprints for artefacts from different periods to see if they match the historical deposit of Badakshan, Afghanistan, despite the alteration products. Indeed, the previous studies conducted on the reference lapis lazuli samples of certified provenance have demonstrated that it is possible to distinguish the lapis sources (Chile, Russia, Tajikistan, Afghanistan) using PIXE [2,3].

[1] Pichon L. C. Pacheco, B. Moignard, T. Guillou, Q. Lemasson, P. Walter, The New AGLAE project, these proceedings

[2] T. Calligaro, Y. Coquinot, L. Pichon, B. Moignard, Advances in elemental imaging of rocks using the AGLAE external microbeam, Nucl Instr and Meth B 269 (2011) 2364–2372

[3] Lo Giudice A., A. Re, S. Calusi, L. Giuntini, M. Massi, P. Olivero, G. Pratesi, M. Albonico, E. Conz, Multitechnique characterization of lapis lazuli for provenance study, Anal Bioanal Chem 395 (2009) 2211–2217

PA32 PIXE-PIGE analysis of size-segregated aerosol samples from remote areas

G. Calzolari^(a), M. Chiari^(a), F. Lucarelli^(a), S. Nava^(a), S. Becagli^(b), C. Ghedini^(b), F. Rugi^(b), D. Frosini^(b), R. Traversi^(b) and R. Udisti^(b)

^(a)Department of Physics and Astronomy – University of Florence and INFN – Florence, Italy

^(b)Department of Chemistry – University of Florence, Italy

The chemical characterization of size-segregated aerosol samples can help in the identification of the main aerosol sources, can give information on the atmospheric processes occurring during atmospheric transportation and it is important for epidemiological studies as the smaller the particles the deeper they can penetrate into the respiratory system (harmful elements may be more dangerous for human health if in small particles). The sampling with multi-stage cascade impactors allows the collection of aerosols as different samples according to the dimensions of the particles. As an example, in Florence a SDI (Small Deposit area Impactor) sampler by Dekati [1] is available. It is a 12-stages impactor, with the following cut-off aerodynamic diameters: 8.57, 4.12, 2.70, 1.68, 1.07, 0.90, 0.60, 0.35, 0.23, 0.15, 0.09, 0.05 μm . With SDI, aerosol particles are collected in non-uniform, multi-spot, point-like deposits enclosed in an 8 mm diameter area on Nuclepore, Kapton or Kimfol foils.

At LABEC, an external beam line is fully dedicated to PIXE-PIGE analysis of aerosol samples. Briefly, the proton beam is extracted in air and the aerosol samples are positioned at a distance of about 1 cm from the extraction window, with the volume of atmosphere between them saturated with helium, to reduce the absorption of the emitted radiation. The beam size is set by a collimator (usually to $1.0 \times 2.0 \text{ mm}^2$) located in the end of the in-vacuum beam line. Two X-ray detectors optimized for low and medium-high X-ray energies, respectively, are used in order to obtain an effective simultaneous detection of all the elements. γ -rays for PIGE analysis are detected by a 60 mm \times 23 mm Ge detector. For the study of SDI samples the beam is de-focused and collimated to obtain a homogeneous spot on the target and a suitable scanning mode is set up in order to analyze uniformly the sampled area. Routinely PIGE is used as a side-kick of PIXE to correct the underestimation of PIXE in quantifying the concentration of the lighter elements, like Na or Al due to X-ray self-absorption inside the individual aerosol particles. Thus PIGE allows the determination of proper bulk correction factors for the light elements depending on the dimension of the particles for every stage and their possible “piling” in the point-like spots; in fact, relevant self-absorption can be observed also when small particles are under study, if they are heavily accumulated on small spots (Figure 1).

Examples from real campaigns performed in different remote areas will be shown.

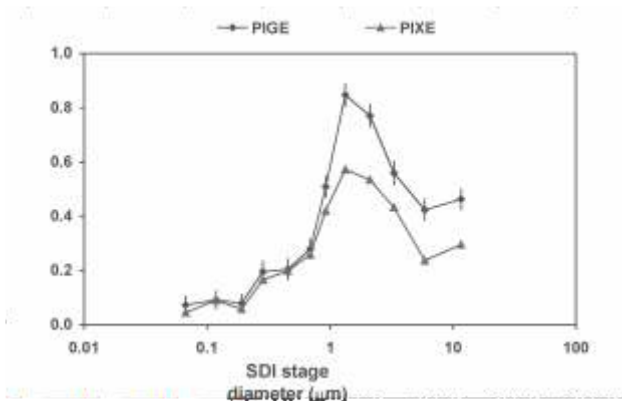


Figure 1: Na PIXE and PIGE concentration on samples from a SDI cascade impactor.

[1] W. Maenhaut, R. Hillamo, T. Mäkelä, J. L. Jaffrezo, M. H. Bergin, C. I. Davidson, Nucl. Instr. & Meth. B, 109/110 (1996), 482.

PA33 PIXE and ICP-AES comparison in evaluating the efficiency of metal extraction and analysis in aerosol samples

F. Rugi^(a), S. Becagli^(a), G. Calzolai^(b), M. Chiari^(b), C. Ghedini^(a), F. Lucarelli^(b), M. Marconi^a, S. Nava^(b), M. Severi^(a), R. Traversi^(a) and R. Udisti^(a).

^(a) Dep. of Chemistry, University of Florence, Via della Lastruccia,3 50019, Sesto F.no (FI), Italy

^(b) Dep. of Physics and Astronomy , University of Florence & INFN, Via G. Sansone,1, 50019, Sesto F.no (FI), Italy

A recent EU regulation (EN 14902 2005) requests the quantification of selected metals in the atmospheric particulate by mineralization with H₂O₂ and HNO₃ in microwave oven. This method might possibly conflict with the determination of the total metal content. In fact, the more the aerosol is enriched in crustal elements the more the difference in the two methods are expected, since the H₂O₂ + HNO₃ extraction is not reliable for metals in silicate form. In order to evaluate the extracted fraction, PIXE and ICP-AES measurements were carried out on the two halves of a series of PM10 and PM2.5 samples collected on Teflon filters in an urban site in the surrounding of Florence (Italy).

An ICP-AES (*Inductively Coupled Plasma - Atomic Emission Spectroscopy*) method was optimized by an ultrasound nebuliser (CETAC 5000 AT⁺), in order to improve reproducibility and detection limit. In these conditions, it was possible quantifying Al, As, Cr, Cu, Fe, Mn, Ni, Pb and V at sub-ppb levels. PIXE analysis using the external beam set-up at LABEC and a 3 MeV proton beam was carried out in order to measure the total elemental content of the metals. By comparing the ICP-AES and the PIXE results, a preliminary evaluation of the efficiency of the H₂O₂ and HNO₃ extraction method was performed.

The obtained results (the mean values for the ICP-AES/PIXE ratio are reported in Table 1) show that the extraction procedure following the EN 14902 directive allows quantitative recoveries (80-120%, including the analytical uncertainties) for the majority of the analysed metals, especially for those mainly emitted by anthropic sources. This result points out that anthropic metals are present in the atmosphere as relatively available species (free metals, labile complexes, carbonates, oxides). On the contrary, lower recoveries were obtained for Al (mean value around 75%), a metal that has a relevant crustal fraction.

	Al	As	Cu	Fe	Mn	Ni	Pb
ICP-AES/PIXE	75	102	92	104	92	103	86

Table 1. Percentage of recovery of ICP-AES versus PIXE determination.

Finally, we will show some examples in which ICP methods are used to determine the "soluble fraction" (in the acidic extraction conditions) of several major (ICP-AES) and trace (ICP-MS) metals. By comparing data obtained by PIXE and by ICP-AES or ICP-MS, we could assess the "soluble fraction" (in different conditions, depending on the strength of the acidic solubilization) of several elements. In this way, PIXE and ICP techniques appear to constitute a powerful complementary method, able to obtain a more complete data set of the aerosol chemical composition.

PA34 External beam milli-PIXE as analytical tool for Neolithic obsidian provenance studies

B. Constantinescu^(a), D.Cristea-Stan^(a), I. Kovács^(b) and Z. Szőkefalvi-Nagy^(b)

^(a)National Institute for Nuclear Physics and Engineering "Horia Hulubei", Str. Reactorului no.30, Bucharest-Magurele, Romania

^(b)Wigner Research Centre for Physics, Institute for Particle and Nuclear Physics, Konkoly-Thege Miklós út 29-33, H-1121 Budapest, Hungary

Obsidian is the most important archaeological material used for tools and weapons before metals appearance. Its geological sources are limited and concentrated in few geographical zones: Armenia, Eastern Anatolia, Italian Lipari and Sardinia islands, Greek Melos and Yali islands, Hungarian and Slovak Tokaj Mountains. Due to this fact, in Mesolithic and Neolithic periods obsidian was the first archaeological material intensively traded even at long distances. To determine the geological provenance of obsidian and to identify the prehistoric long-range trade routes and possible population migrations elemental concentration ratios can help a lot, since each geological source has its "fingerprints". In this work external milli-PIXE technique was applied for elemental concentration ratio determinations in some Neolithic tools found in Transylvania and in the Iron Gates region near Danube, and on few relevant geological samples (Slovak Tokaj Mountains, Lipari, Armenia).

In Transylvania (the North-Western part of Romania, a region surrounded by Carpathian Mountains), Neolithic obsidian tools were discovered mainly in three regions: North-West – Oradea (near the border with Hungary, Slovakia and Ukraine), Centre – Cluj and Southwest - Banat (near the border with Serbia). A special case is Iron Gates - Mesolithic and Early Neolithic sites, directly related to the appearance of agriculture replacing the Mesolithic economy based on hunting and fishing. Three long-distance trade routes could be considered: from Caucasus Mountains via North of the Black Sea, from Greek islands or Asia Minor via ex-Yugoslavia area or via Greece-Bulgaria or from Central Europe – Tokaj Mountains in the case of obsidian. As provenance "fingerprints", we focused on Ti to Mn, and Rb-Sr-Y-Zr ratios.

The measurements were performed at the external milli-PIXE beam-line of the 5MV VdG accelerator of the Wigner RCP. Proton energy of 3MeV and beam currents in the range of 1 ± 10 nA were used. X-ray spectra were taken by an Amptek X-123 SDD spectrometer positioned at 135° with respect to the beam direction. X-ray peak intensities and concentration calculations were made by the GUPIX program package.

External beam milli-PIXE proved to be very suitable in the case of obsidians mainly due to the possibility to analyse flat areas of the multi-faceted mini-tools (blades and arrow heads) and to verify the homogeneity of the samples (e.g. to avoid micro-inclusions of Ti rich soil). The preliminary results show the Transylvanian Neolithic samples have a Slovak Tokaj Mountains provenance. For Iron Gates samples the situation is more complicated: there have at least two different geological sources: for Late Neolithic tools the origin is also Slovak Tokaj Mountains, but for Late Mesolithic-Early Neolithic samples the sources are clearly different, we are supposing Hungarian Tokaj Mountains or Balkan-Aegean sources, but additional analyses and a systematization of literature data are being necessary.

PA35 Improvement of the Tohoku microbeam system for nanoscopic analysis

S. Matsuyama, K. Ishii, A. Terakawa, Y. Kikuchi, M. Fujiwara, H. Sugai, M. Karahashi, Y. Nozawa, S. Yamauchi, K. Watanabe, M. Fujisawa, M. Ishiya and T. Nagaya

Department of Quantum Science and Energy Engineering, Tohoku University

High-energy ion microbeams are versatile tools for analyses in a micrometer-sized region. A microbeam system was installed at Dynamitron laboratory at Tohoku University in July 2002 for biological applications [1]. The primary purpose was to develop a 3D PIXE- μ -CT [2,3,4], in which a microbeam is used to create a monoenergetic point X-ray source. The second was to develop a microscopic analysis system. The system is applicable to simultaneous in-air/in-vacuum PIXE, RBS, SE, and STIM analyses [] and is used for various fields. A beam spot of $0.4 \times 0.4 \mu\text{m}^2$ at a beam current of several tens of pA has been produced [5]. However, μ -PIXE/RBS analyses demand beam currents of ca. 100 pA in our set-up, which restricts the spatial resolution to around $1 \times 1 \mu\text{m}^2$. Recently, higher spatial resolution down to several tenth nm is required e.g. in aerosol study. In *in-vivo* imaging using 3D PIXE- μ -CT, the long measurement time of several hours weakened the specimen. Thus beam currents higher than several hundred pA are required in the 3D PIXE- μ -CT applications.

To meet these requirements, Tohoku microbeam system was redeveloped. A new triplet lens system was installed to get larger demagnification than that of the previous system. The quadrupole lenses are manufactured by TOKIN Machinery Corporation. These lenses are set on fine stages which allow precise adjustment of translation, tilt and rotation. The separation between lenses and working distance can be arranged to meet any requirements. In the separate geometry, demagnification factors are around 60 and 200 for horizontal and vertical planes, respectively, which are seven times higher than those of the previous system. In this arrangement, effect on chromatic aberration is larger and energy resolution should be improved. While an energy analyzing system was installed at the head of the microbeam line, the analyzing system also reduces the brightness of the beam. Thus, we found various source of the voltage ripple of the accelerator and minimize these effects without reducing the brightness. We are now adjusting the whole system to get better performance.

1. S. Matsuyama et al. Nucl. Instr. and Meth. B, 210 (2003) 59
2. K. Ishii et al., Int. J. of PIXE, 15 (3&4) (2005) 111
3. K. Ishii et al., Nucl. Instr. and Meth. B, 249 (2006) 726
4. K. Ishii et al., Nucl. Instr. and Meth. A, 571 (2007) 64
5. S. Matsuyama et al. Nucl. Instr. and Meth. B, 260 (2007) 55

PI X E 2013

FOR TECHNOLOGY AND GLOBAL DEVELOPMENT

POSTER SESSION B

Thursday

Pb01 - PB40

PB01 Nitrogen ionization cross section by electron impact

A. P. L. Bertol^(a), P. Pérez^(b,c), J. Trincavelli^(b,c), G. Castellano^(b,c), R. Hinrichs^(d), M. A. Z. Vasconcellos^(a)

^(a)Instituto de Física, Universidade Federal do Rio Grande do Sul, Porto Alegre, RS, Brasil

^(b)Facultad de Matemática, Astronomía y Física, Universidad Nacional de Córdoba, Argentina

^(c)Instituto Enrique Gaviola, CONICET, Argentina

^(d)Instituto de Geociências, UFRGS, Porto Alegre, RS, Brasil

The electron impact ionization cross sections (σ) of light elements were recently reviewed [1], however the developed models were based on data from the early nineteen-seventies that had used varied experimental setups, e.g. gaseous samples, or organic films of nucleic acid bases sublimated on thin carbon films mounted on TEM copper grids. More recently the σ of heavier elements have been determined with thin mono-elemental films deposited on substrates. It has been shown that the influence of chemical bonding on the σ values is negligible [2], so the ionization cross section can also be experimentally determined measuring the characteristic X-ray spectrum emitted by a thin compound film containing the desired element (e.g. nitrides or oxides).

In this work the nitrogen ionization cross section was determined using films of AlN, Si₃N₄, TiN, and FeN with 10 nm thickness, deposited by magnetron sputtering (AJA International model ATC, ORION 8 UHV, LCN, Instituto de Física of Univ. Federal do Rio Grande do Sul, Brasil) on carbon planchets. The mass thicknesses of the films were determined using Rutherford backscattering spectrometry (RBS) in a 3MeV ion accelerator (High Voltage Engineering, Tandetron 3MV in the Laboratório de Implantação Iônica, IF-UFRGS, Brasil).

Nitrogen X-ray spectra were acquired in an electron microprobe (JEOL JXA 8230 in the Laboratorio de Microscopía Electrónica y Análisis por Rayos X of the Univ. Nacional de Córdoba, Argentina) equipped with a wavelength dispersive spectrometer (WDS) using a synthetic crystal (LDE1) with $2d \approx 60 \text{ \AA}$. The spectra were measured at beam energies of 1.0, 1.2, 1.5, 2.0, 3.0, 4.0, and 5.0 keV (see Figure 1).

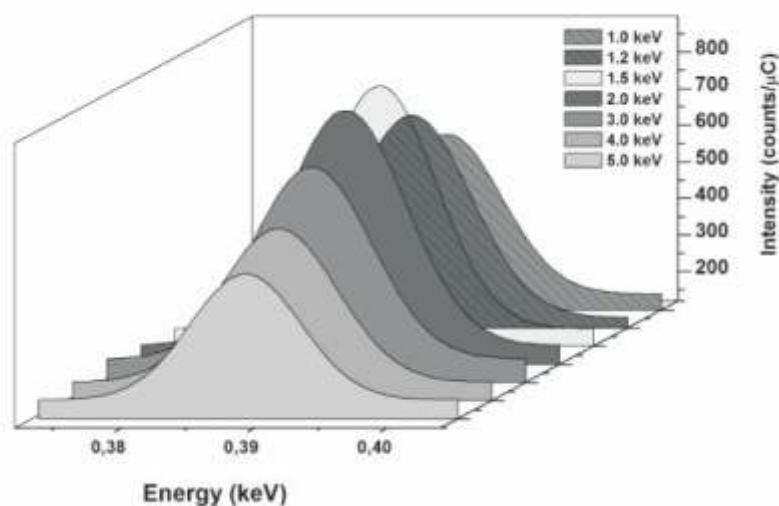


Figure 1: Nitrogen X-ray spectra excited with different electron energies.

The spectrometer efficiency was determined comparing the WDS and EDS spectra of the bremsstrahlung generated on an aluminum substrate when irradiated with 15 keV electrons with simulations using the PENELOPE software [3]. The obtained nitrogen ionization cross sections were compared with the old experimental data sets, and with recent semi-empirical and theoretical models [1,2].

[1] N. Tiwari, S. Tomar. *J. At. Mol. Sci.* 2(2) (2011) 109-116.

[2] S. Limandri, M.A.Z. Vasconcellos, R. Hinrichs, J. Trincavelli, *Phys. Rev. A* 86 (2012) 042701 -10.

[3] F. Salvat, J. M. Fernández-Varea, J. Sempau, in *Proceedings of the OECD/NEA Data Bank, Issy-les-Moulineaux, France* (OECD Publication, Paris, France, 2003).

PB02 Iron L-shell chemical effects in iron nitride films

A.P.L.Berto^(a), S.D.Jacobsen^(a), P. Pérez^(b,c), J. Trincavelli^(b,c), G. Castellano^(b,c), R. Hinrichs^(d),
M.A.Z. Vasconcellos^(a)

^(a)Instituto de Física, Universidade Federal do Rio Grande do Sul, Porto Alegre, RS, Brasil

^(b) Facultad de Matemática, Astronomía y Física, Universidad Nacional de Córdoba, Argentina

^(c) Instituto Enrique Gaviola, CONICET, Argentina

^(d)Instituto de Geociências, UFRGS, Porto Alegre, RS, Brasil

Iron nitride phases have been studied for a long time, due to their application in magnetic recording and because of their wear reducing properties when used as protective surface coatings. These phases can be obtained by various methods. It has been shown that reactive magnetron sputtering can produce phases encompassing the whole composition range in the phase diagram, even disclosing new phases and structures [1].

In this work two iron nitride films were obtained with different deposition atmospheres (Fe_xN_y 1 with 80 vol% N_2 : 20 vol% Ar and Fe_xN_y 2 with 40 vol% N_2 : 60 vol% Ar). The films were deposited on carbon planchets with nominal thickness of 10 nm using the reactive magnetron sputtering process in a ultra-high vacuum equipment. The phase composition of the films was characterized using GIXRD and Mössbauer spectroscopy, and their elemental composition was determined with Rutherford backscattering spectrometry (RBS) in the High Voltage Engineering 3 MV Tandetron of the Laboratório de Implantação Iônica, IF-UFRGS, Brasil.

The spectra of the Fe-L-lines from the two films and a bulk iron standard were acquired using an electron probe microanalyser (JEOL JXA 8230 in the Laboratorio de Microscopía Electrónica y Análisis por Rayos X of the Univ. Nacional de Córdoba, Argentina) equipped with a wavelength dispersive spectrometer (WDS) with a synthetic crystal (LDE1) with $2d \approx 60 \text{ \AA}$. The beam energy was kept at 5 keV. The spectra were processed with the software "POEMA" [2], considering the necessary adjustments of the bremsstrahlung, the characteristic line intensities, the peak shape, and the detector efficiency. The latter factor was obtained calibrating the WDS spectrometer efficiency against the EDS efficiency, measuring reference spectra simultaneously in the EPMA with both spectrometers [3].

The comparison of the spectra showed that the position of the $\text{La}_{1,2}$ line that is due to transitions of the outer M shell was shifted (Figure 1) and that the relative intensities of the La/Lb -lines, were affected by the chemical environment. We propose the use of the chemical effects as an additional phase recognition method, which can be used as a depth sensitive technique in cross sections of thicker films, as those used in wear coatings obtained by conventional glow discharge plasma nitriding.

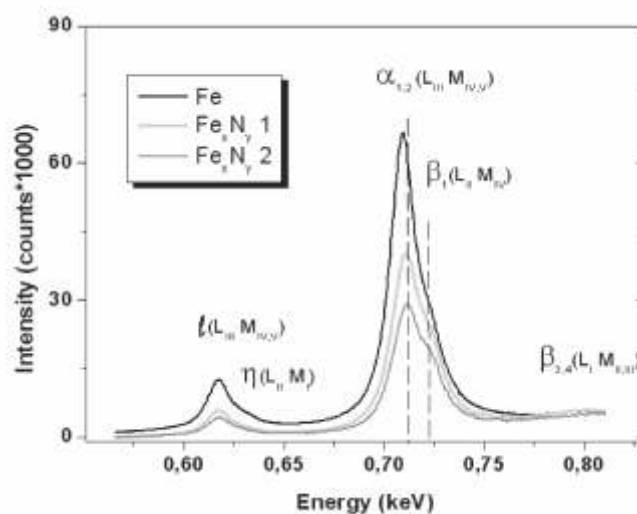


Figure 1: Iron L-lines of the Fe bulk standard and the two Fe_xN_y films.

[1] E. Bradley Easton, Th. Buhrmester, J.R. Dahn, Thin Solid Films 493 (2005) 60 – 66

[2] R. Bonetto, G. Castellano, J. Trincavelli, X-Ray Spectrom. 30 (2001) 313–319.

[3] J. Trincavelli, S. Limandri, A. Carreras, R. Bonetto, Microsc. & Microanal. 14 (2008) 306-314

PB03 L-shell ionization cross sections induced by protons and alpha-particles in the 0.7-2.0 MeV/amu range for Fe, Ni, Ru, and Ag

A.P.L. Berto^(a), T.P. Rodríguez^(b,c), A.H. Sepúlveda^(b,c), J. Trincavelli^(b,c), G. Castellano^(b,c), R. Hinrichs^(d), M.A.Z.Vasconcellos^(a)

^(a)Instituto de Física, Universidade Federal do Rio Grande do Sul, Porto Alegre, RS, Brasil

^(b)Facultad de Matemática, Astronomía y Física, Universidad Nacional de Córdoba, Argentina

^(c)Instituto Enrique Gaviola, CONICET, Argentina

^(d)Instituto de Geociências, UFRGS, Porto Alegre, RS, Brasil

No reliable theoretical or semi-empirical models have been developed to predict L-subshell ionization cross sections induced by protons or alpha-particles [1, 2]. A comprehensive experimental data-base is needed to test the different theories and the impact that perturbations might have on the existing ionization ECPSSR model [3]. The development of new detectors and faster electronics, and ultra-high vacuum facilities for thin film preparation are expected to bring improvements to the dataset available for comparison. This work intends to contribute with experimental data for L-shell ionization cross sections induced by protons and alpha-particles in the 0.7-2.0 MeV/amu range for Fe, Ni, Ru, and Ag.

Thin films of Fe, Ni, Ru, and Ag were deposited on carbon planchets (Ted Pella) by magnetron sputtering (AJA International model ATC, ORION 8 UHV in the Laboratório de Nanoconformação, Instituto de Física of Univ. Federal do Rio Grande do Sul, Brasil) with low deposition rates (0.1 A/s) until a nominal thickness of 10 nm was obtained. The mass thickness was determined with Rutherford backscattering spectrometry (RBS) in a 3MeV ion accelerator (High Voltage Engineering, Tandetron 3MV in the Laboratório de Implantação Iônica, IF-UFRGS, Brasil).

The samples were irradiated in the same ion accelerator with protons and alfa-particles in the 0.7 -2.0 MeV/amu range integrating the total charge during the measurement. Charging was avoided exposing the sample surface to low energy electrons from a nearby filament. Charge normalized PIXE spectra were obtained with an EDX Si(Li) detector (e2V Scientific Instruments, model Sirius 80, with 148 eV energy resolution at the Mn Ka line, takeoff angle of 48.5°). The data acquisition was performed with a Titan pulse processor. The detector efficiency and geometry were tested determining the K-shell ionization cross sections, which compared well to the data in the recent literature.

To determine the L-sub-shell ionization cross sections the relative proportion of the X-ray lines that are generated at the relaxation of the ionized state were taken into account. In view of the considerable overlap of these lines in EDX- spectra, a prior determination of the relative intensities of the X-rays due to transitions from several sub-shell filling the different L-sub-shell vacancies in bulk samples was performed, using an electron microprobe (JEOL JXA 8230) equipped with wavelength dispersive spectrometers (WDS), at the Laboratorio de Microscopía Electrónica y Análisis por Rayos X of the Univ. Nacional de Córdoba, Argentina. The experimental results were compared with ECPSSR theory and tabulated results.

[1] G. Lapicki. Nucl. Instrum. Methods Phys. Res., Sect. B 189 (2002) 8-20.

[2] J.L. Campbell, T.L. Hopman, J.A. Maxwell, Z. Nejedly. Nucl. Instrum. Methods Phys. Res., Sect. B 170 (2000) 193-204.

[3] I. Orlic, C.H. Sow, S.M. Tang. Atomic Data and Nuclear Data Tables 56 (1994) 159-210.

PB04 IBA analysis of TiO₂-doped nanocomposites to be used in orthodontic occlusal restoration

M. Abdelaziz^(a), J. Mars^(b), A. Atbayga^(b), D. Gihwala^(b)

^(a)Dept. of Dental Sciences, Cape Peninsula University of Technology, PO Box 19111, Tygerberg, 7505, South Africa.

^(b)Dept. of Biological Sciences, Cape Peninsula University of Technology, PO Box 1906, Bellville, 7535, South Africa.

Mechanical properties of dental composite, such as wear resistance, continue to be of primary importance when restoring large occlusal areas in posterior teeth. This is especially so in the instance of the cusp tips of artificial teeth that wear down, that is, become flattened. Ultimately, the chewing efficiency is affected.

The objective of this work is to synthesize and characterize TiO₂-doped nanocomposites polymer to be used for occlusal restoration. When dispersed at the nanoscale, TiO₂ could act as visually transparent UV filters and high-thermomechanical-performance materials. The synthesis entails the modification of aggregated TiO₂ by silyl propylmethacrylate derivatives. It is therefore necessary to 1) investigate the surface characteristics with respect to the effect of modifier concentration on the physicochemical properties, 2) establish the size distribution of unmodified and modified TiO₂ nano-size particle powders, 3) the qualitative and quantitative grafting of methacrylate groups on TiO₂ surface and 4) the quantitative elemental distribution (QECDs) in the final product.

For QECDs, PIXE and RBS have extensively been used to quantify elemental concentrations and more so, the quantitative elemental concentration distributions [3,4]. PIXE is used to determine QECDs of elements with atomic number $z > 10$, in the concentration range 1 part per million (1 ppm) and sizes greater than the beam spot size. RBS is used to determine light elements, $z < 11$ quantification, SEM is used for light element quantification and the distribution of particles where the sizes are less than that of the beam spot.

References

- [1] Kusy (1998). *Am. J. Orthod. Dentofacial Orthop.*, vol. 113, pp. 91-95.
- [2] Willems *et. al.* (1997), *J. Dent.*, vol. 25, pp. 263-270.
- [3] Mars (2004), Doctoral Thesis, Cape Peninsula University of Technology, Bellville, South Africa.
- [4] Pineda-Vargas *et. al* (2012) *NIMB*, vol. 273, pp. 153-156.

PB05 Applications of IBA to quantify the effect of Zr on Ti-alloy wires to be used as orthodontic material

K. Ali^(a), J. Mars^(b), A. Atbayga^(b), D. Gihwala^(b)

^(a)Dept. of Dental Sciences, Cape Peninsula University of Technology, PO Box 19111, Tygerberg, 7505, South Africa.

^(b)Dept. of Biological Sciences, Cape Peninsula University of Technology, PO Box 1906, Bellville, 7535, South Africa.

Recent developments in material science have presented newer archwire materials as well as improvements in the properties of existing ones. Proper selection and understanding of the biomechanical requirement of each case requires proper characterization studies on archwire alloys [1] Use of orthodontic archwires has some disadvantages such as high surface roughness, which increases friction at the wire-brace interface during the wire sliding process [2]. The surface quality and the surface roughness of dental materials are of utmost importance; these properties determine the area of the contact surface and thus influence on the friction [3].

Two orthodontic archwires preformed rectangular beta titanium III orthodontic archwires (0.43 × 0.64 mm) and titanium-molybdenum orthodontic archwires (0.040 × 0.64 mm). In addition, pure zirconium was deposited over the archwires. Several thin films of Zr were deposited over titanium orthodontic archwires. Determination of composition and surface roughness of orthodontic wires were performed with Particle-Induced X-ray emission (PIXE) [4] and Backscattering Spectrometry (BS). SEM analysis was performed to determine the major element composition.

Also reported is the strength and composition of archwires before and after deposition with zirconium and immersion in artificial saliva.

References

- [1] Krishnan *et. al.* (2004) Angle Orthodontist, vol. 74 (6). pp. 825-31.
- [2] Kappert *et. al.* (1988). Fortschritte der Kieferorthopadie, vol. 49 (4), pp. 358-367.
- [3] Tecco *et. al.* (2009). The Angle Orthodontist, vol. 79 (1), pp. 111-116.
- [4] Ryan *et. al.* (1995) NIMB, vol. 104, pp. 157-165.

PB06 Comparison of IBA and ICP-OES analyses of trace elements in the serum specimens of rats fed with extracts of anti-oxidant tea to ascertain trace element absorption

C. Kunsevi-Kilola, J.A. Mars, D. Gihwala

Department of Biomedical Sciences, Cape Peninsula University of Technology, PO Box 1906, Bellville, 7535, South Africa.

Antioxidants, generally referred to as reductants, are elements or compounds that easily donate an electron to become "oxidized", while oxidizing agents readily accept these electrons [1]. An antioxidant is thus a molecule capable of slowing or preventing the oxidation of other molecules [2]. Rooibos (*Aspalathus linearis*), a unique South African plant from which herbal tea is prepared, and various other tea extracts are known to be caffeine-free, have an abundance of antioxidants (flavonoids) and to contain several trace elements, those elements in parts per million quantities, such as Ca, K, Mg, Fe, Zn, Na, Co, Mn, and F, to maintain general good health. These trace elements are essentials to biochemical processes of metabolism and are toxic when present in excess. Over the past decades, it has been shown that critical diseases such as heart disease, cancer, and diabetes, associated with free radical. In this study male wistar rats were fed with with Rooibos teas and green tea extracts. Part of the serum obtained was analyzed with ICP-OES. The remainder was freeze-dried and pressed into a pellet and then analyzed with PIXE, RBS and SEM [3,4].

References

[1] Atkins, P. W. (1996) *The Elements of Physical Chemistry* (2nd ed.), London, Oxford University Press.

[2] Vertuani *et. al.* (2004) *Curr. Pharmaceut. Res.*, vol. 10(14), pp. 1677-1694.

[3] Ryan *et. al.* (1995) *NIMB*, vol. 104, pp. 157-165..

[4] Mayer (1999) *Am. Inst. Phys. Conf. Proc.*, vol. 475, pp. 541-544.

PB07 Correlation of element concentrations, determined by IBA, with clinical parameters of HIV-Aids serum specimens

M.L. Maqutu^(a), J.A. Mars^(b), C. Kunsevi-Kilola^(b), M. Saayman^(b), S. Tarr^(c), A. Mohammed^(a)

^(a)HIV-Aids Unit, Cape Peninsula University of Technology, PO Box 1906, Bellville, 7535, South Africa

^(b)Faculty of Health and Wellness Sciences, Cape Peninsula University of Technology, PO Box 1906, Bellville, 7535, South Africa.

^(c)National Health Training College, Private Bag A18, Maseru, Lesotho.

The economic burden of HIV-Aids related death of many individuals, especially those that are economically active, has crippled many countries' economies. More so is the fact that the pathogenesis of human immuno-deficiency virus (HIV) infection is until present not fully understood. To define the pathogenesis, various clinical parameters such as AST, ALT, LDH, bilirubin, uric acid, creatinine, CPK, ALP etc, and specific parameters such as CD4 cell counts have been determined. The ions of elements such as Ca, Mg, Fe, Cu, Zn and Se are incorporated into the structure of many enzymes and are therefore essential to the enzyme function. The focus of this study is the correlation of trace element concentrations, determined by IBA, with the clinical parameters.

Blood obtained from 100 HIV sero-positive males and females attending clinics at the National Health Training College in Maseru metropolis, Lesotho.

The clinical parameters were determined by using Arkray instrumentation. Afterwards the serum specimens were freeze-dried and then pulverized into palettes. The palettes were coated with carbon and then irradiated with a proton beam of 3 MeV energy. X-ray emission and backscattering data were obtained and then quantified with various computational software.

PB08 Application of IBA to determine the effects of Kolaviron (*Garcinia kola*) on the elemental metabolism in the rat liver and kidney

J.A. Mars, C. Kunsevi-Kilola, D. Gihwala

Department of Biomedical Sciences, Cape Peninsula University of Technology, PO Box 1906, Bellville, 7535, South Africa.

Poor or no antioxidant activity has been implicated in the aetiology of various pathologies. Since antioxidants are mostly derived from natural resources, the search for medicinal plants, that can either cure or alleviate ailments, has been phenomenal over the past decades. One plant, *Garcinia kola*, the oil of which is termed kolaviron, has been identified to have possible antioxidant activity [1]. Trace elements such as Fe, Mn, Cu, Zn and Se, form an integral part in antioxidant activity, especially in organ metabolism. In this study organ (liver and kidney) metabolism of major such as C, O, N, S, and trace elements is investigated. The kolaviron was dissolved in corn oil. Two groups (control and experimental) of Wistar rats were selected. The animals were housed in accordance with the WHO animal regulations. Both groups had ad libitum access to standard rat chow and potable tap water. The control group was fed, by gavage, with 200 microlitre of the solution of kolaviron in corn oil once per day for a period of 4 weeks. After this period the animals were sacrificed by intraperitoneal injection of pentobarbitone. The organs were excised and homogenised into smaller parts which were freeze-dried -80°C. The freeze-dried organ was then pulverized and press into a palette. Concentrations of trace elements were determined with proton-induced X-ray emission (PIXE). PIXE was selected since with this technique concentrations down to minimum detection limits (MDLs) of parts per million (ppm) can be determined. A beam of 3 MeV protons was used for bombardment and a Be filter of 125 micrometer thickness for absorption. Backscattering spectrometry (BS) was used to determine the matrix composition. PIXE and BS measurements were determined simultaneously. Scanning electron microscopy was used both as complementary and supplementary to PIXE and BS. Statistical tests of $p < 0.5$ were considered significant.

References

[1] Ogada & Braide (2009) Nig. J. Physio. Sci., vol. 24(1-2), pp. 53-57.

PB09 Ion-beam analysis of plasma of HIV-Aids positive individual patients and comparison to CD4 counts

J.A. Mars^(a), M.L. Maqutu^(b), C. Kunsevi-Kilola^(a), S. Tarr^(c), A. Mohammed^(b)

^(a)Department of Biomedical Sciences, Cape Peninsula University of Technology, PO Box 1906, Bellville, 7535, South Africa.

^(b)HIV-Aids Unit, Cape Peninsula University of Technology, PO Box 1906, Bellville, 7535, South Africa

^(c)National Health Training College, Private Bag A18, Maseru, Lesotho.

HIV-Aids related diseases have claimed the lives of many individuals, especially those that are economically active. This economic burden has crippled many economies since many of the lives claimed are those of individuals with special skills. However, the pathogenesis of human immuno-deficiency virus (HIV) infection is until present not fully understood. Elements such as Ca, Mg, Fe, Cu, Zn and Se are incorporated into the structure of many enzymes and are therefore essential to the enzyme function. The focus of this study is the correlation of trace element concentrations, determined by IBA, and the CD4 count. Blood obtained from 100 HIV sero-positive males and females attending clinics at the National Health Training College in Maseru metropolis, Lesotho.

The CD4 cells of the samples were determined by flow cytometry (Cytoflow SL – S using CD4/CD45 monoclonal antibody and SSC/F12 getting strategy). Afterwards the plasma specimens were freeze-dried and then pulverized into palettes. The palettes were coated with carbon and then irradiated with a proton beam of 3 MeV energy. X-ray emission and backscattering data were obtained and then quantified with various computational software.

PB10 Application of IBA in environmental remediation using skins of cocoa (*Theobroma cacao*) and sweet potatoe (*Ipomoea batatas*)

K. Sumbu^(a), J.A.Mars^(b), D. Gihwala^(b)

^(a)Department of Chemistry, Cape Peninsula University of Technology, PO Box 1906, Bellville, 7535, South Africa.

^(b)Department of Biomedical Sciences, Cape Peninsula University of Technology, PO Box 1906, Bellville, 7535, South Africa.

The industrial sector is one of the most dynamic sectors of the economy and is of cardinal importance in economic development and poverty alleviation. Furthermore, economies with low levels of industrialisation are gradually shifting dependence from agriculture to the industrial sector, while developed economies, with a high level of industrialisation, are shifting from the industrial to the service sector [1]. Amongst the various industrial sectors, a substantial portion of effluents containing heavy metals are generated by electroplating (nickel, lead, zinc and copper), tanneries (chrome) and other chemical industries. Many engineering processes have been designed to remove the heavy metals from the polluted parts of the ecosystem. These processes are however highly capital intensive. To establish a less costly means of removal of heavy metal pollution, the dried skins of cocoa (*Theobroma cacao*) and sweet potatoe (*Ipomoea batatas*) were pulverized and used in the absorption of the heavy metals Ni and Pb. After adsorption by the metals, the powders were dried and then pressed into tablets. For quantification of the elemental adsorption, PIXE, using the GeoPIXE computational software, is a versatile multi-element analytical technique, and has minimum detection limits down to concentration ranges as low as 0.1 parts per million [2, 3]. To determine the composition of the major elements such as C, O and N, Backscattering Spectrometry, using SimNRA software, [4] was used. In this study we report on the economic viability of using the skins of cocoa and sweet potato in the removal of Ni and Pd from polluted waters.

References

[1] Carter et. al. (1993) World Bank Discussion Papers # 224.

PB11 MicroPIXE and microNRA: associated tools for materials characterization

L.A.Bouffleur^(a,b), J.F. Dias^(a,b), and L. Amaral^(a,b)

- (a) Laboratório de Implantação Iônica, Instituto de Física, UFRGS, Porto Alegre, RS, Brazil.
(b) Programa de Pós-Graduação em Ciência dos Materiais, UFRGS, Porto Alegre, RS, Brazil.

Ion beam based analytical techniques are widely used for modification, characterization and analysis of materials. One of the motivations for the continued development and application of these techniques part of its high sensitivity for determining and quantifying trace elements in the order of parts per million (ppm), and create images of their distributions and depth profiles.

The elemental characterization of homogeneous samples is performed in, general, by combining two complementary techniques: PIXE (Particle Induced X-ray Emission) and RBS (Rutherford Backscattering) with stationary beams of the order of mm². However, when there are structures in the sample surface and differences in its elemental distribution, we should use the scanning microbeam system, where it reduces the size of the beam to the order μm². The association between the techniques remain the same. MicroPIXE provides the spatial distribution of elements with Z > 12 and microRBS allows the study of multilayer solids, with good selectivity for thin layers of heavy elements on light elements substrates.

Despite having lower cross sections, the technique of nuclear reaction analysis (NRA - Nuclear Reaction Analysis) can also be used in the microbeam system. The positive point is that through NRA is possible to determine light elements and their isotopes on any substrate.

This study shows the possibility of associating microPIXE and microRNA for elemental characterization of materials. As an example, we present the elemental characterization of a human hair. Through the microRNA was possible to determine the presence of carbon, while microPIXE showed the presence of elements such as: S, K, Ca and Zn in agreement with other studies reported [1].

Samples were irradiated at the Laboratório de Implantação Iônica (IF-UFRGS), utilizing the 3MV tandem accelerator. Proton beams with energy of 1,75 MeV were selected for analysis of particular micro regions of the hair sample with microPIXE and microNRA. The selected regions were scanned with focused proton beam of 4 - 5 μm spot size and currents of ~80 pA. The size of the scan was 200 μm x 200 μm.

[1] C.A. Pineda-Vargas, M. E. M. Eisa; Nucl. Instrum. Methods Phys. Res., Sect. B 268 (2010) 2164-2167.

PB12 Application of IBA in the comparative analyses of fish scales used as biomonitors in the Matola River, Mozambique

J.F. Guambe^(a,b,c), J.A. Mars^(d), J. Day^(a)

^(a)Freshwater Research Unit, Department of Zoology, University of Cape Town, Private Bag, Rondebosch, 7701, South Africa.

^(b)Physics Department, Eduardo Mondlane University, PO Box 257, Maputo, Mozambique.

^(c)Materials Research Department, iThemba LABS, PO Box 722, Somerset West, 7129, South Africa.

^(d)Faculty of Health and Wellness Sciences, Cape Peninsula University of Technology, PO Box 1906, Bellville, 7535, South Africa.

Many natural resources are invariably contaminated by industries located on the periphery of the resources. More so, fish found in the resources are used as dietary supplements, especially by individual that reside near the natural resources. The scale of fish have been proven to be applicable in monitoring contamination of the natural resources. However, the morphology and chemical composition of the scale of various species differ to a significant degree. Consequently, the incorporation of contaminants into the scale structure will be different. There is a need of pilot for contaminants which can harm the biota. The composition of the fish scales is different. To quantify the degree of incorporation onto the scale matrix we have analysed, using PIXE, RBS and SEM, the scale of four types of fish scales, that is, *Pomadasys kaakan* the javelin grunter; *Lutjanus gibbus* the humpback red snapper; *Pinjalo pinjalo* the pinjalo and *Lithognathus mormyrus* the sand streenbras. In this work we report on the viability of using various fish scales as monitors of natural resource contamination.

PB13 Bremsstrahlung in low atomic number thick targets by proton incidence

P. Pérez^(a,b), T. Rodríguez^(a,b), A. Bertol^(c), M. A. Z. Vasconcellos^(c) and J. Trincavelli^(a,b)

^(a)Facultad de Matemática, Astronomía y Física, Universidad Nacional de Córdoba, Argentina

^(b)Instituto de Física Enrique Gaviola, CONICET, Argentina

^(c)Instituto de Física, Universidade Federal do Rio Grande do Sul, Brazil

The subtraction of the continuum from an x-ray spectrum emitted by proton bombardment is usually carried out by means of a mathematical fitting. Thus, the emission lines corresponding to the atoms present in the sample are separated from the background generated in it. The purpose of the present work is to develop an analytical function to model the continuous spectrum generated in a PIXE experiment for different incident beam energies and atomic numbers in thick targets of light elements.

PIXE spectra were measured at the 3 MeV ion accelerator (High Voltage Engineering, Tandetron 3MV) in the Laboratório de Implantação Iônica, IF-UFRGS, Brazil, in thick samples of low atomic number: Be, B, C and BN. The results obtained can be applied to the more general case of thin targets deposited on light substrates like carbon or polymeric materials. The proton beam energies were varied between 700 and 2000 keV.

The spectra analysis was performed taking into account the main four effects underlying the production of the continuous spectrum: Secondary Electron Bremsstrahlung (SEB), Quasi Free Electron Bremsstrahlung (QFEB), Nuclear Bremsstrahlung (NB) and Atomic Bremsstrahlung (AB) [1]. Nevertheless, it was found that for the cases considered, AB is the most important one and the other contributions can be neglected in a first rough approximation.

The experimental spectra from carbon thick targets corrected by self-absorption and detector efficiency are shown in the figure. These spectra generated within the sample were parameterized as a function of the photon energy using an exponential polynomial [2]. Finally, the behavior with atomic number was studied for the light element range.

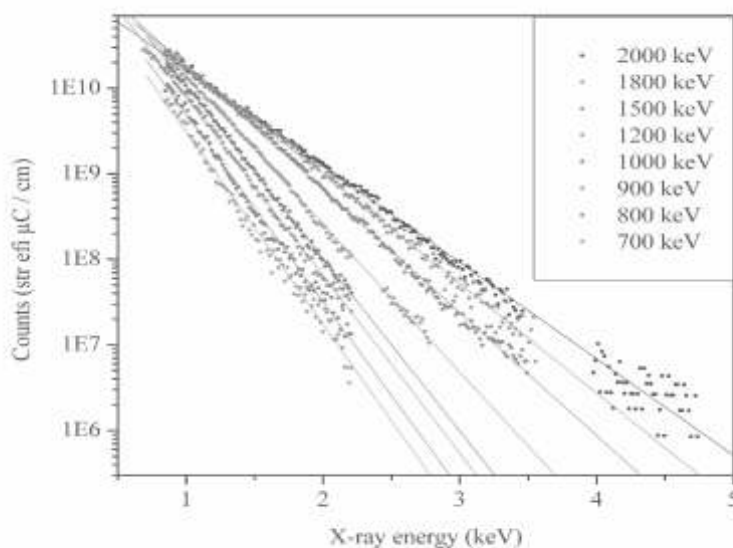


Figure. Continuum spectrum of carbon corrected by absorption and detector efficiency. Dots: experimental; solid line: fitting.

[1] S. Johansson, J. Campbell, K. Malmqvist, Particle-Induced X-Ray Emission Spectrometry (PIXE), first ed., John Wiley & Sons, New York, 1995.

[2] K. Murozono, K. Ishii, H. Yamazaki, S. Matsuyama, S. Iwasaki, Nucl. Instrum. Methods Phys. Res., Sect. B 150 (1999) 76-82.

PB14 L-shell x-ray production cross section for Fe, Ni, Ru and Ag by electron incidence

A. Sepúlveda^(a,b), A. Bertol^(c), M. A. Z. Vasconcellos^(c), R. Hinrichs^(d) and J. Trincavelli^(a,b)

^(a)Facultad de Matemática, Astronomía y Física, Universidad Nacional de Córdoba, Argentina

^(b)Instituto Enrique Gaviola, CONICET, Argentina

^(c)Instituto de Física, Univ. Federal do Rio Grande do Sul, Porto Alegre, RS, Brazil

^(d)Instituto de Geociências, Univ. Federal do Rio Grande do Sul, Porto Alegre, RS, Brazil

Reliable x-ray production cross sections σ_x for inner-shell ionization by electron impact are required for several applications, particularly for electron probe microanalysis and Auger electron spectroscopy. Nevertheless, experimental determinations of these parameters deal mostly with K-shells; while cross-section data for L-shells are scarcer [1].

In this work, σ_x values for L-shells by electron impact were determined from the analysis of the x-ray emission spectra acquired at incident beam energies between 3 and 25 keV from Fe, Ni, Ru, and Ag films. X-ray emission spectra were processed with the software POEMA [2], including the effects due to the substrate and those caused by a spontaneous oxide layer grown on the monoelemental films.

The films were deposited on vitreous carbon planchets, by d.c. magnetron sputtering with an ultrahigh vacuum equipment (AJA International ATC Orion 8). The film thicknesses were determined by Rutherford Backscattering Spectrometry in the ion accelerator TANDEM 3MV. The electron gun of a multibeam SEM-FIB (JEOL JIB-4500) was used to excite the spectra, which were acquired using an energy dispersive x-ray spectrometer (EDX) with a silicon drifted detector (SDD Thermo Scientific Ultradry). All the experimental part of this work was carried out at the Instituto de Física of the Universidade Federal do Rio Grande do Sul.

The absolute determination of σ_x requires the knowledge of the detector intrinsic efficiency and of the solid angle subtended by the x-ray detector. The first one, was estimated from the specifications given by the manufacturer for the detector window and the window supporting grid. The second one was obtained previously [2] from the comparison of the bremsstrahlung measured and simulated with the PENELOPE software [3] when a carbon substrate is irradiated with 15 keV electrons.

One of the main difficulties in the assessment of σ_x for the three L-shells from experimental spectra is the overlapping between lines corresponding to decays to different shells, e. g., L_{II} and L_{III} . In addition, some of the many lines involved have one or more satellite lines associated. To face this problem, the whole structure of the L-spectra of the studied elements was previously investigated by a careful and detailed processing of wavelength dispersive x-ray spectra carried out with the software POEMA [2].

The values obtained for the x-ray production cross sections were compared to those found in the literature for the atomic shells L_I , L_{II} and L_{III} .

[1] C. Campos, M. A. Z. Vasconcellos, X. Llovet, F. Salvat, Phys. Rev. A 66 (2002) 012719 1-9.

[2] S. Limandri, M. A. Z. Vasconcellos, R. Hinrichs, J. Trincavelli, Phys. Rev. A 86 (2012) 042701 1-10.

[3] F. Salvat, J. M. Fernández-Varea, and J. Sempau, in Proceedings of the OECD/NEA Data Bank, Issy-les-Moulineaux, France (OECD Publication, Paris, France, 2003).

PB15 Structure of the x-ray emission L spectra for Fe, Ni, Ru, Ag and Te by electron incidence

T. Rodríguez^(a,b), A. Sepúlveda^(a,b), A. Bertol^(c), G. Castellano^(a,b), A. Carreras^(a,b), M. A. Z. Vasconcellos^(c) and J. Trincavelli^(a,b)

^(a)Facultad de Matemática, Astronomía y Física, Universidad Nacional de Córdoba, Argentina

^(b)Instituto de Física Enrique Gaviola, CONICET, Argentina

^(c)Instituto de Física, Universidade Federal do Rio Grande do Sul, Brazil

X-ray emission spectra excited by electron incidence from Fe, Ni, Ru, Ag and Te targets were measured with a wavelength dispersive spectrometer. To this purpose, spectra were recorded in a JEOL JXA 8230 microprobe at the Laboratorio de Microscopía Electrónica y Análisis por Rayos X of the Universidad Nacional de Córdoba, Argentina. The atomic transitions studied involve decays to states with vacancies in the L shell. A careful spectral processing was carried out, based on a method of parameter refinement previously implemented [1]. With this method, characteristic energies, relative transition probabilities and natural linewidths, fitted by Voigt profiles [2], were determined.

The origin and shape of the satellite bands appearing at the high energy side of the main lines is also discussed, as well as the Auger radiative structures located at the low energy side of the most intense peaks. Finally, the results obtained are compared with the data available in the literature.

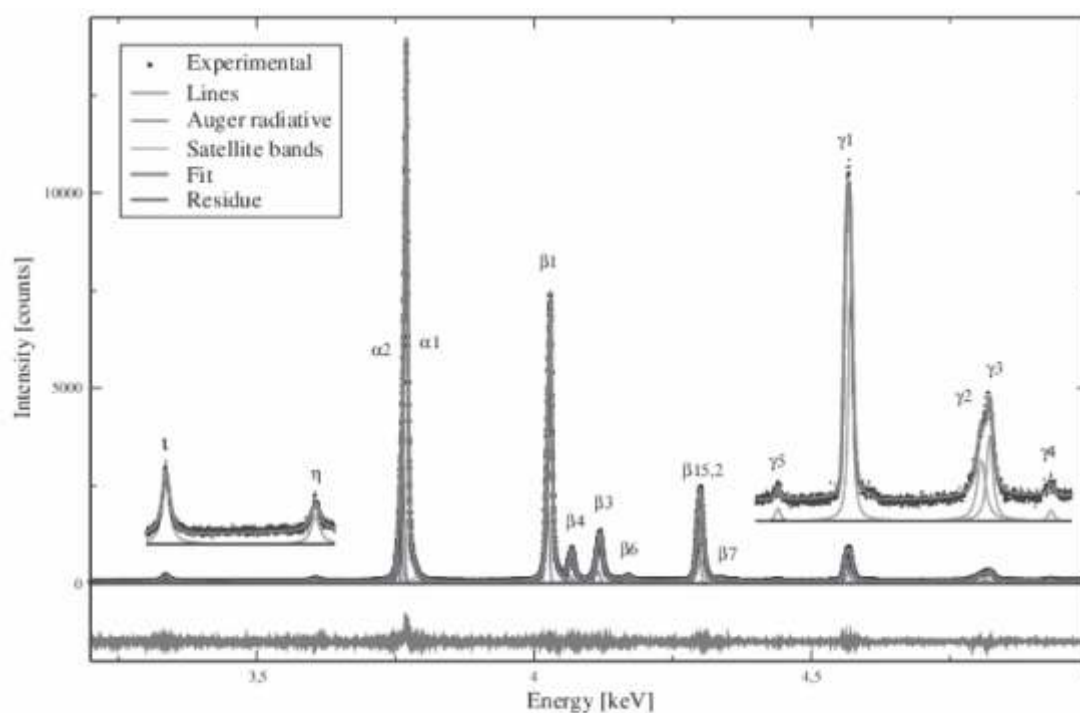


Figure. Tellurium L spectra. The zoomed regions make visible the less intense lines.

[1] S. Limandri, J. Trincavelli, R. Bonetto, A. Carreras, Phys. Rev. A 78 (2008) 022518 1-10.

[2] S. Limandri, R. Bonetto, H. Di Rocco, J. Trincavelli, Spectrochim. Acta B 63 (2008) 962-967.

PB16 Self-consistent simulation of an electron beam for a new autoresonant x-ray generator

Ana M. Herrera, Eduardo A. Orozco, and Valeriy D. Dugar-Zhabon

Universidad Industrial de Santander, Bucaramanga, Colombia

It is shown that an electron beam which is accelerated by TE_{102} microwaves in a rectangular cavity under cyclotron resonance conditions can be used to generate x-rays. An alternative scheme of the x-ray source is shown in Fig 1. The microwave power produced by a magnetron 5 penetrates into a rectangular cavity 1 through waveguide and ferrite isolator 3 and iris window 4. An axially symmetric magnetostatic field is formed by a system of current coils or magnetic rings 2. Electron gun 7 injects the electron beam into the cavity along the magnetic field axis. The magnetic field parameters are those which can maintain the electron beam in the space cyclotron autoresonance regime [1, 2]. To produce x-ray stream, molybdenum target 6 is placed at the acceleration zone end.

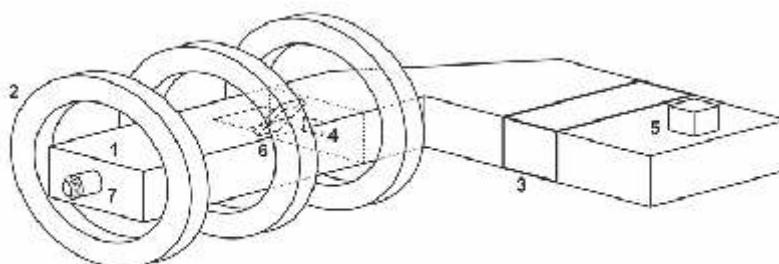


Figure.1. Physical scheme of the autoresonant x-ray source system: 1- cavity, 2- magnets or current coils, 3- waveguide-ferrite isolator, 4- iris microwave window, 5- microwave generator, 6- non-magnetic metal target, 7- electron gun.

To take into consideration the self-consistent electric and magnetic fields of the electron beam, a full electromagnetic particle-in-cell (*PIC*) code is developed. The time dependent electromagnetic field which is defined as the superposition of both the field and the fields generated by the electron beam is simulated at each time step by implementing the finite difference time domain (*FDTD*) method [3]. The beam current density along its trajectory is calculated using the charge conservation method. The cylindrical components of the static magnetic field and the self-consistent fields at simulation particle positions are found by applying bilinear and trilinear interpolations of the mesh node data respectively. The relativistic Newton-Lorentz equation presented in the centered difference form is solved using the Boris algorithm that provides visualization of the beam path and its energy evolution. It is shown that the injected 12 keV electron beam of a 1 A current is accelerated to energy of 250 keV by the 2.45 GHz microwaves of 14 kV/cm in amplitude at a distance of 17 cm. The proposed type of 2.45 GHz x-ray source can be classified as compact with a dimension of the order of 30 cm.

[1] V. D. Dugar-Zhabon and E. A. Orozco. "Modeling of electron cyclotron resonance acceleration in a stationary inhomogeneous magnetic field". *Phys. Rev. ST. Accel. Beams*. 11, 041302 (2008).

[2] V. D. Dugar-Zhabon and E. A. Orozco. "Cyclotron spatial autoresonance acceleration model". *Phys. Rev. ST. Accel. Beams*. 12, 041301 (2009).

[3] C. K. Birdsall and A. B. Langdon, *Plasma Physics via Computer Simulation*, p. 356, (Bristol and Philadelphia: Institute of Physics Publishing, 1991).

PB17 Study of injuries to fish liver with PIXE and micro-PIXE

E. M. Stori^(a), M. L. C. F. Rocha^(b), J. F. Dias^(b), C. T. de Souza^(a), L. Amaral^(a), J.F. Dias^(a)

^(a)Ion Implantation Laboratory, Physics Institute, Federal University of Rio Grande do Sul, Av. Bento Gonçalves 9500, Postal Code 91501-970, Porto Alegre, RS, Brasil

^(b)Oceanographic Institute, University of São Paulo, Praça do Oceanográfico, 191 Butantã, Postal Code 05508-900, São Paulo, SP, Brasil

Fish liver is the primary organ related to the biotransformation of organic contaminants and metals. It is sensitive to contaminants and can accumulate them in relatively higher levels than the environment itself and other organs [1], thus being susceptible to multiple injuries. These injuries are histopathologically characterized as modifications of the cellular structure of the tissue and are usually accompanied by pigmented cells called melanomacrophage centers [2,3]. While these structural modifications are invisible to micro-PIXE, the melanomacrophage centers are distinguishable by this technique. Therefore, these structures were the focus of the present study. For quantitative analysis, broad PIXE measurements were carried out.

Micro-PIXE results show that there is a higher concentration of Fe, P, K, Ti, Cr, Ni, Cu and Zn in melanomacrophage centers. On healthy tissue, the concentration of these elements is homogeneous. In cases where the histopathological study showed injuries without melanomacrophage centers, the micro-PIXE analysis showed much smaller clusters with higher concentrations of these elements, suggesting the presence of melanomacrophage centers too small to be detected by histopathological studies. Broad PIXE results showed that the concentration of Si, Cl, K, Ti, Fe and Cu are directly related to the presence of melanomacrophage centers. Moreover, it could be observed that the concentration of Cr, Mn and Ni is directly related to the injuries but not to melanomacrophage centers.

[1] D. W. T. Au, *Mar. Pollut. Bull.*, v. 48 (2004) 817-834

[2] Leknes I. L., *Melano-macrophage centres and endocytic cells in kidney and spleen of pearl gouramy and platyfish (Anabantidae, Poeciliidae: Teleostei)*. *Acta histochemica*, v. 109, 2007, p. 164.

[3] Saunders H. L., Oko A. L., Scott A. N., Fan C. W., Margor B. G., *The cellular context of AID expressing cells in fish lymphoid tissues*. *Developmental and Comparative Immunology*, v. 34, 2010, p. 669.

PB18 PIXE facility at Centro Atómico Bariloche

S. Limandri^(a), C. Olivares^(b), L. Rodriguez^(a), G. Bernardi^(a,b) and S. Suárez^(a,c)

^(a)Consejo Nacional de Investigaciones Científicas y Técnicas de la República Argentina (CONICET)

^(b)Centro Atómico Bariloche, Comisión Nacional de Energía Atómica, Bustillo 9500, San Carlos de Bariloche, Río Negro, Argentina

^(c)Instituto Balseiro, Universidad Nacional de Cuyo, Bustillo 9500, San Carlos de Bariloche, Río Negro, Argentina

A Tandem accelerator, NEC Pelletron 5SDH, has been recently installed at Centro Atómico Bariloche, Argentina. This facility provides the local scientific community the opportunity to use nuclear techniques in different fields such as material science, environment (air, soil and food), biology, archaeology, etc. The ion beam techniques available in our laboratory includes the ones commonly used in material analysis, i. e., PIXE (proton induced X-ray emission), RBS (Rutherford backscattering spectroscopy), PIGE (proton induced gamma ray emission), channeling and ERDA (elastic recoil detection analysis).

The line used for material analysis consists of a NEC-RC43 Endstation with setups and detectors for all the techniques abovementioned. This communication includes a description of the system facility and the main associated equipment, in particular that for PIXE measurements. In addition, we show some recent applications of PIXE to the study of archaeological ceramics, smokeless gunpowders, and the experimental determination of the efficiency of our SDD detector.

The detector efficiency was estimated for energies between 0.27 and 25 keV. The method applied is based on the comparison of X-ray characteristic intensities excited by 2-MeV protons in bulk samples with theoretical predictions. The results are compared with efficiency values obtained by the product of the window transmission and the detector quantum efficiency.

Element constituents of black, white, brown and ocher pigments from Aguada Culture (600-900 before present) were studied. The results obtained are compared with measurements performed at the Laboratório de Implantação iônica –UFRGS. This study is helpful to interpret the social, political economic and cultural contexts of pre-Inca societies and the interaction among different sites.

Traces amounts present in seven smokeless gunpowders commonly used in Argentina were determined. The powders were deposited on a carbon tape and the contribution of the substrate was taken into account in the spectral processing. The results obtained show that trace element concentration can be used to distinguish the gunpowders.

PB19 Characterization of Ancient Metal Using Non-destructive Methods

Hellen Santos, Nemitala Added

Instituto de Física da Universidade de São Paulo - Departamento de Física Nuclear
hsantos@dfn.if.usp.br

The traditional methods to characterize metal in archaeometry are always destructive or limited to qualitative analysis. The challenge, nowadays, is to make analyses able to give quantitative, reliable information on several topics as conservation status, composition and manufacturing techniques without damaging the artifacts. Some nuclear techniques like IBA (Ion Beam Analysis) can be applied with this purpose. In this work, in order to obtain the elemental composition, the crystallographic pattern and grain size on blade surface of two ancient swords, we used PIXE (Particle Induced X-rays Emission) and XRD (X-rays Diffraction).

The PIXE irradiation was performed in external beam setup installed at Lamfi¹ (Laboratório de análises de material por feixe iônico-Universidade de São Paulo) using a 2.6 MeV energy proton beam to probe the samples. The system of detection is composed by two Si(Li) detector for X-rays with 140eV resolution in Mn region. The beam charge was estimated by X-rays coming from an Au foil, placed immediately after the output window in the external beam line.

XRD analysis were made at Laboratório de Cristalografia², Instituto de Física- Universidade de São Paulo. The results of the present investigation allowed differentiating between the relative concentration of steel alloy elements in the edge and a thick part of blade, suggesting difference in the treatment of those parts.

References

<http://www2.if.usp.br/~lamfi/>

<http://web.if.usp.br/cristal/node/10> (responsible for the laboratory: Dr. Marcia Fantini and Physicist and Technician Antônio Carlos Franco da Silveira)

PB20 Analysis of early 20th century pigments in R. Heintz's paintings using PIXE and mobile analytical systems

C. Defeyt^(a), H. Calvo del Castillo^(a), A. Deneckere^(b), F.-P. Hocquet^(a), P. Vandenaabeele^(b) and D. Strivay^(a)

^(a)Institut de Physique Nucléaire, Atomique et de Spectroscopie & Centre Européen d'Archéométrie, University of Liège (Belgium)

^(b)Archaeometry and Natural Sciences, University of Gent (Belgium)

In this work we will present the evolution of the pigments used by Richard Heintz (Herstal 1871, Sy 1929) in his paintings. He was a Belgian painter from the Impressionist school. We have analyzed several of his masterworks with non-invasive techniques to characterize the changes in pigment use during his life. We have indeed used PIXE in external mode and mobile techniques such as X-ray fluorescence and Raman spectroscopies.

We were able to identify most of the pigments from his palette. We will discuss here the composition as well as the degradation of some of the pigments. For example, the yellow pigments have changed several times during his career. He used iron oxides, chromium, zinc cadmium and barium based pigments.

The palette of Heintz reconstituted through this analysis shows the use of pigments from the industrial era. It also includes pigments mentioned in the correspondence of the painter. The results obtained on the old tubes found in the painter's box ascribed to Richard Heintz are much more equivocal. The presence of copper phthalocyanine in the two boxes of color is an anachronism which challenges its authenticity.

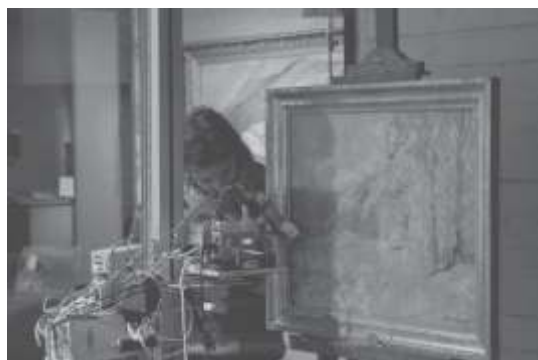


Fig. 1 Mobile XRF analysis of Heintz's painting at the Musée de l'Art Wallon in Liège

PB21 Development of a low-beam-energy PIXE analysis system based on an ion implanter

W. Kada¹, A. Kishi², M. Sueyasu², F. Sato², Y. Kato², and T. Iida²

¹ Takasaki Advanced Radiation Research Institute, Japan Atomic Energy Agency

² Graduate School of Engineering, Osaka University

Elemental-compositions on the surface layers of thin-film materials fascinate growing interest of the analytical researches in determining its behavior and interactions in the nature [1]. Low-beam-energy PIXE has advantages in its penetration depth inside of the target. However there are very few discussions and researches of low-beam-energy PIXE because of its low emission efficiency of characteristics X-rays [2]. In this study, the applicability of low-energy PIXE for surface elemental composition analysis was investigated with collimated 100 keV proton beam generated from a 200 kV ion implanter. Measurement and control system of the irradiation system was modified to fit the requirements of low-beam energy PIXE analysis. The beam parameters like energy of probe protons were precisely controlled by compact reprogrammable logic array with high accuracy 16bit D/A convertor. Electrically cooled Si-PIN detector was installed on the analysis chamber with an angle of 45° to the beam axis and a distance of 15 mm to the analytical target. Elemental analysis of the target was performed using millimeter-sized beam probe of 10-100 keV H^+ with current of 1- 200 $\mu A/mm^2$.

Thin film targets were prepared for the evaluation of this low-beam-energy PIXE analysis by using ion implantation and thermal evaporation techniques. First, film targets of titanium, silver, and gold with thickness of approximately 5 nm were irradiated with proton beam with energy from 10 to 100 keV. Figure 1 shows the relation between the beam-energy of proton and sensitivity to the each element. It was revealed that the sensitivity of each element was proportional to the seventh power of proton energies. Differences were observed in the relation when the depth distribution of the elements was changed in the film targets. Detail would be discussed in the presentation.

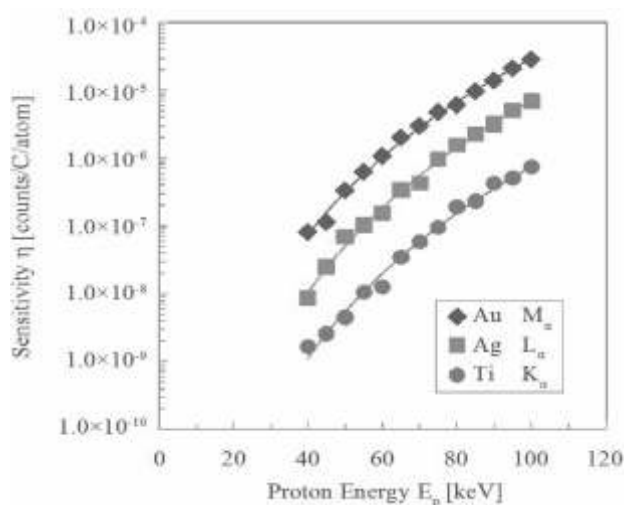


Figure 1. The relation between beam-energy of proton beam probe and sensitivities to each element obtained from thin film target.

[1] The European Palament and the Coucil of the European Union, Official. J. European Union, L37, (2003) 19-23.

[2] J. Miranda and A. Oliver, Nucl. Instr. Meth. B, 34,3 (1988) 362-368.

PB22 Trace Element Analysis of Fly ash Using Proton Induced X-rays Emission (PIXE)

B K Sharma^(a),

Sanskriti Institute of Management & Technology, Mathura, INDIA

B. P. Singh^(a,b)

Deptt of Physics Aligarh Muslim University, Aligarh and

R. Prasad^(c)

Deptt of Physics Aligarh Muslim University, Aligarh^(c)

Abstract:

Fly ash is a major component of solid material created by the coal-fired thermal power stations. In India the total amount of fly ash produced per annum is around 200 million tonnes. Fly ash has a great potential for utilization in making industrial products like cement, bricks as well as building materials, besides being used as a soil conditioner and a provider of micro nutrients in agriculture. However, given the large amount of fly ash that accumulate at thermal power plants, their possible reuse and dispersion and mobilization into the environment of the various elements depend on climate, soils, indigenous vegetation and agriculture practices. Fly ash use in agriculture improved various physico-chemical properties of soil, particularly the water holding capacity, porosity and available plant nutrients. However it is generally apprehended that the application of large quantity of fly ash in fields may affect the plant growth and soil texture. Hence there is a need to characterize trace elements of fly ash. The results of trace element analysis of fly ash and pond ash samples collected from major thermal power plants of India by Particle Induced X-ray Emission (PIXE) has been discussed.

Keywords: fly ash; pond ash; PIXE;

References:

- [1] K.C. Patra, Tapash R. Rautray, B.B. Tripathy, P. Nayak. (2012) Elemental analysis of coal and coal ASH by PIXE technique. Applied Radiation and Isotopes 70:4, 612-616. Online publication date: 1-Apr-2012.
- [2] P. MALAR, TAPASH RANJAN RAUTRAY, V. VIJAYAN, S. KASIVISWANATHAN. (2006) SYNTHESIS AND PIXE CHARACTERIZATION OF $CuInS_{e2}$ AND $Cu_{n3}S_{e5}$. International Journal of PIXE 16:01n02, 127-136. Online publication date: 1-Jan-2006. [Abstract | PDF (730 KB) | PDF Plus (366 KB)]
- [3] R Sivakumar, V Vijayan, V Ganesan, M Jayachandran, C Sanjeeviraja. (2005) Electron beam evaporated molybdenum oxide films: a study of elemental and surface morphological properties. Smart Materials and Structures 14:6, 1204-1209. Online publication date: 1-Dec-2005.
- [4] R. Sivakumar, V. Ganesan, V. Vijayan, M. Jayachandran, C. Sanjeeviraja. (2005) Particle induced X-ray emission spectroscopic (PIXE) and surface morphological (AFM) studies on electron beam evaporated WO_3 thin films. Surface Engineering 21:4, 315-319. Online publication date: 1-Aug-2005.
- [5] B. Mallikharjuna Rao, T. Seshi Reddy, G. A. V. Ramana Murty, Y. Ramakrishna, V. Vijayan, A. Ramani. (2004) Effect of radiation therapy on trace elemental concentrations of hair samples of cervical cancer patients? PIXE technique. X-Ray Spectrometry 33:6, 410-413. Online publication date: 1-Nov-2004.

PB23 PIXE analysis of some anti-diabetic medicinal plants in Nigeria

S.O. Olabanji ^(*, a, b), O.R. Omobuwajo ^(c), D. Ceccato ^(a, d), A.C. Adebajo ^(c), M.C. Buoso ^(a),
and G. Moschini ^(a, d)

^(a)Istituto Nazionale di Fisica Nucleare (INFN), Laboratori Nazionali di Legnaro (LNL), I-35020 (Padova), Italy.

^(b)ICTP Fellow on sabbatical leave from Centre for Energy Research and Development, Obafemi Awolowo University, Ile-Ife, Nigeria.

^(c)Department of Pharmacognosy, Faculty of Pharmacy, Obafemi Awolowo University, Ile-Ife, Nigeria.

^(d)Dipartimento di Fisica, Università di Padova, Padova, Italy.

Diabetes mellitus, a metabolic disease characterized by high blood glucose levels (hyperglycemia) due to defects in insulin secretion, or action, or both. It is a dangerous disease leading to death of many people in the world. Some of the medicinal plants implicated in the herbal recipes for the treatment of diabetes in Nigeria have been reported¹. Additional medicinal plants used for the treatment of diabetes in Nigeria are presented in this work. These medicinal plants are becoming increasingly important and relevant as herbal drugs due to their use as antioxidants, nutraceuticals, food additives and supplements in combating diabetes. Elemental compositions of these anti-diabetic medicinal plants were determined using PIXE technique. The 1.8 MV collimated proton beam from the 2.5 MV AN 2000 Van de Graaff accelerator at Istituto Nazionale di Fisica Nucleare (INFN), Laboratori Nazionali di Legnaro (LNL) Legnaro (Padova) Italy was employed for the work. The results show the presence of twenty two elements at various concentrations in the medicinal plants. The leaves of *Murraya*, *P. amarus*, *O. gratissimum*, *O. subscopodica*, *P. pellucida* and the whole plant of *B. diffusa*, *B. pinnatum* and *C. occidentalis* could be taken as vegetables, food additives, nutraceuticals and supplements in the management of diabetes.

[1.] S.O. Olabanji, O.R. Omobuwajo, D. Ceccato, A.C. Adebajo, M.C. Buoso, G. Moschini. Nucl. Instrum. Methods Phys. Res. Sect. B 266 (2008) 2387-2390.

Keywords: PIXE, Anti-diabetic, Medicinal plants, Nigeria.

*Corresponding author. Tel. +234 803 532 1791

E-mail: skayode2002@yahoo.co.uk

PB24 High energy Ion beam analysis at ARRONAX

C. Koumeir^(a,b), A. Guertin^(a), F. Haddad^(a,b), V. Metivier^(a), N. Michel^(a,b), D. Ragreb^(a) and N. Servagent^(a)

^(a) Subatech, 4 rue A. Kastler, 44000 Nantes, France

^(b) GIP ARRONAX, 1, rue Aronnax, - 44817 SAINT-HERBLAIN, France

ARRONAX, acronym for « Accelerator for Research in Radiochemistry and Oncology at Nantes Atlantique », is a high energy cyclotron. It is characterized by the acceleration of several types of particle beams: 68 MeV alpha, 15-35 MeV deuterons and 30-68 MeV protons.

A platform was implemented on ARRONAX to perform non-destructive materials analysis with X and gamma rays emission (PIXE-PIGE). A proper selection of the projectile type and beam energy allows us to analyze heavy and light elements in thin and thick samples.

Our research activities are oriented along three axes:

- x Measurements of K X-ray production cross section for various elements to complement the databases at high energy. A first experiment has been conducted to measure these cross sections for copper and gold with protons energy between 34 and 68 MeV.
- x Study of the detection sensitivity which depends on the nuclear background and the bremsstrahlung radiations. A dedicated shielding has been developed and detection limits below tens of $\mu\text{g/g}/\mu\text{C}$ have been assessed using different referenced samples from IAEA.
- x Determination of concentration profile as function of the depth in a thick target. Using layered samples, we have showed for a target consisting of three different layers, the possibility to determine the sequence and thickness of each layer by using X and gamma rays measured respectively during and after irradiation.

During this talk, I will present the characteristics and the capabilities of our platform. In the near future we intend to install the PIGE technique and use it with 15 MeV deuterons to analyze lightweight elements.

PB25 Analysis of trace elements in polymers by PIXE

C. T. Souza^{a,b}, L. A. Bouffleur^{a,b}, C.E.I. dos Santos^b, E. M. Stori^{a,b}, D. V. Bauer^b, R. M. Papaléo^c,
L. Amaral^{a,b}, J. F. Dias^{a,b}

^aPrograma de Pós-Graduação em Ciência dos Materiais, Universidade Federal do Rio Grande do Sul, CP 15051, CEP 91501-970, Porto Alegre, RS, Brazil.

^bInstituto de Física, Universidade Federal do Rio Grande do Sul, CP 15051, CEP 91501-970, Porto Alegre, RS, Brazil.

^cPontifícia Universidade Católica do Rio Grande do Sul, Av. Ipiranga 6681, CEP 90619-900, Porto Alegre, RS, Brazil.

The quantitative analysis of trace elements in biological tissues has been widely studied in several laboratories. Usually, elements like phosphorus, chlorine, calcium and iron play important role in biological systems. Other elements like nickel and zinc are also important due to their presence in the so-called metalloproteins. Therefore, the precise quantification of such elements is of utmost interest as far as biological tissues are concerned. In many cases, different types of polymers are used as a backing for biological samples [1-3] due to the relatively low background observed during the experiments [1]. However, some polymers have trace elements which can hamper the proper analysis of tissues using PIXE and micro-PIXE. Thus, it becomes essential to study the elemental composition of polymers prior to their use as backings of biological samples. In the present study, the presence of trace elements in different polymers was determined. Foils of PS (polyestirene - 25 μm), PET (polyethylene terephthalate - 1.5, 2.0, 6.0 and 52.0 μm) and PA (polyamide - 25 μm) were analyzed with PIXE. The measurements were carried out at the Ion Implantation Laboratory of the Physics Institute (UFRGS) using a 3 MV Tandemron accelerator. All PIXE measurements were performed with 2 MeV proton beams. The foils were irradiated with a mean current of 3 nA during 400 seconds, which ensures a low dead time of the data acquisition system. A Si (Li) detector positioned at 135° with respect to the beam direction is used to detect the characteristic X-rays. The results show that different trace elements were observed in different types of polymers. Figure 1 shows a typical PIXE spectrum for some of the samples. It was possible to observe the presence of trace elements such as Al, Si, P, Cl, Ca, Ti, Cr, Fe, Ni, and Zn. The results indicate that some polymers are rich in Ca, Cr and Fe, while others have substantial amounts of P, Ni and Zn.

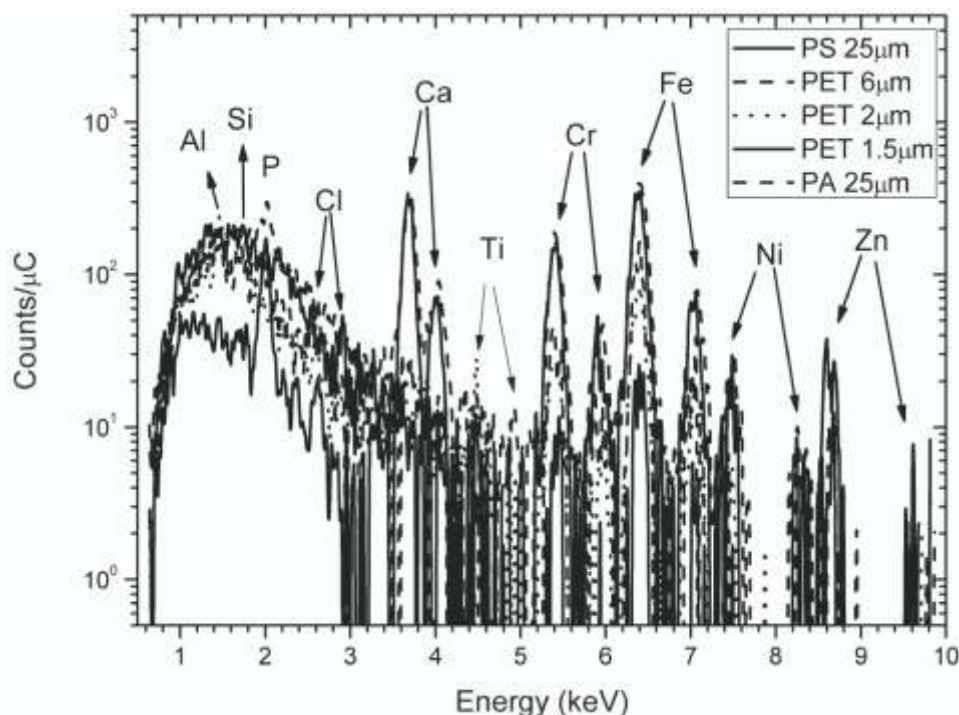


Figure 1: Typical PIXE spectrum showing the number of X-ray counts per unit charge as a function of the energy of each characteristic X-ray.

[1] S. B. Russeli, C. W. Schuite, S. Falq, J. L. Campbell. *Analytical Chemistry*, 53 (1981) 571-574.

[2] G. Flaccavento, M. Folkard, J. A. Noble, K. M. Prise, B. Vojnovic. *Applied Radiation and Isotopes* 67 (2009) 460-463.

[3] C. C. Anamelechi, G. A. Truskey, W. M. *Biomaterials* 26 (2005) 6887-6896.

PB26 PIXE analysis of pre-colonial pottery from Sambaqui do Panaquatira

R. A. Ikeoka^(a), C. R. Appoloni^(a), M. A. Rizzutto^(b), T.F.Silva^(b) and A. M. Bandeira^(c)

^(a) Departamento de Física/CCE, Universidade Estadual de Londrina;
Cx.Postal 6001, CEP 86051-990, Londrina/PR – Brazil
E-mail:renatoikeoka@yahoo.com.br

^(b) Instituto de Física da Universidade de São Paulo, Laboratório de Análise de Materiais por Feixes Iônicos (LAMFI), Rua do Matão Travessa R Nr.187, CEP 05508-090 Cidade Universitária, São Paulo, SP – Brasil

^(c) Museu de Arqueologia e Etnologia, Universidade de São Paulo; Av. Prof. Almeida Prado, 1466 CEP 05508-900, Cidade Universitária, São Paulo/SP – Brazil

The study of cultural heritage of ancient people through fossils, monuments and engines has fundamental importance in the construction of the memory of any society. Such knowledge can be acquired by researches in archaeological sites and the detailed study of the different kind of objects which can be found in these places. This work deals with objects from the Sambaqui of Panaquatira located in São Luís do Maranhão (Brazil). Ancient civilizations that inhabited that territory were characterized as fishing populations - catchers – hunters and ceramists. From a selection of 95 pottery fragments of surface; 5 to 10 cm; 20 to 30 cm; 40 to 50 cm; 65 to 70 cm; 80 to 90 cm; 90 to 100 cm; 130 to 140 cm and 160 to 170 cm stratigraphic levels, a representative set was analyzed using Particle Induced X-ray Emission (PIXE) methodology. PIXE measurements were performed with an external beam setup with ~2.4MeV proton beam in the LAMFI laboratory using three X-ray detectors, two Si-PIN detectors and one HPGe with standard spectrometry electronics; each spectrum was taken for 600s. The spectra analyses were performed with the Quantitative X-Ray Analysis Software (WinQXAS), distributed by International Atomic Energy Agency (IAEA). The elements Si, P, S, Cl, K, Ca, Ti, Cr, Mn, Fe and Zn were identified in the different fragments. It was analysed the kind of applied treatment on the concave and convex sides in relation to the ceramic paste of the fragments. From the determination of the elemental composition of the fragments, it was possible to identify that the elements Ti, Mn, Fe and Zn are present in the fragments with larger amounts at concave and convex sides, compared to the ceramic paste, indicating a different surface treatment that leads to an enrichment of these elements. One fragment from the 20-25cm stratigraphy has a lighter colour region which is characterized by containing the highest concentration of the elements Ti, Ca, Ti, Cr and Mn.

PB27 Trace Elements Level in Serum of Melanoma Patients by PIXE and HR-ICPMS

Suene Bernardes^(a), Manfredo Harri Tabacniks^(a), Jorge Eduardo de Souza Sarkis^(b), Ernesto^(b), Talita Oliveira^(b), Ivan Abranches Oliveira Santos^(c), Francisco de Assis Ribas Bosco^(c), Andrea Fernandes de Oliveira^(c), Janaína Namba Shie^(c)

^(a)Institute of Physics, University of São Paulo, Brazil.

^(b)Instituto de Pesquisas Energéticas e Nucleares – IPEN - Laboratório de Caracterização Química – LCQ, Centro de Química e Meio Ambiente –CQMA - São Paulo, Brazil.

^(c)UNIFESP, São Paulo, Brazil.

Melanoma is a serious skin cancer that, if found and treated in its early stages increases the chance of recovery. Over the last decades its incidence has rapidly risen in world populations, but the reasons for this growth are partly unknown. However it is known that sun exposure and genetic factors are important precursors of melanoma. Nowadays, some studies have correlated some trace elements in blood and tissue with the disease. [1,2]. In this work, trace element concentrations in blood serum of patients with melanoma were measured by PIXE (Proton Induced X-ray Emission) and HR-ICP-MS (High-Resolution Inductively Coupled Plasma Mass Spectrometry) aiming to correlate them with the disease. Blood samples from 30 patients and 116 healthy donors were collected at the Hospital (protocols CEP 1036/08 UNIFESP) in glass tubes without additives, and the serum separated after centrifugation for 15 minutes at 4500 rpm. A total of 10 elements were measured: 4 by HR-ICPMS (Mg, Se, Cu and Zn), 8 by PIXE (P, S, Cl, K, Ca, Br, Cu and Zn). The analytical methods were assessed analyzing reference materials QMEQAS06S-06, QMEQAS08S-06 and NIST 1577b. The analytical precision ranged from 3 % to 9 %. Relevant clinical information of patients has also been included in the statistical analysis (histological type of tumor, level of melanoma, Breslow depth scale, number of lymph nodes, presence or absence of mitosis and/or ulceration). The evaluation of the control group showed different concentrations of P and Mg for individuals aged above and below 40 years. The P, S, Ca, Cu and Zn in healthy individuals differed according to the gender, highlighting the need of inserting the variables age and gender in the case-control analysis. The concentrations of K, S, Ca and Se showed differences between the control group and the melanoma, when considering the clinical variables of the patients ($p < 0.05$). The need for stratification by age, gender and stage of cancer, critically reduced the already limited number of samples, compromising the interpretation of the small differences in elemental concentrations found. The results for the healthy population agreed with the values reported in the literature and contributed to strengthen the database of elemental concentrations in serum of the Brazilian population.

Acknowledgments: FAPESP

[1] M. Bergomi, G. Pellacani, M. Vinceti, S. Bassissi, C. Malagoli, D. Alber, S. Sieri, L. Vescovi, S. Seidenari and R. Vivoli, *Journal of Trace Elements in Medicine and Biology*, 19 (2005) 69-73.

[2] R.A. Desmond and S.J. Soong, *Surg. Clin. North Am.*, 83(1) (2003) 1-29.

PB28 Metallic objects belonging to the first emperor of Brazil studied with PIXE technique

V.C. Ambiel^(a), M.A. Rizzutto^(b), J. F. Curado^(b), P.H.O.V. Campos^(b), E.A.M. Kajiya^(b) and T.F.Silva^(b)

^(a)*Museu de Arqueologia e Etnologia da Universidade de São Paulo, Av. Prof. Almeida Prado, 1466, São Paulo, SP, Brasil;*

^(b)*Instituto de Física da Universidade de São Paulo; Rua do Matão, Travessa R, 187, São Paulo, SP, Brasil, rizzutto@if.usp.br*

First Emperor of Brazil, D. Pedro I is one of the main personalities in the history of Brazil and was responsible for the formation of the 'Brazilian nation', in September 7. With the death of King D. João VI in 1826, was acclaimed King Pedro IV in Portugal, however, held the office for a week and abdicated in favor of her daughter, Maria da Gloria. Due to political problems he also abdicated the Brazilian throne, in 1831, in favor of his son Pedro II. D. Pedro died on September 24 of 1834 at the Palace of Queluz, in Cintra and was buried in the Pantheon of the Royal House of Bragança, in Lisbon, Portugal. However in 1972, during celebrations of the 150th anniversary of the Independence of Brazil, his remains were moved to the Imperial Chapel in Monument Ipiranga installed in the city of São Paulo, Brazil. In the year 2012, was initiated a study in the Emperor including the exhumation, the inventory associated with it and several physical-chemical studies. The analyses have been performed with non-destructive techniques such as X Ray Fluorescence (XRF) in various classes of objects, including bones, tissues and metals and also Particle Induced X-Ray Emission (PIXE) in the metal objects. This article presents the PIXE results obtained for the set of metallic artifacts such as cufflinks and medals that show a wide variation in chemical composition with alloys formed mainly of copper and zinc and also made of alloys containing silver and gold. It was also verified the presence of lead and calcium, probably due to contamination suffered in the environment in which materials were found, particularly the remains were originally kept in a coffin of lead. The analyses also indicate some degree of deterioration of these objects.

PB29 Optimization of PIXE Quantitative System to Assist the Traceability of Pearl and other Gemstones

S. MURAO^(a), K. SERA^(b), S. GOTO^(c), C. TAKAHASHI^(c), L. CARTIER^(d), and K. NAKASHIMA^(e)

^(a)National Institute of Advanced Industrial Science and Technology, Tsukuba, Ibaraki, Japan, Email s.murao@aist.go.jp;

^(b) Cyclotron Research Center, Iwate Medical University, Takizawa, Iwate, Japan

^(c) Takizawa laboratory, Japan Radioisotope Association, Takizawa, Iwate, Japan

^(d) Department of Environmental Science, University of Basel, Switzerland

^(e) Yamagata University, Yamagata, Japan

A recent rise of social attention towards ethical consumerism, ethical jewellery, blood diamonds and the traceability of gemstones has challenged scientists to construct analytical systems to deliver in line with such expectations by offering traceability solutions. It is important to develop traceability protocols for gemstones and pearls that are ethically traded, as this will further encourage members of the trade to engage in ethical and fair trade practices. Of various kinds of available methods, "Proton/particle Induced X-ray Emission (PIXE)" seems to be robust and promising in this context because of its trace element analysis capabilities without destruction. The authors conducted both vacuum and in-air experiments to optimize conditions to identify important peaks and to quantify the signals that correspond to gemstone materials from specific geographic origins. PIXE results for cultured pearls from Micronesia and commercial-quality crystals from Pakistan, both sources of fair trade gemstone materials, will be presented.

PB30 Metabolomics approach regarding the effects of the treatment of undernourished rats with Shiitake mushroom (*Lentinula edodes*)

Patrícia Molz^a, Joel Henrique Ellwanger^a, Carla Eliete Iochims dos Santos^b, Deivis de Campos^a, Marisa Terezinha Lopes Putzke^a, Daniel Prá^a, Valeriano Antonio Corbeline^a, Silvia Isabel Rech Franke^a.

^aUniversidade de Santa Cruz do Sul, Av. Independência, 2293, Bairro Universitário, CEP: 96815-900 Santa Cruz do Sul - RS / Brazil.

^bUniversidade Federal do Rio Grande do Sul, Av. Bento Gonçalves, 9500, Bairro Agronomia, CEP: 91509-900, Porto Alegre – RS/Brazil.

Most diseases are associated with physiological complex patterns, involving multiple metabolic pathways. By having a complex composition, food can affect several metabolic pathways simultaneously, presenting aggravating or curative effects for many diseases. Malnutrition is characterized by decreased metabolic rate as a result of lack of nutrients essential to life. Severe malnutrition can often lead to death. The mushrooms have a significant nutritional composition for the treatment of malnutrition by having good amount of protein and carbohydrates. Shiitake Mushroom (*Lentinula edodes*) can be an alternative to reverse malnutrition because besides having high values of macronutrient with the exception lipids, has functional properties as antioxidant. The aim of this study was to explore the metabolic changes and the concentration of minerals found in undernourished rats reared with Shiitake mushroom. 20 animals were randomly assigned into 2 groups: Undernourished (U) and Undernourished+Shiitake (U+S). For 30 days, groups U and U+S went through the process of calorie restriction (75% - 80% less of the usual intake) to reach the state of undernourished for rats (specific body mass index $<0.45\text{g/cm}^2$)¹. During the next 60 days, the group U+S was supplemented with Shiitake (0.015g/weight/animal). At the end of the experiment, whole blood obtained during the sacrifice was frozen for later processing. For the determination of the level of minerals in the blood, samples were first lyophilized and subsequently measured at the Laboratory of Ion Implantation of the Institute of Physics of UFRGS, through the technique of Particle Induced X-ray Emission (PIXE)². For metabolomics, samples were mixed with KBr and lyophilized and tested under Infrared Fourier Transform Spectroscopy (FT-IR)³ analyzed by DRIFTS in the range of 4000 to 600 cm^{-1} with 16 scans scanning and 4 cm^{-1} resolution and normalization relative to banda amide I. The mineral analysis indicated differences between the groups in relation to minerals Aluminum, Arsenic, Bromine, Calcium, Chloride, Chromium, Copper, Sulphur, Iron, Phosphorus, Magnesium, Nickel, Potassium, Rubidium, Sodium, Zinc and Titanium. Preliminary results of the FTIR analysis show significant differences between the groups U and U+S absorption band at 3750-3500 cm^{-1} (OH and NH water and proteins) with $P < 0.05$. Also, there was a trend for reduced absorption at 2250-2000 cm^{-1} (OH water) from 0.1780 to 1720 cm^{-1} (C = O esters and carboxylic acids) and 1050-800 cm^{-1} (C-O carbohydrates) but with $p < 0.1$. For group U+S, we found significant correlations between the number of spectra and the concentration of Arsenic, Chlorine, Iron, Magnesium and Potassium. The data indicate that supplementation with Shiitake in malnutrition alters the composition of blood proteins, minerals and blood volume. A more detailed study to address the composition of minerals in the mushroom will be accomplished to quantity of heavy metals.

[1] E.L. Novelli, Y.S. Diniz, C.M. Galhardi, G.M. Ebaid, H.G. Rodrigues, F. Mani, A.A. Fernandes, A.C. Cicogna, J.L. Novelli Filho, Anthropometrical parameters and markers of obesity in rats, Lab Anim, 41 (2007) 111-119.

[2] O. Fiehn, W. Weckwerth. Deciphering metabolic networks. European Journal of Biochemistry, 270 (2003) 579-588.

[3] S.A.E. JOHANSSON, J.L. CAMPBELL, K.G. MALMQVIST. (Eds.). Particle-induced x-ray emission spectrometry (PIXE). New York: John Wiley, 1995.

PB31 External beam PIXE and ionoluminescence micro-imaging of Mesoamerican jade

T. Calligaro^(a), C. Andrieu^(b), Y. Coquinot^(a), C. Delobelle^(c), J. Gazzola^(d), F. Gendron^(e), V. Gonzalez^(a), O. Jaime-Riveron^(f), B. Moignard^(a), Q. Lemasson^(a), C. Pacheco^(a), L. Pichon^(a), S. Ramos^(d)

^(a) Centre de recherche et de restauration des musées de France (C2RMF), Louvre, Paris, France

^(b) UMR 8096 CNRS ArchAm - Université Paris 1 Panthéon-Sorbonne, France

^(c) Université Bordeaux III, Bordeaux, France

^(d) Instituto Nacional de Antropología e Historia (INHA), Mexico City, Mexico

^(e) UMR 7194 CNRS Dpt préhistoire, Muséum National d'Histoire Naturelle (MNHN), Paris, France

^(f) University of Kentucky, Lexington, Kentucky, USA

e-mail: thomas.calligaro@culture.fr

Mesoamerican jade was an important raw material for manufacturing sumptuary artifacts during Prehispanic times. To establish long-distance exchange of jade, the fingerprinting of this very heterogeneous rock made of various minerals (jadeite $\text{NaAlSi}_2\text{O}_6$, omphacite, phlogopite, titanite, amphiboles, etc.) would rely on mineralogical methods that require sampling such as petrography. The alternative approach presented here provides a detailed mineralogical characterization of the samples in a fully non-destructive manner relies on the coupling of PIXE and ionoluminescence (IL) using a scanning external nuclear microprobe.

This setup is installed in the New AGLAE external beamline and uses a 3-MeV proton beam of a few nA with a diameter of 30 μm . The beam is scanned over an area of a few millimeters on the sample by vertical magnetic deflection of the beam and mechanical translation of the target [2]. The IL spectra in the 200 to 1000 nm domain are recorded using a Peltier-cooled spectrometer Ocean Optics QE-65000 using a 1000 μm optical fiber placed at an angle of 45° and 3 mm away from the beam impact point. The data acquisition system of the New AGLAE beam line allows to collect PIXE/PIGE/RBS/IL spectra maps.

Some 130 jade samples were analyzed, sixty geological samples and seventy archaeological ones. The reference jade come from the Northern and Southern banks of the Motagua river in Guatemala, the only reported jade deposit in Mesoamerica [4]. The archaeological jade samples are craps recovered from workshops from the Maya archaeological site of Cancuén, Guatemala [5], and small artefacts such as beads and carvings recently excavated near the Quetzalcoatl temple at Teotihuacán, Mexico. The majority of the mineralogical phases could be identified by the quantitative composition in major elements - confirmed using μ -Raman spectrometry - along with their respective trace elements. The comparison between the IL and the PIXE maps suggested possible elements implied in the IL production. The statistical correlation between the intensity of the three main IL bands at 340, 560, 710 nm and the concentrations of these elements confirm this behavior, such as for instance the band at 560 nm with calcium. The archaeological samples from Cancuén and Teotihuacán appear to have markedly different IL spectra and chemical compositions.

[1] T. Calligaro, Y. Coquinot, L. Pichon, B. Moignard, Nucl Instr and Meth B 269 (2011) 2364

[2] Pichon L., C. Pacheco, B. Moignard, T. Guillou, Q. Lemasson, P. Walter, The New AGLAE project, these proceedings

[3] Pichon L., Beck L., Walter Ph., Moignard B., Guillou T., Nucl Instr and Meth B 269 (2010) 2028

[4] Gendron F., D.C. Smith and A. Gendron-Badou. J. Archaeological Sciences, 29 (8) (2002) 837

[5] Andrieu C., Forné M. and Demarest A., 2012. El valor del jade: producción y distribución del jade en el sitio de Cancuén, Guatemala. Instituto Nacional de Arqueología e Historia, colección científica, México.

PB32 Elemental concentrations in hepatic and renal tissues of *Mugil curema* Valenciennes, 1836 in two coastal systems in southeastern Brazil

W.S. Fernandez^(a,b), J.F. Dias^(a), L.A. Bouffleur^(b), C.E.I. dos Santos^(b), M.L. Yoneama^(b), L. Amaral, J.F. Dias^(b)

^(a)Oceanographic Institute, University of São Paulo, Praça do Oceanográfico 191, Cidade Universitária, CEP 05508-120, São Paulo, SP, Brazil

^(b)Physics Institute, Federal University of Rio Grande do Sul, CP 15051, CEP 91501-970, Porto Alegre, RS, Brazil

This study investigated the presence and the concentration of elements in hepatic and renal tissues of white mullet *Mugil curema* from two areas of the state of São Paulo (SP, Brazil) by Particle-Induced X-ray Emission (PIXE). Fish sampling was carried out from March/09 to February/10 in Santos estuary and from May/08 to April/09 in the Cananéia-Iguape coastal estuarine system using gillnet, cast net, and fish trap. For the elemental analysis, the tissues (N=470) were pooled according to the location, freeze-dried, ground into a fine powder and pressed in pellets. The samples were irradiated with 2.0 MeV proton beam and the induced X-rays were detected by a Si(Li) detector placed at 135 in relation to the beam direction. Typical Limits of Detection (LOD) were 2.97, 3.02, 3.48, 3.54 and 8.35 ppm for Fe, Cu, Zn, Cr and Br respectively. Specimens presented difference in elemental concentrations in liver and kidney tissue, being Fe > Cr > Zn > Br > Cu and Fe > Cu > Zn > Br > Cr respectively (Figure 1). The concentrations of Cu, Cr and Zn showed statistical significant differences among the tissues of *M. curema* ($p < 0.05$). The kidney tissue showed high concentrations of Cr, while the liver tissue presented relatively higher concentrations of Cu and Zn. Between the two study areas there was no significantly difference in the elemental concentrations. *M. curema* presented concentrations of Cu, Cr and Zn in hepatic and renal tissues above the maximum limits for consumption, according to the United States Environmental Protection Agency (EPA) and Brazilian National Health Surveillance Agency (Agência Nacional de Vigilância - ANVISA). Despite its relative minor commercial importance, it feeds on detritus and can be a good indicator of environmental characteristics and bioavailability of elements in the sediment.

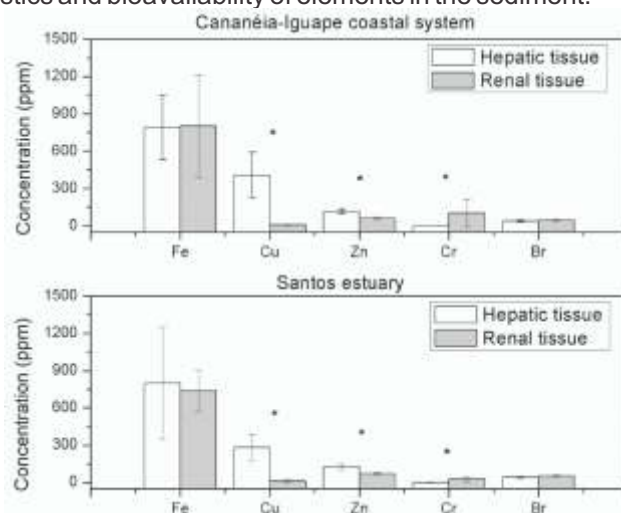


Figure 1. Elemental concentrations in hepatic and renal tissues of *Mugil curema* in Santos estuary and

PB33 Elemental detection in muscle of flatfish *Achirus lineatus* and *Trinectes paulistanus* (Actinopterygii, Pleuronectiformes) from Santos Bay, Southeastern Brazilian coast

Maria Luiza Chiste Flaquer da Rocha^(a), Johnny Ferraz Dias^(b) and June Ferraz Dias^(a)

^(a) Instituto Oceanográfico da Universidade de São Paulo
Laboratório de Ecologia Reprodutiva e do Recrutamento de Organismos Marinhos (Praça do Oceanográfico, 191, 05508-120 São Paulo, SP, Brasil)

^(b) Instituto de Física da Universidade Federal do Rio Grande do Sul
Laboratório de Implantação Iônica (Av. Bento Gonçalves, 9500, 91501-970 Porto Alegre, RS, Brasil)

Studies on the presence of elements, including metals, in organisms can prevent both degradation of aquatic systems and the bioaccumulation of elements especially those that offer risk to human health. The aim of this study was to investigate the presence elements in the muscle of two species of flatfish, *Achirus lineatus* and *Trinectes paulistanus* (Achiridae, Pleuronectiformes), using Particle Induced X-Ray Emission (PIXE). This technique is considered one of the most sensitive for detecting trace metals in biomaterials. These flatfish specimens are considered residents in Santos Bay, central coast of São Paulo state, and they were caught monthly throughout the year 2005 and sorted by size and maturity stage as juveniles and adults. The two species have no spatial overlap and this allows a mapping of the Santos Bay for the presence of bioavailable metals and other elements. Sampling was done in six distinct points in the Bay, under different antropic influences: two along the beaches, one in the vicinity of the outfall diffuser and three along the entrance of the bay. Results from 54 samples of muscle allowed detect the following elements: aluminium (Al), arsenic (As), lead (Pb), copper (Cu), chromium (Cr), iron (Fe), strontium (Sr), manganese (Mn), mercury (Hg), nickel (Ni), selenium (Se) and zinc (Zn). There were no correlation with the levels of sediment contamination for most metals analyzed in muscles, with the exception of copper and also no clear pattern of differential level of metals between young and adult specimens of *A. lineatus* and *T. paulistanus*. According to the maximum tolerance values of the Brazilian National Health Surveillance Agency (Agência Nacional de Vigilância Sanitária -ANVISA), fish muscle presented levels of contamination above the permitted for human consumption, mainly for some elements: mercury, in samples from the internal area; arsenic, in samples from west side and selenium, in samples from east side of the bay.

PB34 PIXE applications to the toxicological field

C.E.I. dos Santos^(a), J.F. Dias^(a), P. F. C. Jobim^(a), M. L. Yoneama^(a), V.M. Andrade^(b),
L. Amaral and J. da Silva^(c)

^(a)Laboratório de Implantação Iônica, Instituto de Física, Universidade Federal do Rio Grande do Sul. Av. Bento Gonçalves, 9500, Porto Alegre, Brazil.

^(b)Laboratório de Biologia Celular e Molecular, Universidade do Extremo Sul Catarinense. Av. Universitária, 1105, Criciúma, Brazil.

^(c)Laboratório de Toxicologia Genética, Universidade Luterana do Brasil. Av. Farroupilha, 8001, Canoas, Brazil.

Several studies have been carried out in order to investigate the toxicological properties of some chemical elements in different type of biological samples. Ion beam techniques, in particular PIXE, have been successfully used to analyze the elemental composition of food, beverage, plants and animal tissues. In this context, the PIXE line of the Ion Implantation Laboratory (Porto Alegre, Brazil) have been used in the last few years to study food and beverage processing and biological specimens exposed to contaminated environment. The aim of this study is to present some of our results using PIXE analysis applied to toxicological research field. For instance, a recent published research [1] investigated the genotoxic and mutagenic effects in tobacco farmers exposed to metal-based formulated pesticides. Levels of Mg, Al, Cl, Zn, Cr and Br, elements associated with DNA damage, were higher in the blood samples of tobacco farmers exposed to pesticide than in the non-exposed group. The occupational genotoxicity among copper smelters was also investigated [2]. The elemental content of blood samples were analyzed by PIXE. DNA damage in the peripheral blood lymphocytes of workers exposed to copper smelter was observed. However, no clear correlation was found between the metal content and DNA damage.

[1] F. R. da Silva, J. da Silva, M. C. Allgayer, C. F. Simon, J. F. Dias, C. E. I. dos Santos, M. Salvador, C. Branco, N. B. Schneider, V. Kahl, P. Rohr, K. Kvitko, J. Hazard. Mat., 225-226 (2012) 81-90.

PB35 Structural changes in quantum dots core-shell CdSe/ZnS by thermal treatment and proton irradiation

L. G. Almeida^(a), M. A. Sortica^(a), P. L. Grande^(a), C. Radtke^(b), R. Debastiani^(a), J. F. Dias^(a), A. Hentz^(a)

^(a) Instituto de Física, Universidade Federal do Rio Grande do Sul (IF-UFRGS)

^(b) Instituto de Química, Universidade Federal do Rio Grande do Sul (IQ-UFRGS)

Compound quantum-dots (QDs) are promising materials used in many fields of technological development. In spite of that, the accurate knowledge of their compositional depth-profiling is still a technological challenge. Recently, we used the MEIS (medium energy ion-scattering) technique, combined with PIXE and RBS (Rutherford backscattering spectrometry) to characterize core-shell nanostructures of CdSe/ZnS [1]. In this work, we use the same characterization methods to survey the changes of elemental distribution in the the core and shell regions of these QDs, when submitted to a range of thermal treatments and proton irradiation conditions. Our preliminary results show that for temperatures below the melting point of the bulk CdSe compound, there is already a decrease in the amount of cadmium, accompanied by an overall decrease in the diameter of the CdSe QD nuclei.

Financial support by CNPq and PRONEX

[1] M. A. Sortica, P. L. Grande, C. Radtke, L. Almeida, R. Debastiani, J. F. Dias, A. Hentz, Applied Physics Letters, 101 (2012) 023110.

PB 36 Swift-heavy ion-sputtered CaF₂ nanoparticles characterized by medium energy ion scattering

M. Hatori¹, M. A. Sortica¹, J. F. Dias¹, P. L. Grande¹, W. Assmann², A. Weizmüller², M. Toulemonde³, C. Trautmann^{4,5}

¹*Institute of Physics, Universidade Federal do Rio Grande do Sul (IF-UFRGS)*

²*Ludwig-Maximilians-Universität, Munich, Germany*

³*CIMAP-GANIL, CEA, CNRS, ENSICAEN, Univ. Caen, Caen, France*

⁴*GSI Helmholtzzentrum, Darmstadt, Germany*

⁵*Technische Universität Darmstadt, Darmstadt, Germany*

hatori.masa@gmail.com

When swift heavy ions penetrate into a target, they deposit energy by electronic excitation processes and induce the ejection of particles from the sample surface, so-called electronic sputtering. For ionic crystals such as LiF and CaF₂, the emission has a jet-like component normal to the target surface superimposed on a broad cosine angular distribution [1]. The jet like emission is probably due to the ejection of nanoparticles (NPs), but the origin of this jet effect is not well understood.

In this work, we characterize the nanoparticles ejected when irradiating CaF₂ crystals with 210-MeV Au ions using Medium Energy Ion Scattering (MEIS). MEIS is a well-established characterization technique to analyze surfaces and thin films. The method was recently extended to allow for the characterization of size and composition of nanoparticles [2]. CaF₂ crystals were irradiated under tilted beam incidence ($\alpha=70^\circ$, 45° , and 20° with respect to the surface) at the tandem laboratory of Munich. The ejected particles were collected on Si foils positioned at $\theta=11^\circ$, 33° , and 55° on an arc-shaped catcher. Under the same conditions, sputtered particles were collected on TEM grids for high resolution electron microscopy analysis. The resulting TEM and MEIS data agree well with respect to size and size distribution of the nanoparticles. In addition, MEIS shows the presence of atomic Ca on the catcher foils for $\alpha=70^\circ$ and $\theta=55^\circ$. The amount of atomic Ca vanishes for other emission angles.

In all cases, the NPs can be described by little spheres partially embedded in the substrate. The present results are consistent with the two sputtering components described in [1]: within the jet, mainly NPs are ejected while the sputtering at larger angles originates predominantly from ejected surface atoms. We are going to do PIXE on the samples to measure the fluor of the CaF₂, the Ca isotopes saw by MEIS and to check if there is any other impurity on the sample.

References:

- [1] M. Toulemonde, W. Assmann, C. Trautmann, F. Grüner, Phys. Rev. Lett. **88**, 057602 (2002).
- [2] M.A. Sortica, P.L. Grande, G. Machado, L. Miotti, J. Appl. Phys. **106**, 114320 (2009).

PB37 Evaluation of radioactive transfer of soils contaminated with radioactive cesium by micro-PIXE analysis

F. Fujishiro^(a), K. Ishii^(a), S. Matsuyama^(a), H. Arai^(a), A. Ishizaki^(a), N. Osada^(a), H. Sugai^(a), K. Kusano^(a), Y. Nozawa^(a), S. Yamauchi^(a), M. Karahashi^(a), S. Oshikawa^(a), K. Kikuchi^(a), S. Koshio^(a), K. Watanabe^(a) and Y. Suzuki^(b)

^(a) Graduate School of Engineering, Tohoku University

^(b) Graduate School of Biomedical Engineering, Tohoku University

Radioactive cesium, which was scattered from Fukushima daiichi nuclear power plant accident, had fallen out on a vast expanse of area of Fukushima prefecture in Japan, and has contaminated soils in field, road, schoolyard, garden and paddy. As a result, people who live in region with a high ambient dose (20 mSv/year) have been forced to live as refugees. Even in region with lower ambient dose, farm products are occasionally contaminated by radioactive cesium, which causes a serious problem for farmers due to restriction of shipment as farm products by government.

In a village where ambient dose is more than 3 mSv/h, cesium concentration of paddy soils is ca. 63000 Bq/kg. Cesium concentration of plants grown up in this region exceeds ca. 600 Bq/kg, which indicates that the radioactive transfer factor from soil to plant is ca. 0.01. On the other hand, the radioactive transfer factor of less than 0.01 has been observed at another area. In a river park area located in the downstream of a river that flows from high ambient dose area in Fukushima Prefecture, cesium concentration of soil is ca. 10000 Bq/kg. These highly contaminated soils have been thrown from the upstream, and piled up in this park at the flood. Plants grown up in this park have cesium concentration less than 10 Bq/kg. If the same radioactive transfer factor was 0.01, cesium concentration should be ca. 100 Bq/kg.

Since more than 70 % of cesium in the soil is strongly bound as a layer atom instead of original potassium in clay crystals [1], these bounded cesium could not be absorbed by plant root. Therefore, rest 30 % of cesium would affect the transfer factor from soil to plants.

In this study, soils are classified and analyzed individually by using microbeam analysis system at Tohoku University. Since bulk analysis is averaging over many particles, individual particle analysis can determine the chemical composition of these particles and is superior for better understanding. Micro-PIXE analysis is performed for several soils to evaluate a relationship between the radioactive transfer factors and elemental concentration of the soils. By comparing elemental concentration maps obtained from these soils, the radioactive cesium transfer has been discussed.

[1] H. Tsukada, A. Takeda, S. Hisamatsu and J. Inaba, J. Environ. Radioact. 99 (2008) 875-881.

PB38 Improvement of the stability of X-ray emission by the thermal excitation of pyroelectric crystals

F. Naruse^(a), H. Honda^(a), Y. Nakanishi^(a), S. Fukao^(a), Y. Ito^(b), Y. Sato^(a), and S. Yoshikado^(a)

^(a)Graduate School of Science and Engineering, Doshisha University, Kyotanabe, Kyoto, 610-0321, Japan

^(b)Institute of Chemical Researches, Kyoto University, Uji, Kyoto, 611-0011, Japan

Spontaneous polarization of a pyroelectric crystal such as LiTaO_3 or LiNbO_3 is dependent on the temperature of the crystal, and electric charge appears on the crystal surface by heating or cooling of the crystal. This pyroelectricity causes intense electric fields to appear around the crystal when the temperature changes. When a target is placed across the crystal, the electric fields accelerate electrons toward the target or the crystal, and the chamber walls. X-rays are then emitted by the impact of electrons against these surfaces [1].

A miniaturized electron accelerator based on pyroelectric crystals can be used in portable analytical instruments. The X-ray emission for a long time requires the crystal temperature to be periodically changed to form intense electric fields. Therefore, X-ray is emitted discontinuously. Continuous emission can be achieved by using multiple crystals, however, the X-ray intensity is still unstable. The electric charge density on a crystal is determined by both the polarization charges and adsorbed charges supplied from ionized ambient gas. When the net amount of charge becomes large, electrostatic discharge occurs along the crystal surface. Accordingly, sudden cessation of the X-ray emission occurs periodically. To avoid such discharge and achieve the stable emission of X-rays, the initial amount of electric charge on a crystal for each temperature cycle must be equal. It is suggested that the amount of accumulated charges on the surface is dependent on the pressure of ambient gas, amount of electrons supplied, and period of the temperature cycle. In this study, the time dependence of the net amount of electric charge was simulated using a simple model [2]. Furthermore, the stability of the X-ray emission using one or six crystal(s) was investigated by changing the temperature cycle period.

Nonstoichiometric LiTaO_3 single crystals were used. In the case of one crystal, a target was an oxygen-free copper foil of 20 μm thickness and was placed 15 mm above the negatively charged surface ($-z$ surface) of the crystal in a chamber made from stainless steel (SUS 304). Each crystal temperature was controlled by the application of triangular voltages to the Peltier device. The temperature range ΔT , was approximately 30 or 40°C. The temperature change period L , was varied from 200 to 2000 s. The ambient gas was air and the pressure was approximately 10^{-4} Pa. X-ray emission was measured using a Si-PIN X-ray detector.

Fig. 1 shows the energy spectra of X-rays per period with one crystal for $L = 1000$ s. Cu K_α and Cu K_β X-rays originated from the target, and Ta L_α X-rays from the crystal. Fig. 2 shows the average count rate of photons of Cu K_α X-rays with six crystals for $L = 1000$ and 2000 s. When L was varied, the long-term stability of the X-ray emission was changed. It was suggested that the amount of electrons supplied to the space around the target changed.

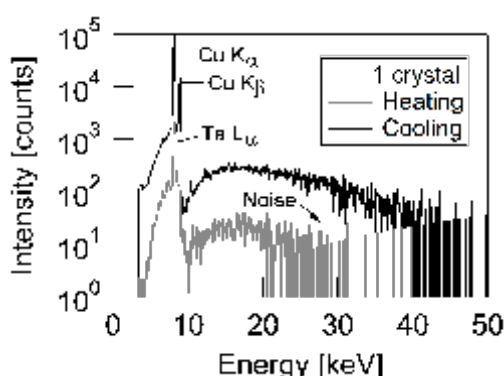


Fig. 1 Energy spectra of X-rays per period for $L = 1000$ s.

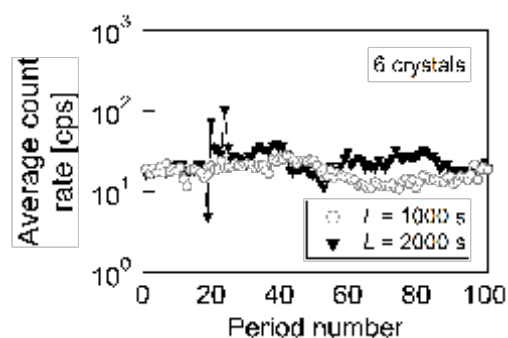


Fig. 2 Average count rate of photons of Cu K_α X-rays for $L = 1000$ and 2000 s.

[1] J. D. Brownridge, "Pyroelectric X-ray generator", *Nature*, **358**, 1992, pp. 287-288.

[2] T. Z. Fullem et al., "Electrostatics of pyroelectric accelerators", *J. Appl. Phys.*, **106**, 2009, pp. 074101.h

PB39 An evaluation of the radiocesium retention ability by root-mat horizon using micro PIXE analysis

H. Arai^(a), K. Ishii^(a), S. Matsuyama^(a), K. Kusano^(a), Y. Nozawa^(a), S. Yamauchi^(a), M. Karahashi^(a), S. Oshikawa^(a), K. Kikuchi^(a), S. Koshio^(a), K. Watanabe^(a), Y. Suzuki^(b), F. Fujishiro^(a), A. Ishizaki^(a), H. Sugai^(a), A. Terakawa^(a), Y. Kikuchi^(a), and N. Osada^(a)

^(a) Department of Quantum Science and Energy Engineering, Graduate School of Engineering, Tohoku University

^(b) Graduate School of Biomedical Engineering, Tohoku University

Root-mat horizon, which is mainly consisted of concentrated plant roots and soil particles, is often formed under litter layer in pastures and grasslands. This horizon plays an important role for plant growth as the main nutrient acquisition site [1]. Therefore, the quality and quantity of above-ground plant biomass is strongly affected by the nutrient status in the root-mat horizon.

After the Fukushima Dai-ichi Nuclear Power Plant accident, the radiocesium contamination of pasture soils and grass hays caused serious problems relating to food safety and stock-farming. A lot of the deposited radiocesium on the pastures is accumulated in root-mat horizon comparing with above-ground plant body and mineral soil layer [2]. Therefore, the ability and mechanism of radiocesium retention by root-mat horizon is an issue of great concern. Here, we investigated the accumulation of radiocesium into root-mat by an addition of stable cesium (as the form of $^{133}\text{Cs}_2\text{CO}_3$ solution) and micro PIXE analysis.

A soil block including root-mat and mineral soil was sampled at the Kawatabi Field Science Center, Tohoku University, Miyagi prefecture, Japan. The sampled soil block was brought back to laboratory. The solution of $^{133}\text{Cs}_2\text{CO}_3$ (60000 ppm, 500 ml) was poured to the surface of the soil block. The soil block was divided into three compartments (root, soil in root-mat horizon, soil under root-mat horizon). Some roots were washed by water to estimate the relative contribution of each the adsorption onto the surface and the transportation into the internal tissues by root uptake. All samples were dried at 40 °C for the subsequent micro PIXE analysis.

Cesium was detected in all samples by micro PIXE analysis. The distribution pattern of Cs was similar between non-wash and wash root sample, which were relatively homogeneous through the root. This result suggests that plant root retains Cs both inter- and external tissues, and the uptake of Cs by plant roots should be one of the important pathway for the retention of Cs in root-mat horizon. Soil samples in and under root-mat showed similar distribution pattern of Si, Al, Fe, and K. This result suggests that clay particles adsorbed Cs into/onto them. Therefore, it is concluded that both biotic and abiotic factors contribute to the retention of Cs in root-mat horizon.

References

[1] S. Okano, M. Nishio, and Y. Sawada. *Soil Sci. Plant Nutr.* 33. (1987) 373–386.

[2] Fukushima Prefecture. available from URL:

<http://www1.town.bandai.fukushima.jp/data/download/pdf/2011/ganba18bokusoH230922.pdf>. (2011) (In Japanese)

PB40 Concentration of Cs in plants and Water for the radioactive pollution due to Fukushima first nuclear power plant disaster

A. Ishizaki^(a), K. Ishii^(a), S. Matsuyama^(a), S. Koshio^(a), S. Yamauchi^(a), K. Kusano^(a), Y. Nozawa^(a), M. Karahashi^(a), S. Oshikawa^(a), K. Kikuchi^(a), K. Watanabe^(a), S. Itoh^(a), K. Kasahara^(a), S. Toyama^(a), Y. Suzuki^(b), F. Fujishiro^(a), N. Osada^(a), H. Arai^(a), A. Terakawa^(a), Y. Kikuchi^(a) and H. Takahashi^(a)

^(a)Department of Quantum Science and Energy Engineering, Tohoku University, Aramaki-Aza-Aoba 6-6-01, Aoba-ku, Sendai, 980-8579, Japan

^(b)Graduate School of Biomedical Engineering, Tohoku University, Aramaki-Aza-Aoba 6-6-04, Aoba-ku, Sendai, 980-8578, Japan

Due to the Fukushima first nuclear power plant disaster, radioactive materials are released. Then surface soil is contaminated. Many problems were caused by the radioactive contamination. One of the most important problems is on agricultural crops. So, it is important to research the relationship between concentration of radioactive materials in plants and soil conditions.

In this study, plants were cultivated in some kinds of conditions which have different Cs concentration. As samples, the white radish sprouts (fig.1) were selected because the growing period is seven days. Then amounts of Cs included in plants were analyzed with PIXE at Tohoku University [1]. The samples were planted in water with Cs_2CO_3 where Cs is normal.

It is known that too much concentration of Cs in soil makes plants poorly grew or kill. First it was carried out to exam upper limit of concentration of Cs for plants to grow up normally. As the result, it was 500 ppm.

Second, we examined a variation of Cs concentration in plants to each Cs concentration in water. The Cs concentration in leaves and stems were analyzed with submilli-PIXE camera. The result is shown in fig.2. The concentration of Cs in water of 500ppm is the highest. The others have a little difference each other.

In future work, we will have the relationship of the absorbed Cs concentration in plants and in soil for many kinds of soil conditions.

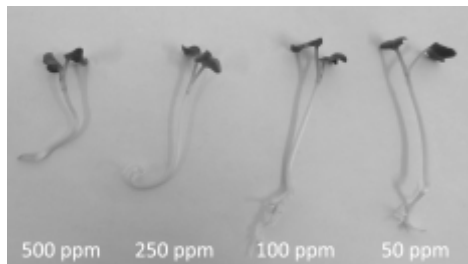


Figure1. The photograph of white radish sprout.

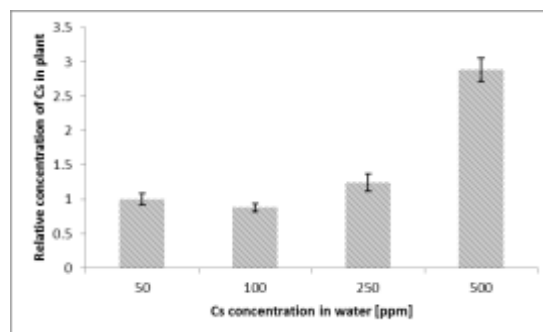


Figure2. The result of relationship between the concentration of incorporated Cs in plants and in water.

[1] S.Matsuyama, K. Gotoh, K.Ishii, H. Yamazaki, T. Satoh, K Yamamoto, A. Sugimoto, Y. Tokai, H. Endoh and H. Orihara, International Journal of PIXE, 8(2&3), (1998), 209-216.

PI X E 2013

FOR TECHNOLOGY AND GLOBAL DEVELOPMENT

AUTHOR INDEX

A

Abdelaaziz, M.	PB04
Added, N.	PB19
Adebajo, A.C.	PB23
Agarwal, A.	PA05
Ali, K.	PB05
Almeida, L.G.	O10, PB35
Almeida, S.M.	PA13, PA21
Almeida-Silva, M.	PA13
Alves, E.	PA18
Alves, L.C.	PA18, PA22
Amaral, L.	O32, PA12, PA23, PA25, PB11, PB17, PB25, PB34
Ambiel, V.C.	O26
An, K.	PA08
Andrade, V.M.	PB34
Andreae, M.O.	I9
Andrieu, C.	PB31
Angelici, D.	PA31
Angyal, A.	O24, O16, PA29
Antwis, L.	I4
Appoloni, C.R.	PB26
Arai, H.	I5, O30, PB37, PB39, PB40
Aspiazu, J.	O1
Assmann, W.	PB36

Atanacio, A.	I8,O4
Atbayga, A.	PB04, PB05
B	
Bailey, M.	I14
Bandeira, A.M.	PB26
Barradas, N.P.	PA24
Bauer, D.V.	PB25
Becagli, S.	PA32,PA33
Beckers, A.	PA06
Behar, M.	O3
Bernardes, S.	PB27
Bernardi, G.	PB18
Bertol, A.P.L.	PB01, PB02,PB03, PB13, PB14, PB15
Bhuloka Reddy, S.	O21, PA07
Bichler, M.	O27
Bohic, S.	O19
Borba, C.E.	PA04
Bosco, F.A. R.	PB27
Bouffleur, L.A.	PB11, PB25, PB32
Buoso, M.C.	PB23

C

Calligaro, T.	I12, PA30, PA31, PB31
---------------	-----------------------

Calvo del Castillo, H.	PB20
Calzolari, G.	O23, PA32, PA33
Campbell, J.L.	O5
Campos, P.H.O.V.	O26
Carcenac, C.	O19
Cardoso, J.	PA13
Carmona, A.	O19
Carreras, A.	PB15
Carrez, D.	O19
Cartier, L.	PB29
Carvalho, M.L.	I2, PA14
Cassen, S.	PA30
Castellano, G.	PB01, PB02,PB03, PB15
Ceccato, D.	PB23
Champion, C.	O2
Chaves, P.C.	I2, O2, O18, O31, PA13, PA14, PA17, PA20, PA21, PA22, PA24
Chêne, G.	O6
Chiari, M.	O23, PA32, PA33
Chilukusha, D.	O9
Christopher, M.	I14
Chu, J.	PA08
Cohen, D.	I8,O4
Colaax, J.	O17

Comrie, C.M.	O9
Constantinescu, B.	PA34
Coquinot, Y.	PA31, PB31
Corbeline, V.A.	PB30
Corregidor, V.	PA18, PA22
Cosic, D.	O11
Costa, E.M.	PA18
Crawford, J.	I8,O4
Cristea-Stan, D.	PA34
Cruz, J.	PA22
Csedreki, L.	O16
Curado, J.F.	O26

D

da Rocha, M.L.C.F.	PB33
da Silva, J.	PB34
Day, J.	PB12
de Campos, D.	PB30
de Campos, P.	PA31
de Oliveira, D.P.S.	O18
de Souza Sarkis, J.E.	PB27

de Souza, C.T.	PB17, PB25
Debastiani, R.	O10, PA23, PA25, PB35
Dedavid, B.A.	PA18
Defeyt, C.	PB20
Delobelle, C.	PB31
Deneckere, A.	PB20
Desnica, V.	O11
Dias, J.F.	O10, O32, PA12, PA23, PA25, PB11, PB17, PB25, PB32, PB33, PB34, PB35, PB36
Dias, June F.	PB32, PB33
Díaz, R. V.	O1, PA02
Doherty, G.	O4
Domínguez-Bella, S.	PA30
Dran, J.-C.	I12
Duarte, A.	O32, PA12
Dugar-Zhabon, V.D.	PB16
Dupuis, T.	O6
E	
Eder, F.M.	O27
Ehara, S.	O22
Ellwanger, J.H.	PB30
Enastu, M.	O22
Espinosa, A.A.	PA02

Espinoza-Quiñones, F. R.	PA04
Eulitz, J.	O29
F	
Fadanelli, R.C.	O3
Fajfar, H.	O28
Fang, K.H.	PA16
Farenzena, L.S.	PA15
Fawole, O.G.	PA21
Fazinic, S.	O11
Ferenczi, Z.	PA29
Fernandes de Oliveira, A.	PB27
Fernandes, A.	O31, PA21
Fernandez, W.S.	PB32
Fisher, D.	O13
Franke, S.I.R.	PB30
Freemantle, C.S.	O8
Frosini, D.	PA32
Fuchs, S.	O14
Fujisawa, M.	PA35
Fujishiro, F.	I5, O30, PB37, PB39, PB40
Fujiwara, M.	PA35
Fukao, S.	PB38

Funaki, Y.	O20
Furu, E.	O16, O24, PA27, PA29
Furumoto, S.	O20
G	
Garg, M.L.	O33
Gazzola, J.	PB31
Gendron, F.	PB31
Ghedini, C.	PA32, PA33
Gihwala, D.	PB04, PB05, PB06, PB08, PB10
Gisbert, P.E.	PA15
Gonzalez, V.	PB31
Goto, S.	I13, O22, PB29
Govil, I.M.	O33
Grande, P.L.	O10, PB35, PB36
Grime, G.	I4, I11, I14, O17
Grlj, N.	I3
Guambe, J.F.	PB12
Guan, X.C.	PA16
Guerquin-Kern, J.L.	O19
Guertin, A.	PB24
Guillou, T.	O7
Gunnelius, K.	PA26

H

Habanyama, A.	O9
Haddad, F.	PB24
Hägerstand, H.	PA26
Harada, S.	O22
Harju, L.	PA26
Hasselmeyer, L.	O29
Hatori, M.	PB36
Heirwegh, C.M.	O5
Henkel, R.	O13
Hentz, A.	O10, PB35
Herrera, A.M.	PB16
Heselius, S-J.	PA26
Himberg, M.	PA26
Hinrichs, R.	PB01, PB02, PB03, PB14
Hocquet, F.P.	PA06, PB20
Homem, M.G.P.	PA15
Honda, H.	PB38
Hubert-Ferrari, A.	PA06
Huszánk, R.	O16

I

Iida, T.	PB21
Ikeoka, R.A.	PB26
Incerti, S.	O2

Ishii, K.	I5, O20, O22, O30, PA35, PB37, PB39, PB40
Ishiya, M.	PA35
Ishizaki, A.	I5, O30, PB37, PB39, PB40
Ito, N.	O20
Ito, Y.	O20, PB38
Itoh, S.	PB40
Ivantchenko, V.	O2
J	
Jacobsen, S.D.	PB02
Jaime-Riveron, O.	PB31
Jaksic, M.	O11
Jeromel, L.	I3
Jeršek, M.	O28
Jeynes, C.	I14, O17
Jobim, P.F.C.	PB34
Jones, B.N.	I4, I14, PA15
Joseph, D.	PA01
K	
Kada, W.	O15, PB21
Kajiya, E.A.M.	O26
Kalkur, N.	PA01
Kamiya, T.	O15, O22
Karahashi, M.	O20, O30, PA35, PB37, PB39, PB40

Karnieli, A.	I9
Karydas, A.G.	O11
Kasahara, K.	PB40
Kato, Y.	PB21
Kavčič, M.	PA14, PA27
Kearsley, A. T.	O17
Kelemen, M.	I3
Kertész, Zs.	O16, O24, PA27, PA29
Khumalo, Z.	PA11
Kikuchi, K.	O30, PB37, PB39, PB40
Kikuchi, Y.	I5, O20, O30, PA35, PB39, PB40
Kirkby, K.	I14
Kishi, A.	PB21
Kiss, Á.Z.	O16
Knific, T.	O28
Koka, M.	O15
Koshio, S.	O30, PB37, PB39, PB40
Koumeir, C.	PB24
Kovács, I.	PA34
Kržič, A.	O28
Kukec Mezek, G.	I3
Kunsevi-Kilola, C.	PB06, PB07, PB08, PB09
Kusano, K.	O20, PB37, PB39, PB40

L

Lapicki, G.	I1, O4
Lemasson, Q.	O7, PB31
Li, X.	PA08
Lill, J-O.	PA26
Limandri, S.	PB18
Lindroos, A.	PA26
López-Monroy, J.	O1, PA02
Lucarelli, F.	O23, PA32, PA33
Lugo, M.	O1
Lux, J.	O28

M

Maenhaut, W.	I9
Manfredi da Silva, L. R.	O32, PA12
Manjunatha, H.C.	PA09
Mantero, A.	O2
Maqutu, M.L.	PB07, PB09
Marchal, A.	O6
Marco, S.	O19
Marconi, M.	PA33

Marques, J.P.	I2, PA14, PA20, PA24
Mars, J.A.	O13, PB04, PB05, PB06, PB07, PB08, PB09, PB10, PB12
Mathis, F.	O6
Mathpal, M.C.	PA05
Matsuyama, S.	I5, O20, O30, PA35, PB37, PB39, PB40
Méndez, B.	O1
Merchel, S.	O27
Mesjasz-Przybylowicz, J.	I6
Metivier, V.	PB24
Michel, N.	PB24
Migliori, A.	O11
Miranda, J.	O1, PA02
Mochi, D.	O23
Módenes, A.N.	PA04
Mohammed, A.	PB07, PB09
Moignard, B.	O7, PB31
Molz, P.	PB30
Moschini, G.	PB23
Mudronja, D.	O11
Murao, S.	PB29
Murillo, G.	O1
N	
Naga Raju, G.J.	O21, PA07

Nagakubo, K.	I5
Nagaya, T.	PA35
Nakanishi, Y.	PB38
Nakashima, K.	PB29
Nardi, L.V.	PA15
Naruse, S.	PB38
Nava, S.	O23, PA32, PA33
Neelmeijer, C.	O27, O29
Nemutudi, R.	O9
Nozawa, Y.	O20, O30, PA35, PB37, PB39, PB40
Nunes, T.	PA13
O	
Ogrinc, N.	I3
Ogundele, L.T.	PA21
Olabanji, S.O.	O12, PB23
Oladele, A. T.	O12
Olaniyi, H.B.	PA21
Olise, F.S.	O31, PA21
Olivares, C.	PB18
Oliveira Santos, I.A.	PB27
Oliveira, T.	PB27
Omobuwajo, O.R.	PB23
Orozco, E.A.	PB16

Ortega, R.	I7, O19
Osada, N.	I5, O30, PB37, PB39, PB40
Osinkolu, G.A.	O12
Oshikawa, S.	PB37, PB40
Owoade, O.K.	PA21

P

Pacheco, C.	O7, PB31
Palcsu, L.	O16
Palitsin, V.	I4, I14, O17
Papaléo, R.M.	PB25
Pearce, N.J.G.	O27
Pelemo, D.A.	O12
Pelicon, P	I3
Pérez, P.	PB01, PB02, PB13
Perrin-Verdugier, L.	O19
Petersen Xavier, A.A.	PA12
Pichon, L.	O7, PA31, PB31
Pierrat-Bonnefois, G.	PA31
Pineda-Vargas, C.A.	O8, O9, PA11
Pio, C.A.	PA13

Plá Cid, C.C.	PA15
Plá Cid, J.	PA15
Pongrac, P.	I3
Prá, D.	PB30
Pradler, I.	O5
Przybylowicz,W. J.	I6, O14
Puri, N.K.	O33, PA03
Putzke, M.T.L.	PB30
Q	
Querré, G.	PA30
R	
Radtke, C.	O10, PB35
Ragreb, D.	PB24
Rajta, I.	O16
Ramos, M.M.	PA23, PA25
Ramos, S.	PB31
Ravir Kumar, M.	PA07
Re, A.	PA31
Regvar, M.	I3
Reis, M.A.	I2, O2, O18, O31, PA13, PA14, PA17, PA20, PA21, PA22, PA24
Rizzutto, M.A.	O26, PA04, PB26
Rocha, M.L.C.F.	PB17

Rodriguez, L.	PB18
Rodríguez, T.P.	PB03, PB13, PB15
Rosa, L.F.S.	PA15
Roudeau, S.	O19
Rugi, F.	PA32, PA33
S	
Saayman, M.	PB07
Sacks, N.	O8
Saitoh, Y.	I13
Sakurada, T.	I5
Santos, G.H.F.	PA04
Santos, H.	PB19
Sarita, P.	O21, PA07
Sato, F.	PB21
Sato, T.	O22
Satoh, T.	O15
Sato, Y.	PB38
Savasta, M.	O19
Sepúlveda, A.H.	PB03, PB14, PB15
Sera, K.	I13, O20, O22, PB29

Servagent, N.	PB24
Severi, M.	PA33
Shameena, A.	PA01
Sharma, B.K.	PB22
Shie, J.N.	PB27
Silva, T.F.	O26, PB26
Simon, A.	I10
Singh, M.K.	PA05
Småtått, J-H.	PA26
Šmit, Ž.	O28
Sortica, M.A.	O10, PB35, PB36
Souza, V.S.	PA23, PA25
Stelcer, Ed	I8, O4
Sterba, J.H.	O27
Stori, E.M.	PB17, PB25
Streicher, M.	PA18
Strivay, D.	O6, PA06, PB20
Suárez, S.	PB18
Sueyasu, M.	PB21
Sugai, H.	O20, O30, PA35, PB37, PB39
Sugai, K.	I5
Sumbu, K.	PB10
Suzuki, Y.	PB37, PB39, PB40
Szikszai, Z.	O16, PA29

Szoboszlai, Z.	O16, O24, PA29
Szőkefalvi-Nagy, Z.	PA34
T	
Tabacniks, M.H.	PB27
Taborda, A.	I2, O2, O18, O31, PA13, PA14, PA17, PA20, PA21, PA24
Takahashi, C.	I13, PB29
Takahashi, H.	O30, PB40
Tarr, S.	PB07, PB09
Terakawa, A.	I5, O20, O30, PA35, PB39, PB40
Thanigai, A.	PA01
Topic, M.	O8, PA11
Török, Zs.	O16, O24, PA29
Toulemonde, M.	PB36
Toyama, S.	PB40
Trautmann, C.	PB36
Traversi, R.	PA32, PA33
Trincavelli, J.	PB01, PB02, PB03, PB13, PB14, PB15
U	
Udisti, R.	PA32, PA33
Uzonyl, I.	O16
V	
Vandenabeele, P.	PB20
Vasconcellos, M.A.Z.	PB01, PB02, PB03, PB13, PB14, PB15
Vavpetič, P.	I3

Villaseñor, P.	O1
Vogel-Mikuš, K.	I3
W	
Wada, S.	O20
Walter, Ph.	O7
Wang, G.	O25, PA08
Wang, T.S.	PA16
Warmenhoven, J.	I14
Watanabe, K.	O30, PA35, PB37, PB39, PB40
Webb, R.	I4, I14, PA15, O17
Weitz, F.	O13
Weizmüller, A.	PB36
Wu, T.D.	O19
Wu, B.	PA08
X	
Xu, X.X.	PA16
Y	
Yamauchi, K.	I13
Yamauchi, S.	O20, O30, PA35, PB37, PB39, PB40
Yamazaki, H.	O20
Yokoyama, A.	O15
Yoneama, M.L.	PA12, PA23, PA25, PB32, PB34
Yoshikado, S.	PB38

Yu, L.

O25, PA08

Z

Zhang, R.

O25, PA08

Zhang, S.

PA16

Zhao, J.T.

PA16

Impressão:

